

Seismic Analysis and Retrofitting Measures for Bridge No. 2001 in Highway PR-22, Bayamón, PR

By

REINALDO SILVESTRY ACOSTA

A project submitted in partial fulfillment of
the requirements for the degree of

**MASTER OF ENGINEERING
IN
CIVIL ENGINEERING**

**UNIVERSITY OF PUERTO RICO
MAYAGUEZ CAMPUS
May 2013**

Approved by:

Manuel Coll Borgo, Ph.D.
Member, Graduate Committee

Date

José A. Martínez Cruzado, Ph.D.
Member, Graduate Committee

Date

Ricardo R. López Rodríguez, Ph.D.
President, Graduate Committee

Date

Pedro Vásquez Urbano, D. Sc.
Representative of Graduate School

Date

Ismael Pagán Trinidad, M. Sc.
Chair of Civil Engineering and Surveying Department

Date

Abstract

The Commonwealth of Puerto Rico has over 2200 in-service bridges as part of their inventory and more than 50% of these bridges were constructed over 30 years ago. Seismic design requirements are updated frequently due to research and innovations, and bridges are essential structures in the transportation systems that must be designed to withstand seismic events. Because of this, the seismic analysis of bridges designed and constructed at a time when seismic design provisions were insufficient according to current standards should be considered as a required step to determine their performance and capacity to withstand lateral loads during seismic events. In this study, a detailed seismic analysis was performed on Bridge No. 2001 in Highway PR-22 over Bayamón River & Rio Hondo Channel in Bayamón, Puerto Rico. The seismic analysis of this bridge was completed following the Component Capacity/Component Demand Ratio (C/D Ratio) methodology of the FHWA publication entitled *Seismic Retrofitting Manual for Highway Bridges*. C/D ratios were determined for various bridge components and it was found that some of these bridge components are in need of possible retrofitting. Bridge components in need of retrofitting include: hinge connections, shear keys, piers, pile caps, piled foundations and soils. Retrofitting measures for the strengthening of these bridge components were presented, as part of this study, to improve their seismic performance as well as the seismic performance of the bridge.

Resumen

El Estado Libre Asociado de Puerto Rico cuenta con sobre 2200 puentes en servicio actualmente como parte de su inventario y más del 50% de estos fueron construidos sobre 30 años atrás. Como sabemos, los requisitos de diseño sísmico son actualizados continuamente como consecuencia de las investigaciones e innovaciones y los puentes son estructuras esenciales dentro de los sistemas de transportación que deben ser diseñados para resistir cargas sísmicas. Por tal razón se considera el análisis sísmico de aquellos puentes que pudieran no estar en cumplimiento con los requisitos sísmicos actuales como un paso necesario para evaluar su comportamiento y capacidad para resistir cargas laterales durante eventos sísmicos. En este estudio se realizó un análisis sísmico detallado para el Puente No. 2001, construido a mediados de los años 70, en la Autopista PR – 22 sobre el Río Bayamón y el Canal de Río Hondo en Bayamón, Puerto Rico. El análisis sísmico se llevó a cabo siguiendo el método Capacidad/Demanda de la publicación titulada *“Seismic Retrofitting Manual for Highway Bridges”* de la Autoridad Federal de Carreteras. La razón Capacidad/Demanda se determinó para varios componentes del puente y se concluyó que varios de estos componentes requieren ser rehabilitados. Entre los componentes del puente que requieren ser rehabilitados se encuentran: las conexiones articuladas entre tramos, dientes de cortante, columnas, pilastras, fundaciones profundas y los suelos. Varias medidas de rehabilitación para reforzar los componentes del puente fueron presentadas como parte de este estudio con el propósito de mejorar el desempeño sísmico de los componentes así como el desempeño sísmico del puente.

Dedicated to my family...

My mother: María L. Acosta

My sister: Aimee Silvestry

And

To the memory of my father:

Luis A. Silvestry

Acknowledgements

First of all, I would like to thank God Almighty for the completion of this work. I thank God for the wisdom, strength, and perseverance He bestowed on me during the completion of this thesis.

I would like to express my deepest gratitude to Dr. Manuel Coll, Bridge Engineer with the Puerto Rico Highway and Transportation Authority (PRHTA) and Dr. Jeffrey Ger, Bridge Engineer with the Federal Highway Administration (FHWA) in Florida and Puerto Rico, who expertly assisted me through the completion of this thesis. The vast knowledge and expertise they shared with me were very useful to understand complex concepts to apply to my thesis. Both are more than advisors to me, they are very good friends and role models.

I would like to express my sincere appreciation to Dr. Ricardo López Rodríguez and Dr. José Martínez Cruzado, Faculty members at the University of Puerto Rico at Mayagüez, for being part of my graduate committee. They provided unconditional guidance and spent much time to review this manuscript.

I would like to thank Dr. Ricardo Ramos, Faculty member of the Geotechnical Department at the University of Puerto Rico at Mayagüez, for not only sharing his knowledge and expertise in the geotechnical matter, but also important resources as the computer program GROUP7, used during the completion of this project.

I also want to thank to the administrative staff, Myriam Hernández from the Civil Engineering Department for the unconditional help and assistance with the administrative affairs.

Finally, I want to thank my family and friends, from deep inside my heart, for their prayers, love and full support because without them, the completion of this thesis would not have been possible at all. Very special thanks to my father, who passed away while the thesis writing was in progress, thanks for being my biggest motivation to achieve this goal.

Table of Contents

Abstract	ii
Resumen.....	iii
Dedication	iv
Acknowledgements	v
Table of Contents.....	vi
List of Figures.....	viii
List of Tables	x
Unit's Abbreviations.....	xii
CHAPTER I: Introduction	1
1.1 Problem Statement.....	1
1.2 Justification.....	2
1.3 Objective	3
1.4 Bridge Description.....	4
1.5 Seismic Analysis Methodology	11
1.5.1 Introduction	11
1.5.2 Bridge Analytical Model.....	12
1.5.3 Spectral Analysis Model.....	13
1.5.4 Load Combinations.....	14
1.5.5 Procedure for C/D Ratios Calculation	14
1.6 Project Organization	19
1.6.1 Development of the Bridge Analytical Model.....	19
1.6.2 Bridge Analysis and C/D Ratios Determination	19
1.6.3 Retrofitting Measures.....	19
CHAPTER II: Development of the Analytical Model	20
2.1 Introduction	20
2.2 Bridge Analytical Model.....	20
2.3 Bridge Loads	27
2.4 Piled Foundation Model.....	30
2.5 Seismic Spectral Analysis.....	40
CHAPTER III: Bridge Analysis and C/D Ratios Determination	43
3.1 Introduction	43
3.2 C/D Ratios for Reinforced Concrete Columns, Walls and Footings	43
3.2.1 Piers.....	43
3.2.2 Foundation.....	51
3.2.3 Pile Cap.....	57

3.2.3.1 Flexure.....	57
3.2.3.2 Punching Shear	59
3.3 C/D Ratios for Anchorage of Longitudinal Reinforcement.....	61
3.4 Splices of Longitudinal Reinforcement.....	63
3.5 C/D Ratios for Column Shear.....	65
3.5.1 Strong Direction Analysis.....	65
3.5.2 Weak Direction Analysis	66
3.6 Force C/D Ratios.....	67
3.6.1 Transverse Forces.....	68
3.6.2 Vertical Forces.....	69
3.6.3 Axial Forces	71
3.7 Displacement C/D Ratios	72
3.8 C/D Ratios for Abutments.....	73
3.9 C/D Ratios for Soil Liquefaction	74
CHAPTER IV: Retrofitting Measures	78
4.1 Introduction	78
4.2 Cantilever Connection Strengthening	78
4.2.1 Hinge Connection.....	78
4.2.2 Shear keys	80
4.3 Diaphragm Strengthening	81
4.4 Substructure Strengthening.....	82
4.4.1 Piers.....	82
4.4.2 Pile Cap and Piled Foundation	83
4.5 Ground Improvement.....	94
4.5.1 Compaction Grouting.....	94
4.5.2 Permeation Grouting	95
4.5.3 Jet Grouting.....	96
4.5.4 In Situ Soil Mixing.....	96
CHAPTER V: Conclusions and Recommendations	98
5.1 Conclusions.....	98
5.2 Recommendations	101
References	102
APPENDIX A: Seismic Demand Loads on Piles	103

List of Figures

Figure 1. 1. Collapsed bridge in I-5, SR-14 Overpass: San Fernando earthquake	1
Figure 1. 2. Damaged bridge in San Francisco, CA: Loma Prieta earthquake	2
Figure 1. 3. Bridge location	4
Figure 1. 4. Bridge No. 2001, highway PR-22, Bayamon, PR.	5
Figure 1. 5. Elevation view of bridge No. 2001.....	5
Figure 1. 6. Bridge components.	6
Figure 1. 7. Cross section view of bridge superstructure.....	6
Figure 1. 8. Piers cross-section view.....	7
Figure 1. 9. Piers elevation view (see dimensions in Table 1.1).	7
Figure 1. 10. Reinforcement details for piers 2 and 3.	8
Figure 1. 11. Reinforcement details for piers 1, 4, and 5.....	8
Figure 1. 12. Plan view of piles configuration for piers.	9
Figure 1. 13. Piles cross section and reinforcement details.....	10
Figure 2. 1. Bridge analytical mode.	21
Figure 2. 2. Stress zone overlapping for group of piles.....	30
Figure 2. 3. Boring logs: Piers 1, 2, 3, and 4.....	32
Figure 2. 4. Boring logs: Pier 5 and Abutments.....	32
Figure 2. 5. Group7: Pile configuration requirements.....	33
Figure 2. 6. Pile cap principal axes and arbitrary lodas application.....	39
Figure 2. 7. Stiffness matrix for piled foundation.....	40
Figure 3. 1. Interaction diagram for Pier 1 about X axis.....	46
Figure 3. 2. Interaction diagram for Pier 1 about Y axis.....	46
Figure 3. 3. Interaction diagram for Piers 2 and 3 about X axis.	47
Figure 3. 4. Interaction diagram for Piers 2 and 3 about Y axis.	47
Figure 3. 5. Interaction diagram for Piers 4 and 5 about X axis.	48
Figure 3. 6. Interaction diagram for Piers 2 and 3 about X axis.	48
Figure 3. 7. Plastic hinging analysis at pier–superstructure connection.....	50
Figure 3. 8. Cross-section properties and reinforcement details for superstructure.....	51
Figure 3. 9. Foundation analysis: West abutment.....	53
Figure 3. 10. Foundation analysis: Pier 1.....	54
Figure 3. 11. Foundation analysis: Pier 2.....	54
Figure 3. 12. Foundation analysis: Pier 3.....	55
Figure 3. 13. Foundation analysis: Pier 4.....	55
Figure 3. 14. Foundation analysis: Pier 5.....	56
Figure 3. 15. Foundation analysis: East abutment.....	56
Figure 3. 16. Plan view of pier's pile cap and pile configuration.....	57
Figure 3. 17. Elevation view for pier's pile cap and piles.....	58
Figure 3. 18. Anchorage of longitudinal reinforcement.....	61
Figure 3. 19. Elevation view for hinge beams and shear key.....	68
Figure 3. 20. Hinge beam location.....	70
Figure 3. 21. Cross-section view of the hinge beam.	71
Figure 3. 22. Modified penetration resistance.....	76
Figure 3. 23. Relationship between C_N and σ'	76

Figure 4. 1. Proposed steel section for hinge connection retrofitting.....	79
Figure 4. 2. Side view of the proposed hinge connection retrofitting.....	79
Figure 4. 3. Cross-section view of the proposed retrofitting measure for shear keys.	80
Figure 4. 4. Plan view of the proposed retrofitting measure for shear keys.....	81
Figure 4. 5. Diaphragm strengthening.	81
Figure 4. 6. Piers strengthening, plan view.....	82
Figure 4. 7. Pile caps and pile foundations strengthening, plan view.....	83
Figure 4. 8. Pile cap strengthening.	84
Figure 4. 9. Piled foundations strengthening.	84
Figure 4. 10. Cross-section view and reinforcement for new piles.....	85
Figure 4. 11. Piled foundation retrofitting, existing piles analysis (Pier 1).....	86
Figure 4. 12. Piled foundation retrofitting, new piles analysis (Pier 1).	86
Figure 4. 13. Piled foundation retrofitting, analysis for new piles only (Pier 1).....	87
Figure 4. 14. Piled foundation retrofitting, existing piles analysis (Pier 2).....	87
Figure 4. 15. Piled foundation retrofitting, new piles analysis (Pier 2).	88
Figure 4. 16. Piled foundation retrofitting, analysis for new piles only (Pier 2).....	88
Figure 4. 17. Piled foundation retrofitting, existing piles analysis (Pier 3).....	89
Figure 4. 18. Piled foundation retrofitting, new piles analysis (Pier 2).	89
Figure 4. 19. Piled foundation retrofitting, existing piles analysis (Pier 5).....	90
Figure 4. 20. Piled foundation retrofitting, new piles analysis (Pier 5).	90
Figure 4. 21. Piled foundation retrofitting, analysis for new piles only (Pier 3).....	91
Figure 4. 22. Piled foundation retrofitting, existing piles analysis (East Abutment).	91
Figure 4. 23. Piled foundation retrofitting, new piles analysis (East Abutment).....	92
Figure 4. 24. Piled foundation retrofitting, analysis for new piles only (East Abutment).....	92
Figure 4. 25. Piled foundation retrofitting, existing piles analysis (West Abutment).....	93
Figure 4. 26. Piled foundation retrofitting, new piles analysis (West Abutment).....	93
Figure 4. 27. Piled foundation retrofitting, analysis for new piles only (West Abutment).....	94
Figure 4. 28. Compaction grouting process (Andrus and Chung, 1995).....	95
Figure 4. 29. Permeation grouting process (Andrus and Chung, 1995)	95
Figure 4. 30. Jet grouting process (Baez, 1996).	96
Figure 4. 31. In situ soil mixing technique (Andrus and Chung, 1995).....	97

List of Tables

Table 1. 1. Pier dimensions and average pile length per pier	8
Table 1. 2. Material properties for bridge elements.....	10
Table 1. 3. Seismic analysis methods included in the SRMHB	11
Table 1. 4. Site class definition	13
Table 1. 5. Summary of bridge components to be analyzed with Method C.	15
Table 1. 6. Procedure for the evaluation of piers and footings.....	15
Table 1. 7. Procedure for the evaluation of anchorage for longitudinal reinforcement.....	16
Table 1. 8. Procedure for the evaluation of splice length for longitudinal reinforcement.	17
Table 1. 9. Procedure for the evaluation of shear in columns.....	18
Table 2. 1. Cross-section properties: First span.	21
Table 2. 2. Cross-section properties: Second span.....	22
Table 2. 4. Cross-section properties: Third span.....	23
Table 2. 6. Cross-section properties: Fourth span.	24
Table 2. 8. Cross-section properties: Fifth span.....	25
Table 2. 10. Cross-section properties: Sixth span.	26
Table 2. 11. Piers cross-section properties.....	26
Table 2. 12. Abutment cross-section properties.....	26
Table 2. 13. Pile cross-section properties.....	27
Table 2. 14. Loads due to superstructure, parapets and asphalt overlay.....	27
Table 2. 15. Pier loads.....	29
Table 2. 16. Abutment loads.....	29
Table 2. 17. Pile cap loads.....	30
Table 2. 18. Soil parameters for granular soils.....	31
Table 2. 19. Soil parameters for cohesive soils.....	31
Table 2. 20. Piles configuration: Piers 1, 4 and 5, first row.	33
Table 2. 21. Piles configuration: Piers 1, 4 and 5, second row.	34
Table 2. 22. Piles configuration: Piers 1, 4 and 5, third row.	34
Table 2. 23. Piles configuration: Piers 1, 4 and 5, fourth row.....	35
Table 2. 24. Piles configuration: Piers 1, 4 and 5, fifth row.	35
Table 2. 25. Piles configuration: Piers 2 and 3, first row.....	36
Table 2. 26. Piles configuration: Piers 2 and 3, second row.....	36
Table 2. 27. Piles configuration: Piers 2 and 3, third row.....	37
Table 2. 28. Piles configuration: Piers 2 and 3, fourth row.	37
Table 2. 29. Piles configuration: Piers 2 and 3, fifth row.....	38
Table 2. 30. Piles configuration: Piers 2 and 3, sixth row.	38
Table 2. 31. Equivalent stiffness for piled foundation.....	40
Table 2. 32. Site coefficient (F_a) in short period acceleration.....	41
Table 2. 33. Site coefficient (F_v) in long period acceleration.	42
Table 2. 34. Seismic zone and seismic design category	42
Table 3. 1. Biaxial flexure analysis: Top of Piers.....	49
Table 3. 2. Biaxial flexure analysis: Bottom of Piers.....	50
Table 3. 3. Plastic hinge location analysis.....	51
Table 3. 4. Flexural analysis at pile cap.....	59

Table 3. 5. Punching shear analysis at pile cap.....	60
Table 3. 6. Anchorage of longitudinal reinforcement: Top of Piers.	63
Table 3. 7. Anchorage of longitudinal reinforcement: Bottom of piers.....	63
Table 3. 8. Splices of longitudinal reinforcement: Bottom of Piers.....	64
Table 3. 9. Splices of longitudinal reinforcement: Top of piers.	65
Table 3. 10. Column shear C/D ratios: Bottom of Piers.	66
Table 3. 11. Column shear C/D ratios: Top of piers, weak direction.....	67
Table 3. 12. Column shear C/D ratios: Bottom of piers, weak direction.....	67
Table 3. 13. Transverse shear C/D ratios.	69
Table 3. 14. Vertical shear C/D ratios.....	71
Table 3. 15. Axial forces C/D ratios.	72
Table 3. 16. Displacement C/D ratios.....	73
Table 3. 17. Abutments C/D ratios.	74
Table 3. 18. Liquefaction C/D ratios: M = 6%.	77
Table 3. 19. Liquefaction C/D ratios: M = 7%.	77
Table 3. 20. Liquefaction C/D ratios: M = 8%.	77
Table 4. 1. Piled foundation retrofitting summary.....	85
Table A. 1. Piles reactions: East Abutment.....	103
Table A. 2. Piles reactions: West Abutment.	103
Table A. 3. Piles reactions: Pier 1.	104
Table A. 4. Pile reactions: Pier 2.	106
Table A. 5. Piles reactions: Pier 3.	109
Table A. 6. Piles reactions: Pier 4.	111
Table A. 7. Piles reactions: Pier 5.	114

Unit's Abbreviations

kN = kilonewtons.

kPa = kilopascal.

ksf = kips per square foot.

m = meters.

m² = square meters.

m³ = cubic meters.

m⁴ = meters to the fourth.

mm² = square millimeters.

MPa = megapascal.

N = newton.

pcf = pound per cubic foot.

pci = pound per cubic inch.

rads = radians.

s² = square seconds.

CHAPTER I: Introduction

1.1 Problem Statement

The seismic evaluation and rehabilitation of older bridges in regions of high seismicity, which were designed prior to the advent of seismic design codes and have not yet been subjected to a severe earthquake, is a matter of growing concern (Harik et al., 1998). San Fernando earthquake (1971, California) was one of the first earthquakes that brought to the public's attention the seismic risks to bridges and elevated structures. This earthquake has been cited as a watershed event in bridge engineering since it demonstrated quite dramatically that the bridge design practices of the time did not guarantee that bridges would perform well during an earthquake, even if the earthquake was of moderate intensity (FHWA, 2006). Figure 1.1 presents a picture of a collapsed bridge as consequence of San Fernando earthquake in 1971.



Figure 1. 1. Collapsed bridge in I-5, SR-14 Overpass: San Fernando earthquake (FHWA 2011).

Years later, Loma Prieta earthquake (1989) and Northridge earthquake (1994) also caused severe damage to transportation infrastructure with the partial collapse of bridges in San Francisco and Los Angeles, California, respectively. Figure 1.2 presents an image of damages caused by Loma Prieta earthquake in 1989. It is known that seismic design requirements are updated frequently due to research and innovations,

and bridges are essential structures in the transportation systems that must be designed to withstand seismic events. Because of this, the seismic analysis of old bridges should be considered as a required step to determine their performance and capacity to withstand lateral loads during seismic events.



Figure 1. 2. Damaged bridge in San Francisco, CA: Loma Prieta earthquake, (FHWA 2011).

1.2 Justification

The Commonwealth of Puerto Rico has over 2200 in-service bridges as part of their inventory. Data provided by the Puerto Rico Highway and Transportation Authority (PRHTA) reveals that more than 50% of their bridges were constructed over 30 years ago. Puerto Rico is located in a seismic zone and most of these bridges may have been designed and constructed at a time when bridge codes had no seismic design provisions, or when these provisions were insufficient according to current standards. It means that bridges in P.R. could be in non-compliance with actual seismic requirements and may suffer severe damage during a seismic event. In this study a seismic analysis will be performed on a bridge constructed during the 70's in one of the main routes of the National Highway System to determine its seismic vulnerability and evaluate possible retrofit measures if necessary

1.3 Objective

The purpose of this study is to perform a detailed seismic analysis for Bridge No. 2001 in Highway PR-22 over Bayamon River & Rio Hondo Channel in Bayamon, Puerto Rico. The Capacity/Demand Ratio (C/D) methodology will be implemented in order to determine the performance of the bridge and its capacity to withstand lateral loads during seismic events. In addition to the seismic analysis, retrofitting alternatives will be presented for this bridge in case it does not meet actual code requirements. The objectives can be summarized as follows:

- Perform a seismic analysis for Bridge No. 2001 using the guidelines of the FHWA publication: Seismic Retrofitting Manual for Highway Bridges.
- Determine the Capacity/Demand ratio for various bridge components in order to evaluate the seismic vulnerability of this bridge to the adverse effects of an earthquake event.
- Present retrofitting measures to improve the seismic performance of the bridge if necessary.

1.4 Bridge Description

Bridge No. 2001 is a 435m length six span reinforced concrete cantilever bridge that goes from Km. 11.6 to Km. 12.0 in highway PR-22, Bayamón, PR. This bridge, constructed during the mid-70's, has four lanes on each direction and carries an approximate average daily traffic of 130,000 vehicles in one of the main routes of the National Highway System. Figures 1.3 and 1.4 present an aerial view of bridge location. The superstructure of this bridge consists of two spine concrete box girder sections. The lengths of the six spans are 42.5m, 92.5m, 100m, 87.5m, 75m and 37.5m. Figures 1.5 and 1.6 present a cross section and elevation view of this cantilever concrete box girder bridge. The interior spans are connected with hinges at the center of each span and the superstructure is supported with five rectangular (hollow) reinforced concrete wall-piers. The connection between the superstructure and substructure (piers) is monolithic. Piers reinforcement (vertical & horizontal) consist of #4 to # 6 bars. Figures 1.7 to 1.10 present the cross section view, elevation view and reinforcement details for wall-piers, while Table 1.1 presents a summary of geometric properties for piers.



Figure 1. 3. Bridge location (Google Earth, 2011).



Figure 1. 4. Bridge No. 2001, highway PR-22, Bayamon, PR (Google Earth, 2011).

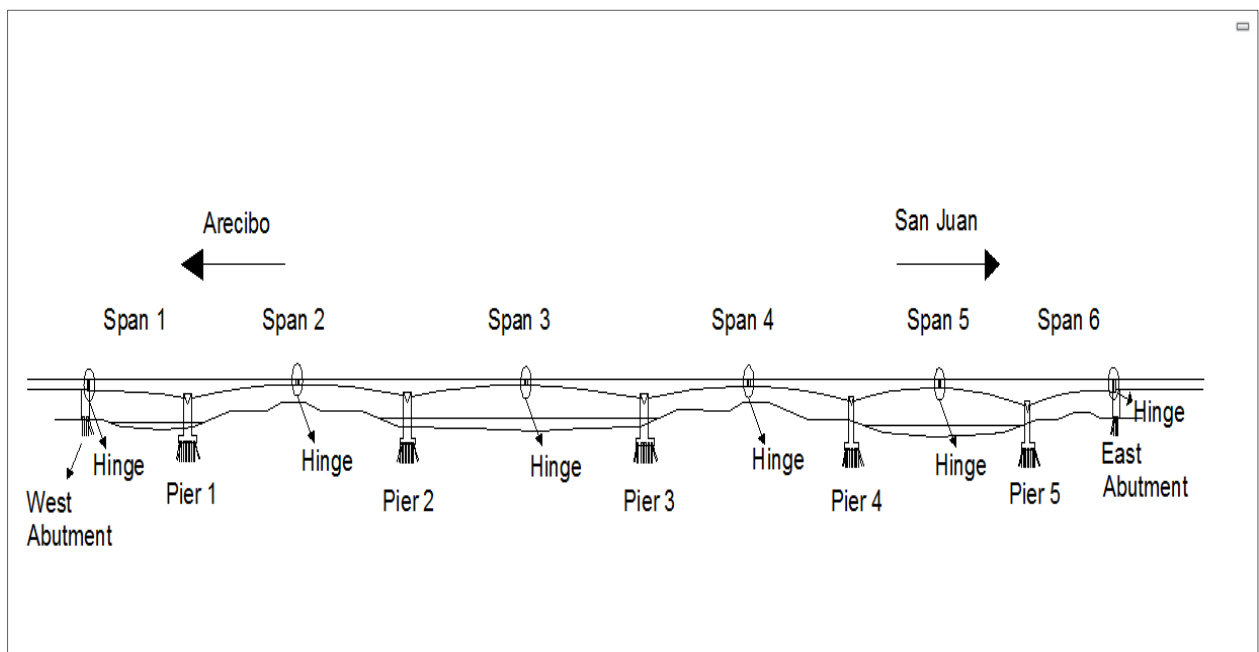


Figure 1. 5. Elevation view of bridge No. 2001.

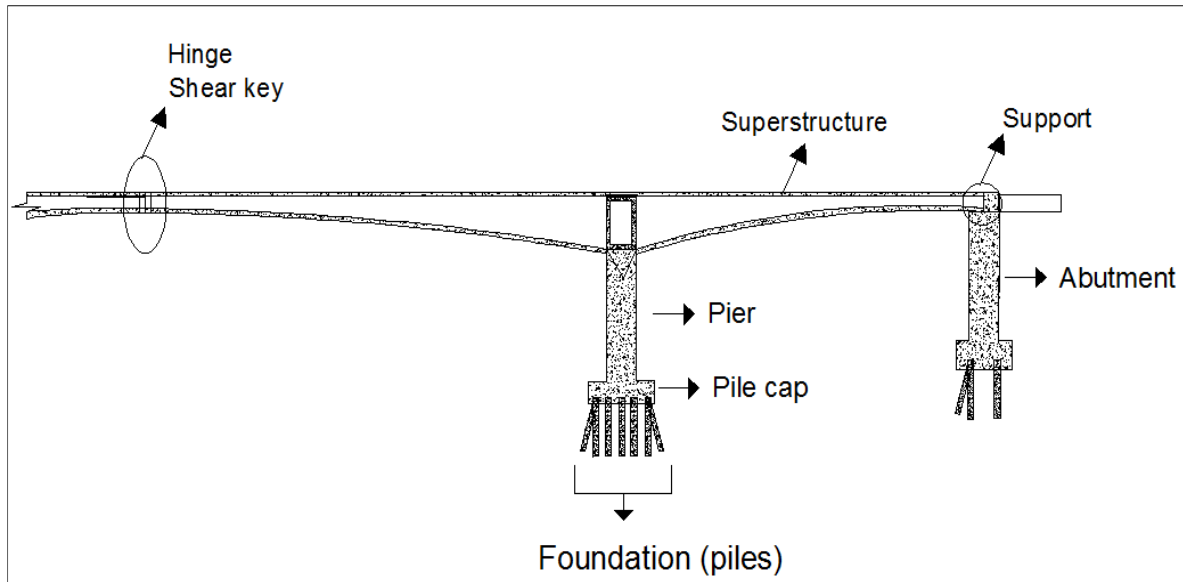


Figure 1. 6. Bridge components.

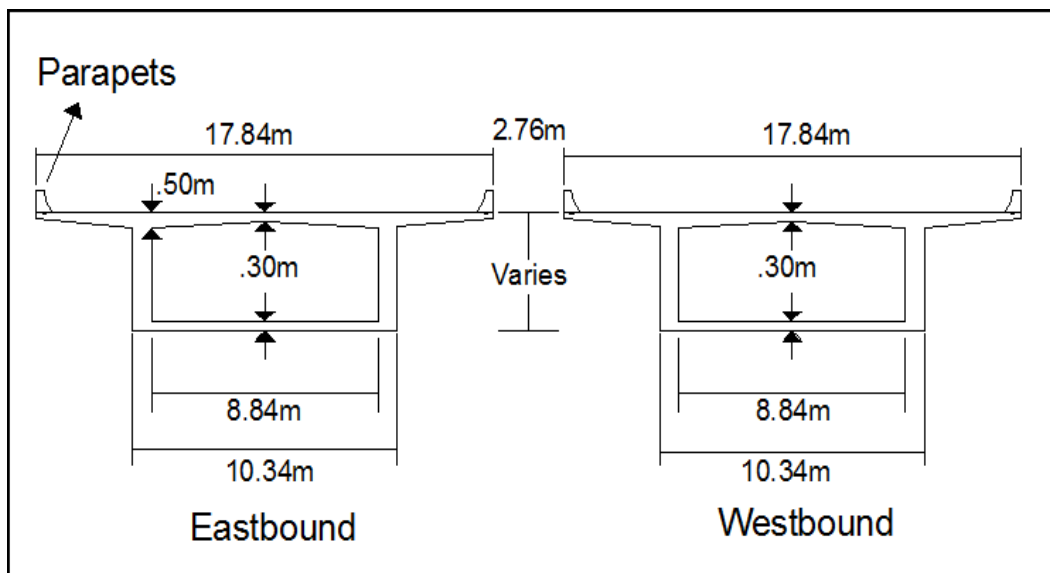


Figure 1. 7. Cross section view of bridge superstructure.

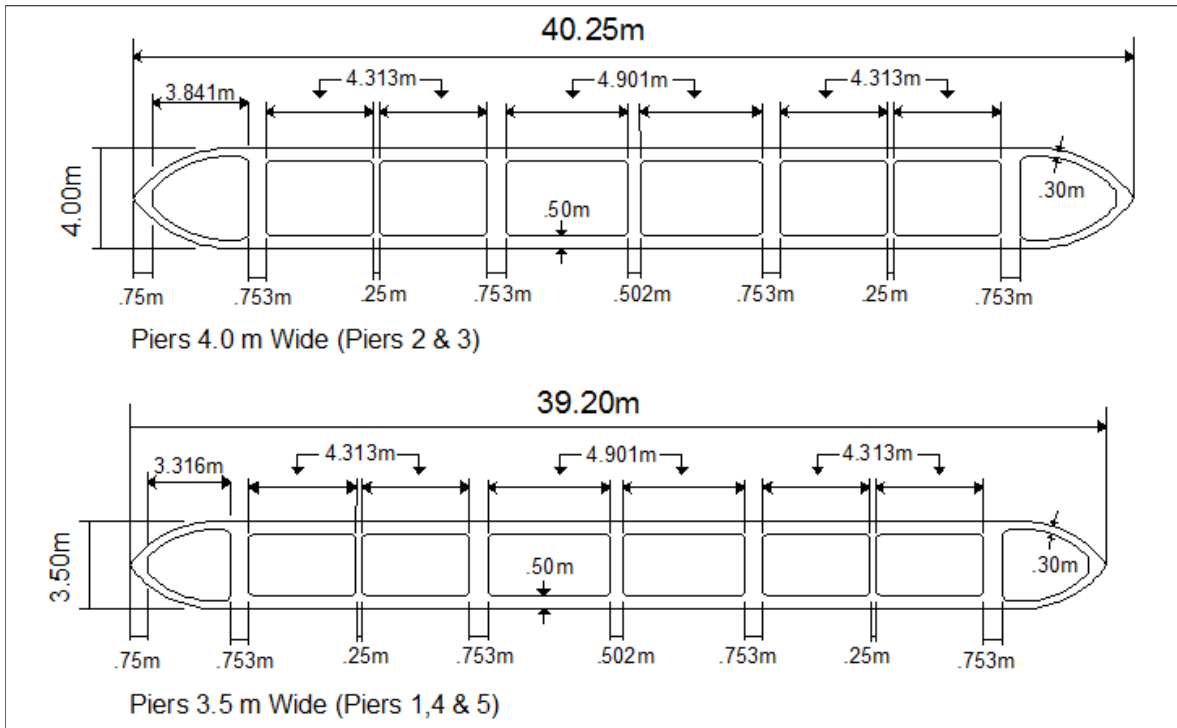


Figure 1. 8. Piers cross-section view.

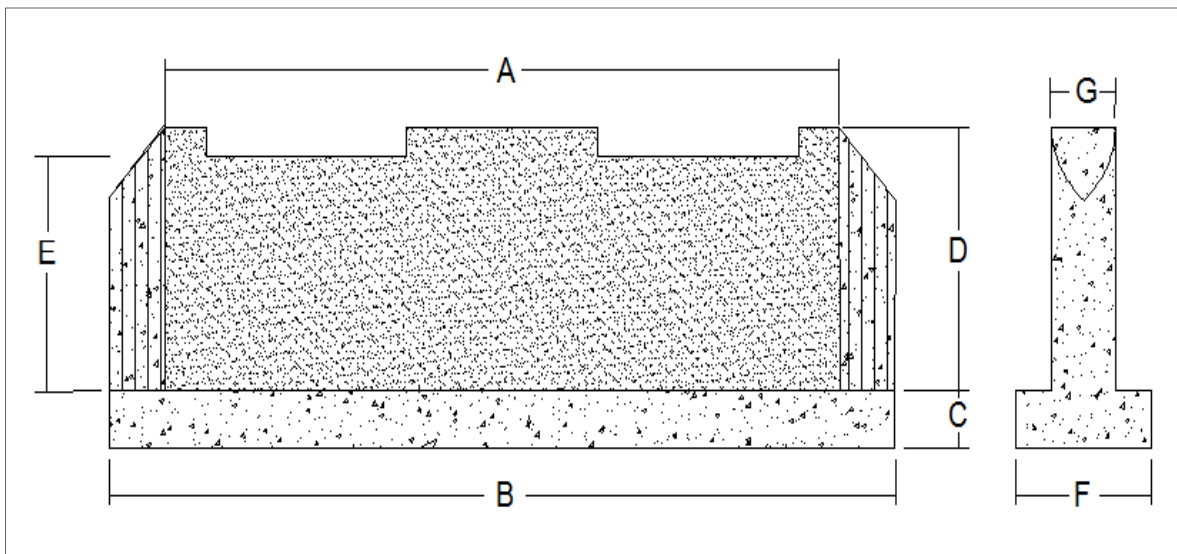


Figure 1. 9. Piers elevation view (see dimensions in Table 1.1).

Table 1. 1. Pier dimensions and average pile length per pier.

Pier Properties								
Pier #	A (m)	B (m)	C (m)	D (m)	E (m)	F (m)	G (m)	Avg. pile length (m)
1	31.06	39.20	2.20	8.74	7.09	5.80	3.50	28.35
2	31.06	40.25	2.20	7.44	5.79	7.15	4.00	22.25
3	31.06	40.25	2.20	8.40	6.75	7.15	4.00	23.47
4	31.06	39.20	2.20	4.08	2.43	5.80	3.50	21.34
5	31.06	39.20	2.20	5.34	3.69	5.80	3.50	25.00

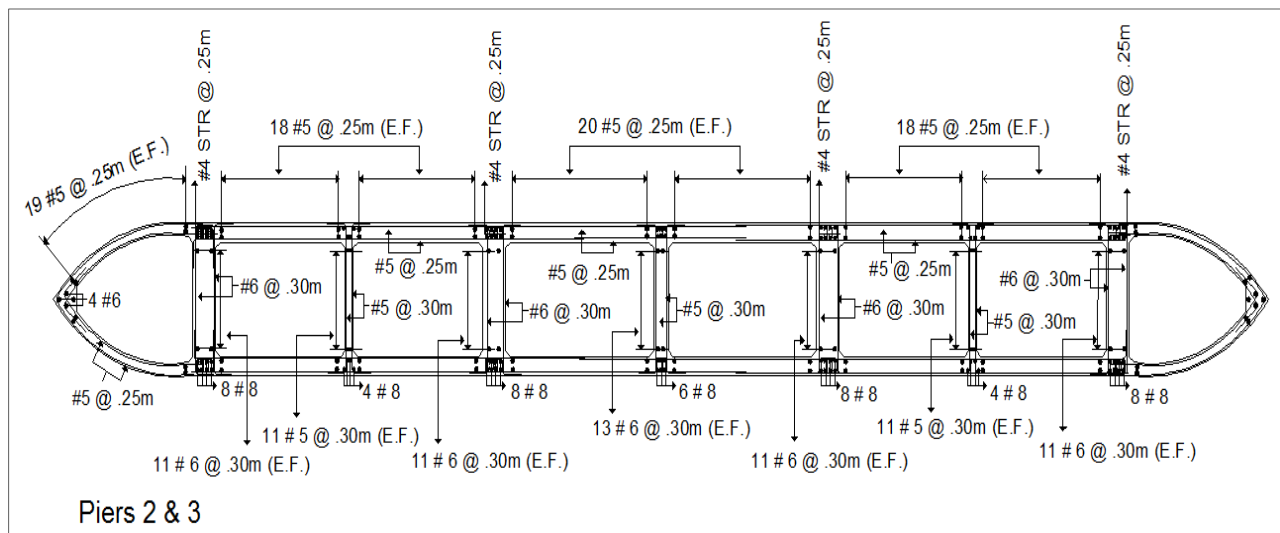


Figure 1. 10. Reinforcement details for piers 2 and 3.

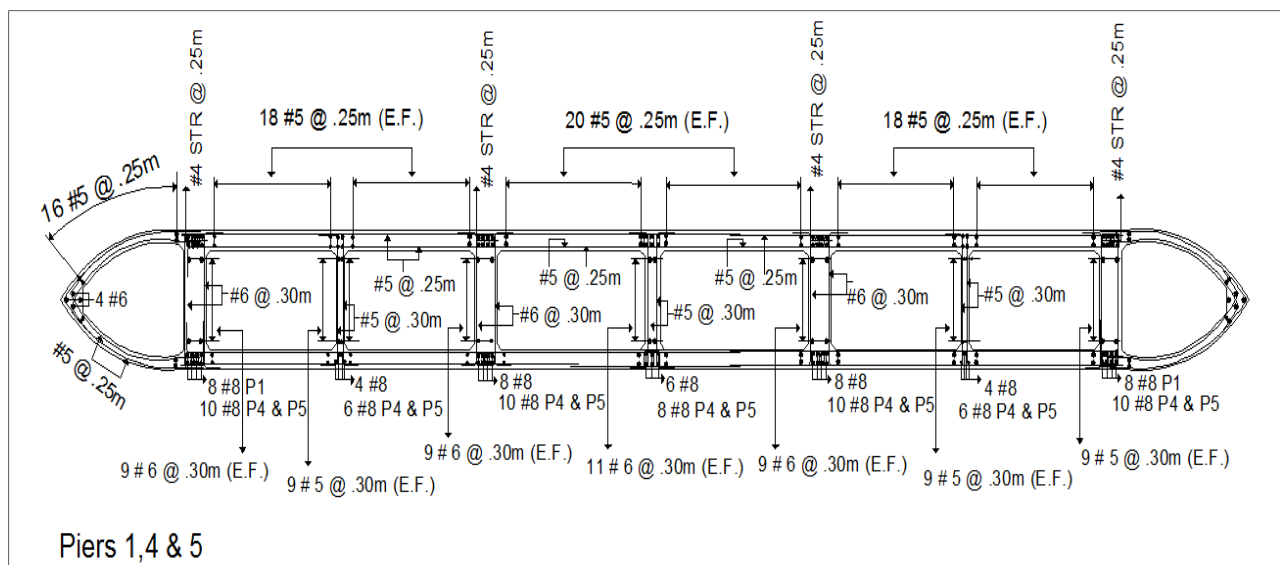


Figure 1. 11. Reinforcement details for piers 1, 4, and 5.

Bridge piers and abutments are founded on deep foundations consisting on vertical and batter (11.3°) reinforced concrete piles. Piers 1, 4 and 5 have a total of 118 piles; 76 inclined and 42 vertical piles. Piers 2 and 4 have a total of 138 piles; 84 inclined and 54 vertical piles. These concrete piles, with .46m (18 in) diameter, have vertical reinforcement consisting of 8 #6 bars and transverse spiral reinforcement consisting of #4 bars. Piles spacing is 1.35m in the transverse direction and 1.20 m in the longitudinal direction. A plan view of the piles configuration can be observed in Figure 1.11. Figure 1.12 presents a cross section and elevation view of the reinforced concrete pile and Table 1.2 presents a summary of the material properties for bridge components.

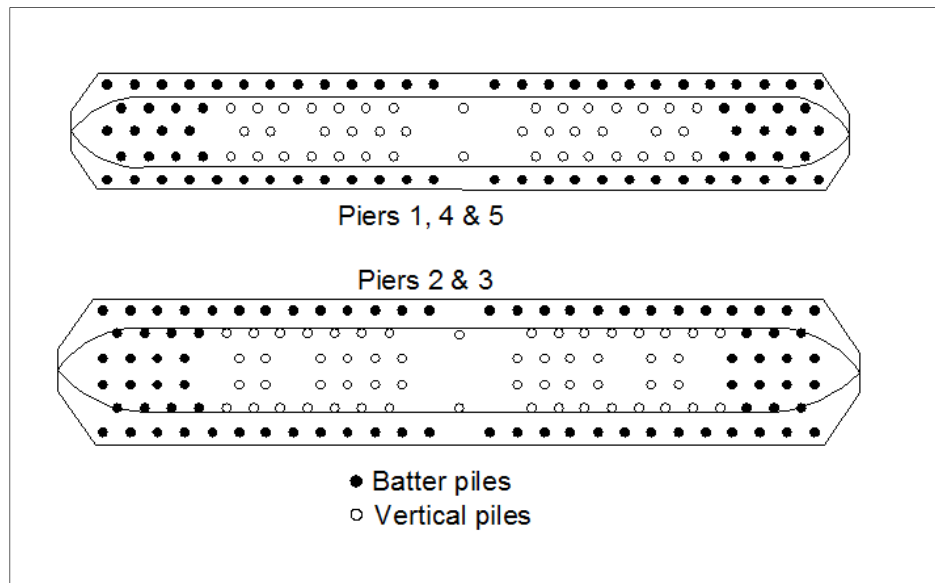


Figure 1. 12. Plan view of piles configuration for piers.

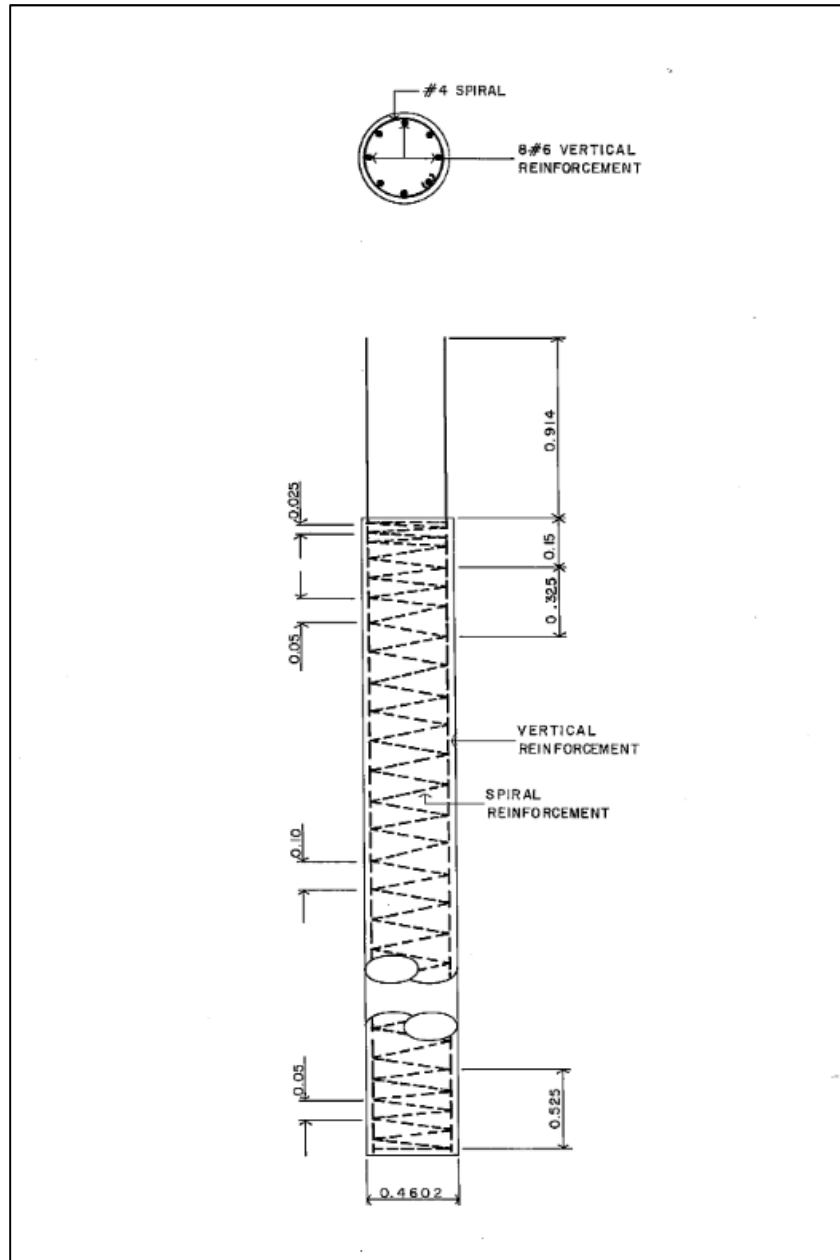


Figure 1. 13. Piles cross section and reinforcement details.

Table 1. 2. Material properties for bridge elements.

Material Properties for bridge elements		
Element	Concrete - f'_c	Steel Reinforcement - f_y
	MPa (ksi)	MPa (ksi)
Box girder	34.47 (5.0)	275.79 (40)
Piers	31.02 (4.5)	
Pile cap	27.57 (4.0)	
Abutments	31.02 (4.5)	
Piles	41.36 (6.0)	

1.5 Seismic Analysis Methodology

1.5.1 Introduction

The methodology to be implemented for the seismic analysis of bridge No. 2001 consists mainly in the FHWA publication entitled *Seismic Retrofitting Manual for Highway Bridges 2006* (SRMHB). The SRMHB presents six different procedures for the seismic evaluation and retrofitting of bridge structures. Table 1.3 presents a summary of each method described in this manual. Method C “Component Capacity/Demand Method” (C/D) will be implemented to complete the seismic analysis of bridge No. 2001. The C/D procedure is based on an elastic modal analysis of the bridge and the estimation of the individual element capacities (Coll, 2003). These C/D ratios provide a percentage of the design earthquake that is likely to cause serious damage to the bridge component and are used to indicate the need for retrofitting. Ratios greater than one indicate sufficient capacity to resist the earthquake demand while ratios less than one indicate components in need of attention and possible retrofitting (FHWA, 2006).

Table 1. 3. Seismic analysis methods included in the SRMHB (FHWA, 2006).

METHOD		CAPACITY ASSESSMENT	DEMAND ANALYSIS	APPLICABILITY		COMMENTS
				SRC-UL ¹	Bridge Type	
A1/A2	Connection and Seat Width Checks	Uses default capacity due to non-seismic loads for connections and seat widths.	Not required	A – D B	All single span bridges. Bridges in low hazard zones.	Hand method, spreadsheet useful.
B	Component Capacity Checks	Uses default capacity due to non-seismic loads for connections, seats, columns and foundations.	Not required	C	Regular bridges, but subject to limitations on $F_v S_1$.	Hand method, spreadsheet useful.
C	Component Capacity/Demand Method	Uses component capacities for connections, seat widths, column details, footings, and liquefaction susceptibility (11 items).	Elastic Methods ² : • ULM • MM • TH	C & D	Regular and irregular bridges that respond almost elastically, such as those in low-to-moderate seismic zones and those with stringent performance criteria.	Calculates C/D ratios for individual components. This is the C/D Method of previous FHWA highway bridge retrofitting manuals. Software required for demand analysis.
D1	Capacity Spectrum Method	Uses bilinear representation of structure capacity for lateral load, subject to restrictions on bridge regularity.	Elastic Methods ² : • ULM	C & D	Regular bridges that behave as single-degree-of-freedom systems and have 'rigid' in-plane superstructures.	Calculates C/D ratios for complete bridge, for specified limit states. Spreadsheet useful.
D2	Structure Capacity/Demand Method	Uses pushover curve from detailed analysis of superstructure, individual piers and foundation limit states.	Elastic Methods ² : • ULM • MM • TH	C & D	Regular and irregular bridges.	Calculates C/D ratios for bridge superstructure, individual piers, and foundations. Also known as <i>Nonlinear Static Procedure</i> or <i>Displacement Capacity Evaluation Method</i> . Software required for demand and capacity analysis.
E	Nonlinear Dynamic Method	Uses component capacities for connections, seat widths, columns and footings.	Inelastic Methods ² • TH	D	Irregular complex bridges, or when site specific ground motions are to be used such as for bridges of major importance.	Most rigorous method, expert skill required. Software essential.
Notes: 1. SRC = Seismic Retrofit Category for upper level earthquake; for the lower level earthquake, the recommended method of evaluation is Method C. 2. ULM = Uniform Load Method; MM = Multi-Mode Spectral Method; TH = Time History Method						

1.5.2 Bridge Analytical Model

In addition to the SRMHB, two computer software programs will be used to perform the analytical modeling of the bridge structure. Computer programs SAP2000 and GROUP7 will be implemented to develop the analytical model of the bridge. Bridge model will be represented with two lines of frame elements for the superstructure and one line of frame elements for bridge wall-piers. Due to the parabolic variation of the spine box girder, each span will be divided in span elements. The first and last spans will be divided in four span elements while the interior spans will be divided in eight elements. Section properties will be calculated at the start/end points of each span element and assigned to the nodes, and then the computer software will be in charge of the variation along each span element. Dead loads due to superstructure (box girder), substructure (piers, pile cap and diaphragms) and superimposed loads (wearing surface and parapets) will be also calculated and assigned to the nodes. The connection between the superstructure and the substructure will be represented with rigid links (body constraints) due to the monolithic construction of this bridge. The connection between bridge piers and piled foundation will be represented with stiffness springs. Computer software GROUP7 will be implemented to model the soil-foundation interaction. Soil profile and soil properties (unit weight (γ), internal friction angle (ϕ), unit strain (ϵ) and soil stiffness (k)) will be provided to the program for the soil modeling. Dimensions of the pile cap will also be provided to the program to take into account the passive pressure of the surrounding soil. Arbitrary loads and moments will be applied to the pile cap within the principal axes. Pile cap displacements, for these arbitrary loads, will be obtained with software GROUP7. These loads and displacements will be combined with Method II – Matrix Coefficient Definition, described in WSDOT 2012, to obtain the springs stiffness. Once analyzed the bridge model, pile cap loads will be distributed to the piles using the same computer program GROUP7.

1.5.3 Spectral Analysis Model

According to the AASHTO 2007, Bridge Design Specifications, bridge No. 2001 can be classified as a regular structure. It means that a Multimode Spectral Analysis method could be implemented to determine the elastic seismic force demands of the structure. Parameters required to generate the response spectrum include: Spectral Acceleration at short period (S_s), Spectral Acceleration at long period (S_1), site class and site coefficients (F_a and F_v). Site class parameter will be determined with the average standard penetration test (SPT) blow count (N). The N value will be calculated using the boring logs of each pier, then, an average N value will be calculated for the overall site. With this value and Table 1.4 an appropriate site class parameter will be defined. Once determined the site class and with the location of the bridge (latitude and longitude), computer program SAP 2000 will be used to determine the remaining parameters.

Table 1. 4. Site class definition (FHWA, 2006).

Site Class	Description
A	Hard rock with measured shear wave velocity, $\bar{v}_s > 1500$ m/sec (5,000 ft/sec)
B	Rock with $760 \text{ m/sec} < \bar{v}_s \leq 1500 \text{ m/sec}$ ($2,500 \text{ ft/sec} < \bar{v}_s \leq 5,000 \text{ ft/sec}$)
C	Very dense soil and soil rock with $360 \text{ m/sec} < \bar{v}_s \leq 760 \text{ m/sec}$ ($1,200 \text{ ft/sec} < \bar{v}_s \leq 2,500 \text{ ft/sec}$) or with either $\bar{N} > 50$ blows/0.30m (50 blows/ft) or $\bar{s}_u > 100$ kPa (2,000 psf)
D	Stiff soil with $180 \text{ m/sec} \leq \bar{v}_s \leq 360 \text{ m/sec}$ ($600 \text{ ft/sec} \leq \bar{v}_s \leq 1,200 \text{ ft/sec}$) or with either $15 \leq \bar{N} \leq 50$ blows/0.30m ($15 \leq \bar{N} \leq 50$ blows/ft) or $50 \text{ kPa} \leq \bar{s}_u \leq 100 \text{ kPa}$ ($1,000 \leq \bar{s}_u \leq 2,000$ psf)
E	Soil profile with $\bar{v}_s < 180$ m/sec (600 ft/sec) or with either $\bar{N} < 15$ blows/0.30m ($\bar{N} < 15$ blows/ft) or $\bar{s}_u < 150$ kPa (1000 psf), or any profile with more than 3 m (10 ft) of soft clay defined as soil with $PI > 20$, $w \geq 40$ percent and $\bar{s}_u < 25$ kPa (500 psf)
F	Soils requiring site-specific evaluations <ol style="list-style-type: none"> 1. Peats or highly organic clays ($H > 3$ m [10 ft] of peat or highly organic clay where H = thickness of soil) 2. Very high plasticity clays ($H > 8$ m [25 ft] with $PI > 75$) 3. Very thick soft/medium stiff clays ($H > 36$ m [120 ft])
Exception: When the soil properties are not known in sufficient detail to determine the site class, site class D may be used. Site classes E or F need not be assumed unless the authority having jurisdiction determines that site classes E or F could be present at the site or in the event that site classes E or F are established by geotechnical data.	

1.5.4 Load Combinations

Load combinations will be as specified in Section 3.10.8 of the AASHTO 2007. It means that elastic force demands will be computed considering the earthquake in two perpendicular directions: longitudinal direction, which means parallel to the traffic flow and transverse direction, which means perpendicular to the traffic flow. Both of these analyses will be combined to generate the two earthquake load combinations:

$$100\% \text{ EL}(x) \pm 40\% \text{ EL}(y) \quad (1 - 1)$$

$$100\% \text{ EL}(y) \pm 40\% \text{ EL}(x) \quad (1 - 2)$$

where:

EL(x) = earthquake load in longitudinal direction, and

EL(y) = earthquake load in transverse direction.

1.5.5 Procedure for C/D Ratios Calculation

As aforementioned, the methodology to be implemented during the seismic analysis of bridge No. 2001 consists on the Component Capacity/Component Demand ratio (Method C) of the *Seismic Retrofitting Manual for Highway Bridges*. Tables 1.5 to 1.9, obtained from the SRMHB, present the bridge components to be evaluated with Method C and summarized flowcharts with procedures to determine the C/D ratios. As noted, Table 1.5 does not include the analysis of the superstructure by itself. The main reason is that Method C focuses on those components that are more vulnerable to damage during the seismic event; connections, bearings, seats, piers, foundations, abutments and soils. Although the performance of a bridge is based on the interaction of all its components, certain bridge components are more vulnerable to damage than others (FHWA, 2006). Damage on the superstructure is expected to occur if there is not enough seat provided or if there is a failure at connections, bearings or piers. However, it is important to verify that plastic hinge occurs first at the pier than at the superstructure. This plastic hinging analysis at the pier-superstructure connection will be considered as part of this study.

Table 1. 5. Summary of bridge components to be analyzed with Method C.

Bridge Components
Superstructure
Support Length
Hinge Connections
Shear Keys
Substructure
Piers
Pile Cap
Deep Foundations
Soils (Liquefaction)
Abutments

Table 1. 6. Procedure for the evaluation of piers and footings (FHWA, 2006).

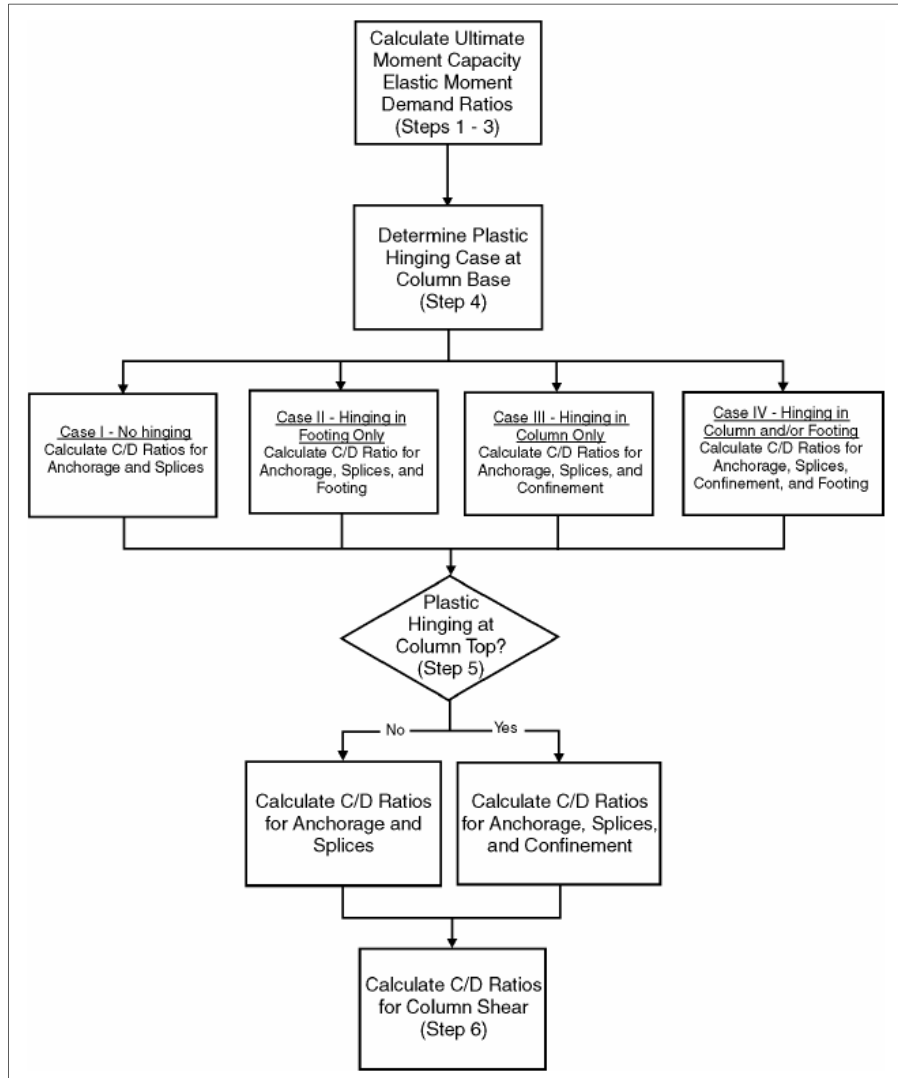


Table 1. 7. Procedure for the evaluation of anchorage for longitudinal reinforcement (FHWA, 2006).

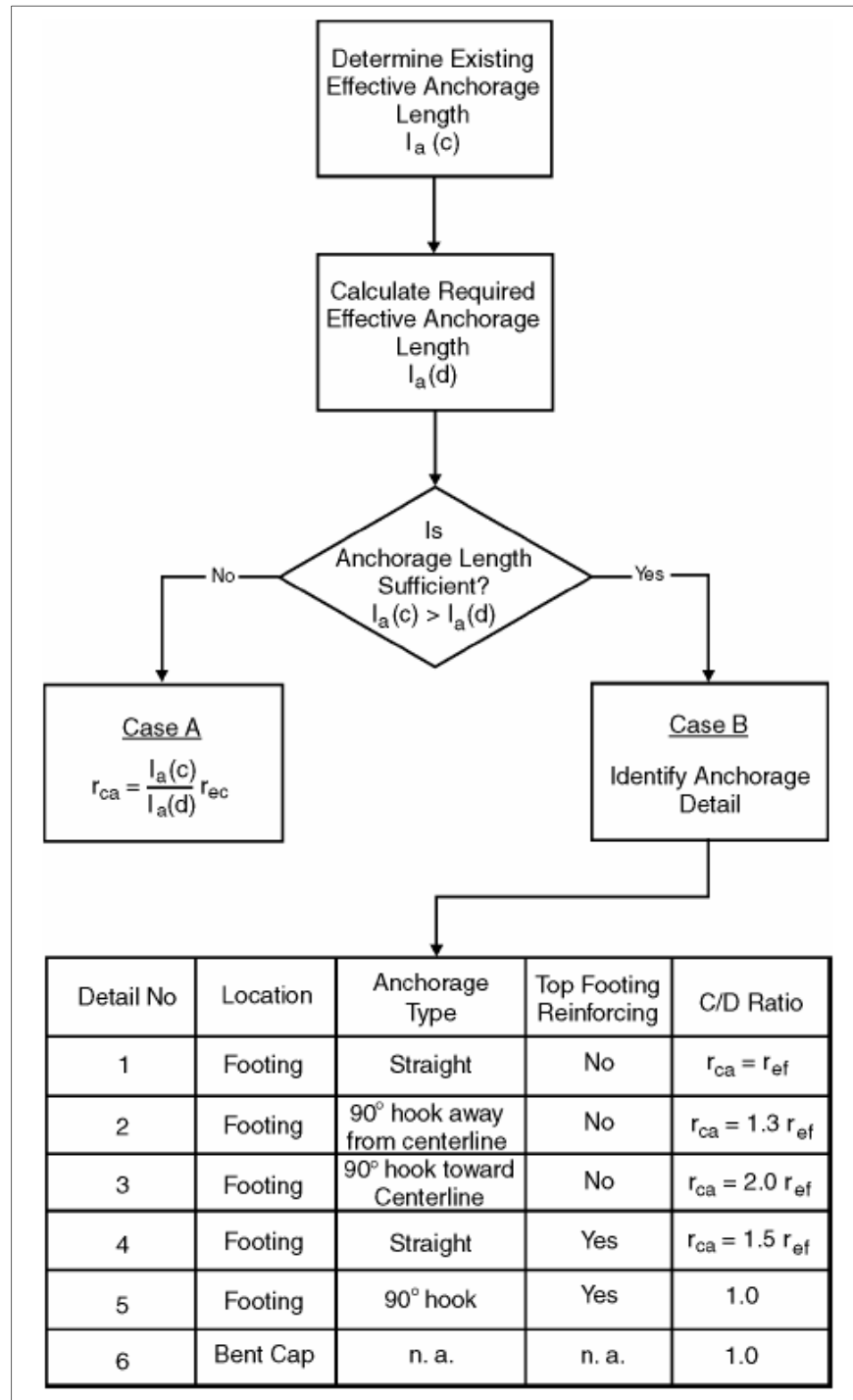


Table 1. 8. Procedure for the evaluation of splice length for longitudinal reinforcement (FHWA, 2006).

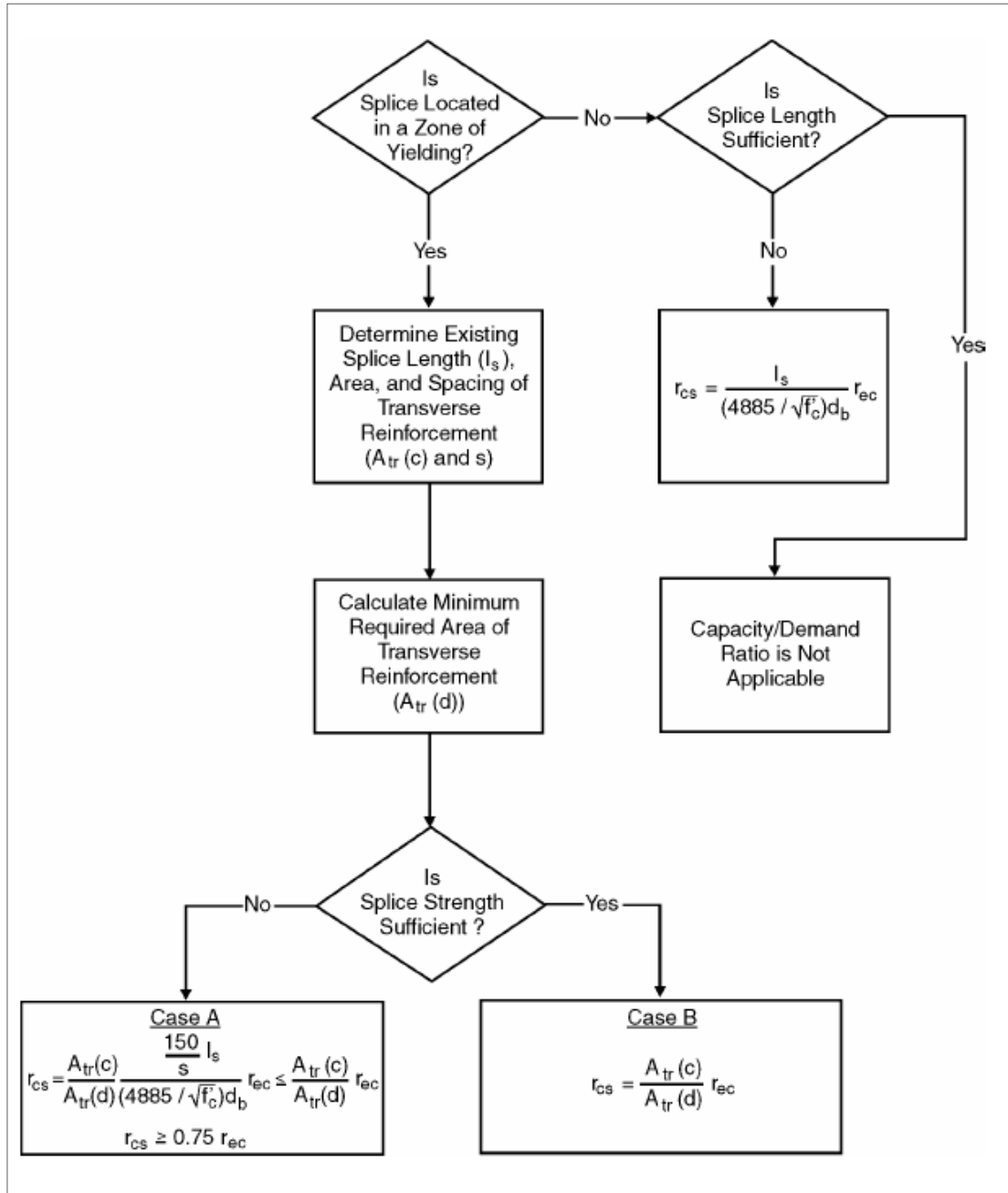
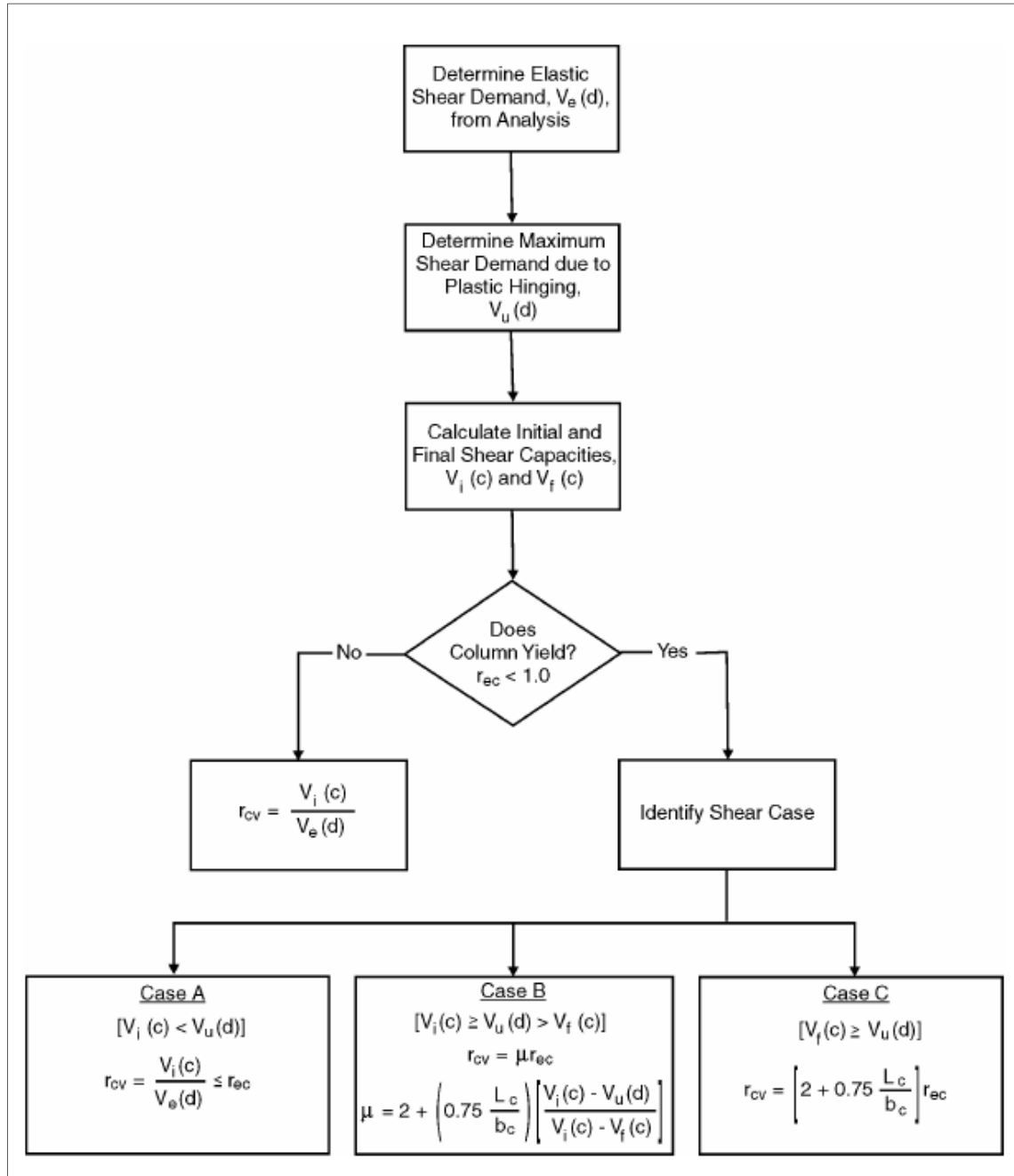


Table 1. 9. Procedure for the evaluation of shear in columns (FHWA, 2006).



1.6 Project Organization

1.6.1 Development of the Bridge Analytical Model

Chapter II presents all the considerations taken into account to develop the analytical model for Bridge No. 2001. It includes bridge geometric properties, determination of dead loads, stiffness springs to represent the pile foundation, and the development of the response spectrum to represent the seismic load.

1.6.2 Bridge Analysis and C/D Ratios Determination

Chapter III present the results obtained after analyzing the bridge with computer program SAP 2000. It includes reactions and displacements due to the load combinations and the distribution of the pile cap loads to the piles. In addition, this chapter present the results obtained after the implementation of the C/D ratio methodology.

1.6.3 Retrofitting Measures

Chapter IV present a summary of the results obtained after the seismic analysis of bridge No.2001. This chapter includes different retrofitting measures to be considered in order to improve the seismic performance of the bridge if it is determined that the bridge is vulnerable.

CHAPTER II: Development of the Analytical Model

2.1 Introduction

The seismic analysis of bridge No. 2001 was performed using two computer software programs: SAP2000 and GROUP7. SAP2000 software was used to generate the multimodal response spectrum and also the analytical model of the bridge. GROUP7 software was implemented to perform the analysis of the piled foundation. Bridge modeling and computers software programs implementation will be discussed further in this chapter.

2.2 Bridge Analytical Model

The analytical model of bridge No. 2001 was developed using computer program SAP2000. This model was represented with frame elements, nodes, body constraints and stiffness springs. The exterior spans of the superstructure were divided in four span elements while interior spans were divided in eight span elements. Wall-type piers and abutments were also represented with frame elements and divided in sub elements. Gross Section properties, areas and inertias, were determined for both sides of each frame element and assigned to the nodes. Due to the monolithic connection between the superstructure and substructure, this connection was represented with body constraints within the analytical model. Figure 2.1 presents a 3D view of the SAP2000 bridge analytical model. Tables 2.1 to 2.13 present a summary of the gross section properties determined for bridge components. These properties include:

- L = span length (m),
- A = area (m^2),
- I_{33} = moment of inertia about Y axis (m^4),
- I_{22} = moment of inertia about X axis (m^4), and
- J = torsional constant (m^4).

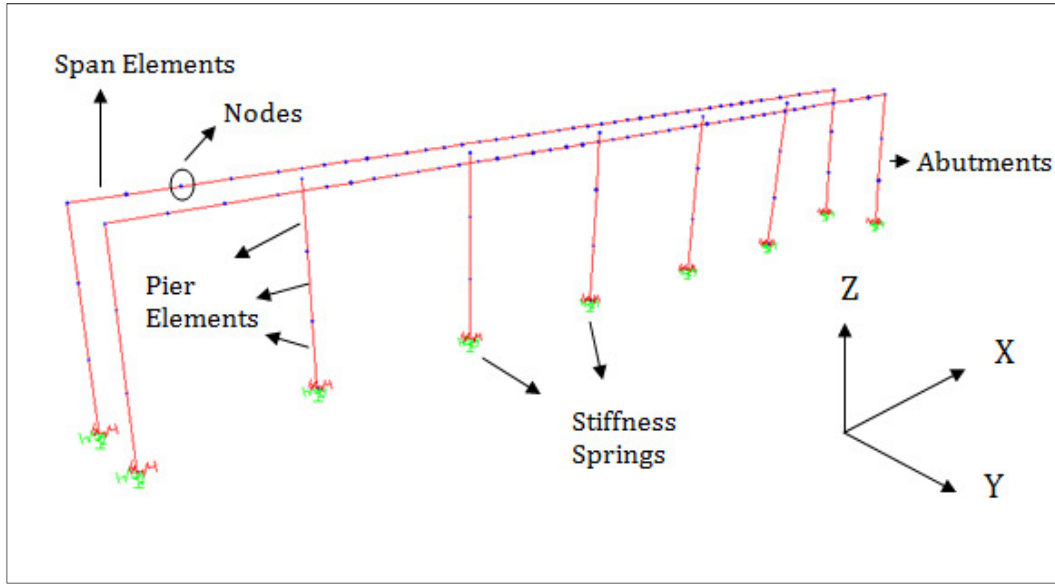


Figure 2. 1. Bridge analytical mode

Table 2. 1. Cross-section properties: First span.

Span # 1, L = 42.5 m		
Property	Left Side	Right Side
Element # 1, L = 15.50 m		
Node #	1	2
A (m ²)	11.81	12.17
J (m ⁴)	15.38	22.07
I 33 (m ⁴)	5.62	8.38
I 22 (m ⁴)	232.29	244.38
Element # 2, L = 12.0 m		
Node #	2	3
A (m ²)	12.17	13.01
J (m ⁴)	22.07	40.78
I 33 (m ⁴)	8.38	16.74
I 22 (m ⁴)	244.38	270.53
Element # 3, L = 8.0 m		
Node #	3	4
A (m ²)	13.01	14.02
J (m ⁴)	40.78	64.67
I 33 (m ⁴)	16.74	28.63
I 22 (m ⁴)	270.5	296.6
Element # 4, L = 7.0 m		
Node #	4	5
A (m ²)	14.02	14.73
J (m ⁴)	64.67	99.49
I 33 (m ⁴)	28.63	49.28
I 22 (m ⁴)	296.56	333.20

Table 2. 2. Cross-section properties: Second span.

Span # 2, L = 92.5 m		
Property	Left Side	Right Side
Element # 1, L = 5.0 m		
Node #	5	6
A (m ²)	14.73	14.17
J (m ⁴)	99.49	72.46
I 33 (m ⁴)	49.28	32.76
I 22 (m ⁴)	333.20	303.93
Element # 2, L = 8.0 m		
Node #	6	7
A (m ²)	14.17	13.20
J (m ⁴)	72.46	45.77
I 33 (m ⁴)	32.76	19.13
I 22 (m ⁴)	303.93	276.52
Element # 3, L = 12.0 m		
Node #	7	8
A (m ²)	13.20	12.26
J (m ⁴)	45.77	24.11
I 33 (m ⁴)	19.13	9.25
I 22 (m ⁴)	276.52	247.72
Element # 4, L = 17.5 m		
Node #	8	9
A (m ²)	12.26	11.93
J (m ⁴)	24.11	15.38
I 33 (m ⁴)	9.25	5.62
I 22 (m ⁴)	247.72	232.29
Element # 5, L = 23.0 m		
Node #	9	10
A (m ²)	11.93	12.57
J (m ⁴)	15.38	31.62
I 33 (m ⁴)	5.62	12.54
I 22 (m ⁴)	232.29	258.78
Element # 6, L = 12.0 m		
Node #	10	11
A (m ²)	12.57	13.84
J (m ⁴)	31.62	49.98
I 33 (m ⁴)	12.54	21.20
I 22 (m ⁴)	258.78	281.47
Element # 7, L = 8.0 m		
Node #	11	12
A (m ²)	13.84	15.09
J (m ⁴)	49.98	99.19
I 33 (m ⁴)	21.20	47.78
I 22 (m ⁴)	281.47	326.74
Element # 8, L = 7.0 m		
Node #	12	13
A (m ²)	15.09	15.85
J (m ⁴)	99.19	148.84
I 33 (m ⁴)	47.78	81.34
I 22 (m ⁴)	326.74	371.66

Table 2. 3. Cross-section properties: Third span.

Span # 3, L = 100.0 m		
Property	Left Side	Right Side
Element # 1, L = 9.0 m		
Node #	13	14
A (m ²)	15.85	14.88
J (m ⁴)	148.84	88.35
I 33 (m ⁴)	81.34	41.55
I 22 (m ⁴)	371.66	317.99
Element # 2, L = 8.0 m		
Node #	14	15
A (m ²)	14.88	13.89
J (m ⁴)	88.35	56.18
I 33 (m ⁴)	41.55	24.29
I 22 (m ⁴)	317.99	288.15
Element # 3, L = 12.0 m		
Node #	15	16
A (m ²)	13.89	13.46
J (m ⁴)	56.18	28.74
I 33 (m ⁴)	24.29	11.26
I 22 (m ⁴)	288.15	254.75
Element # 4, L = 21.0 m		
Node #	16	17
A (m ²)	13.46	12.20
J (m ⁴)	28.74	15.38
I 33 (m ⁴)	11.26	5.62
I 22 (m ⁴)	254.75	232.29
Element # 5, L = 23.0 m		
Node #	17	18
A (m ²)	12.20	12.57
J (m ⁴)	15.38	31.62
I 33 (m ⁴)	5.62	12.54
I 22 (m ⁴)	232.29	258.78
Element # 6, L = 12.0 m		
Node #	18	19
A (m ²)	12.57	13.84
J (m ⁴)	31.62	62.84
I 33 (m ⁴)	12.54	27.66
I 22 (m ⁴)	258.78	294.61
Element # 7, L = 8.0 m		
Node #	19	20
A (m ²)	13.84	15.09
J (m ⁴)	62.84	99.19
I 33 (m ⁴)	27.66	47.78
I 22 (m ⁴)	294.61	326.74
Element # 8, L = 7.0 m		
Node #	20	21
A (m ²)	15.09	15.96
J (m ⁴)	99.19	148.84
I 33 (m ⁴)	47.78	81.34
I 22 (m ⁴)	326.74	371.66

Table 2. 4. Cross-section properties: Fourth span.

Span # 4, L = 87.5 m		
Property	Left Side	Right Side
Element # 1, L = 5.0 m		
Node #	21	22
A (m ²)	15.96	15.29
J (m ⁴)	148.84	110.08
I 33 (m ⁴)	81.34	54.25
I 22 (m ⁴)	371.66	335.15
Element # 2, L = 8.0 m		
Node #	22	23
A (m ²)	15.29	14.09
J (m ⁴)	110.08	70.82
I 33 (m ⁴)	54.25	31.90
I 22 (m ⁴)	335.15	302.55
Element # 3, L = 12.0 m		
Node #	23	24
A (m ²)	14.09	12.71
J (m ⁴)	70.82	35.44
I 33 (m ⁴)	31.90	14.28
I 22 (m ⁴)	302.55	264.08
Element # 4, L = 25.0 m		
Node #	24	25
A (m ²)	12.71	11.95
J (m ⁴)	35.44	15.38
I 33 (m ⁴)	14.28	5.62
I 22 (m ⁴)	264.08	232.29
Element # 5, L = 14.5 m		
Node #	25	26
A (m ²)	11.95	12.03
J (m ⁴)	15.38	21.17
I 33 (m ⁴)	5.62	8.00
I 22 (m ⁴)	232.29	243.00
Element # 6, L = 8.0 m		
Node #	26	27
A (m ²)	12.03	12.64
J (m ⁴)	21.17	31.07
I 33 (m ⁴)	8.00	12.30
I 22 (m ⁴)	243.00	258.09
Element # 7, L = 8.0 m		
Node #	27	28
A (m ²)	12.64	13.39
J (m ⁴)	31.07	48.36
I 33 (m ⁴)	12.30	20.39
I 22 (m ⁴)	258.09	279.52
Element # 8, L = 7.0 m		
Node #	28	29
A (m ²)	13.39	14.02
J (m ⁴)	48.36	75.44
I 33 (m ⁴)	20.39	35.09
I 22 (m ⁴)	279.52	311.19

Table 2. 5. Cross-section properties: Fifth span.

Span # 5, L = 75.0 m		
Property	Left Side	Right Side
Element # 1, L = 5.0 m		
Node #	29	30
A (m ²)	14.02	13.55
J (m ⁴)	75.44	54.83
I 33 (m ⁴)	35.09	23.59
I 22 (m ⁴)	311.19	286.54
Element # 2, L = 8.0 m		
Node #	30	31
A (m ²)	13.55	12.74
J (m ⁴)	54.83	34.64
I 33 (m ⁴)	23.59	13.90
I 22 (m ⁴)	286.54	262.81
Element # 3, L = 12.0 m		
Node #	31	32
A (m ²)	12.74	12.05
J (m ⁴)	34.64	19.70
I 33 (m ⁴)	13.90	7.38
I 22 (m ⁴)	262.81	240.35
Element # 4, L = 12.5 m		
Node #	32	33
A (m ²)	12.05	11.75
J (m ⁴)	19.70	15.38
I 33 (m ⁴)	7.38	5.62
I 22 (m ⁴)	240.35	232.29
Element # 5, L = 10.5 m		
Node #	33	34
A (m ²)	11.75	11.97
J (m ⁴)	15.38	18.44
I 33 (m ⁴)	5.62	6.87
I 22 (m ⁴)	232.29	238.28
Element # 6, L = 12.0 m		
Node #	34	35
A (m ²)	11.97	12.56
J (m ⁴)	18.44	31.07
I 33 (m ⁴)	6.87	12.30
I 22 (m ⁴)	238.28	258.09
Element # 7, L = 8.0 m		
Node #	35	36
A (m ²)	12.56	13.39
J (m ⁴)	31.07	48.36
I 33 (m ⁴)	12.30	20.39
I 22 (m ⁴)	258.09	279.52
Element # 8, L = 7.0 m		
Node #	36	37
A (m ²)	13.39	14.02
J (m ⁴)	48.36	75.44
I 33 (m ⁴)	20.39	35.09
I 22 (m ⁴)	279.52	311.19

Table 2. 6. Cross-section properties: Sixth span.

Span # 6, L = 37.5 m		
Property	Left Side	Right Side
Element # 1, L = 5.0 m		
Node #	37	38
A (m ²)	14.02	13.55
J (m ⁴)	75.44	54.83
I 33 (m ⁴)	35.09	23.59
I 22 (m ⁴)	311.19	286.54
Element # 2, L = 8.0 m		
Node #	38	39
A (m ²)	13.55	12.74
J (m ⁴)	54.83	34.64
I 33 (m ⁴)	23.59	13.90
I 22 (m ⁴)	286.54	262.81
Element # 3, L = 12.0 m		
Node #	39	40
A (m ²)	12.74	12.05
J (m ⁴)	34.64	19.70
I 33 (m ⁴)	13.90	7.38
I 22 (m ⁴)	262.81	240.35
Element # 4, L = 12.5 m		
Node #	40	41
A (m ²)	12.05	11.76
J (m ⁴)	19.70	15.38
I 33 (m ⁴)	7.38	5.62
I 22 (m ⁴)	240.35	232.29

Table 2. 7. Piers cross-section properties.

Piers Cross Section Properties			
Pier - A (3.5m Wide)		Pier - B (4m Wide)	
Piers # 1, # 4, # 5		Piers # 2, # 3	
A (m ²)	47.342	A (m ²)	50.164
J (m ⁴)	275.703	J (m ⁴)	376.722
I 33 (m ⁴)	84.922	I 33 (m ⁴)	118.388
I 22 (m ⁴)	5510.939	I 22 (m ⁴)	6058.261

Table 2. 8. Abutment cross-section properties.

Abutments Cross Section Properties	
East & West	
A (m ²)	8.770
J (m ⁴)	14.740
I 33 (m ⁴)	4.710
I 22 (m ⁴)	102.590

Table 2. 9. Pile cross-section properties.

Pile Cross Section Properties	
A (m ²)	0.1663
J (m ⁴)	0.004403
I ₃₃ (m ⁴)	0.002202
I ₂₂ (m ⁴)	0.002202

2.3 Bridge Loads

Loads assigned to the analytical model include dead loads and superimposed dead loads. Dead loads due to superstructure (box girder), substructure (piers, pile cap and diaphragms) and superimposed dead loads (wearing surface and parapets) were calculated using cross section areas and tributary lengths. Six inches of asphalt pavement were assumed as part of the superimposed loads. All loads were added and assigned to the corresponding node. Tables 2.14 to 2.17 present a summary of loads determined for each bridge component. Nodes 101 to 141 were used to define the superstructure of the east bound bridge while nodes 201 to 241 were used to define the superstructure of the west bound bridge. Nodes 401 to 420 were used to define bridge piers while nodes 501/601 to 506/606 were used to define the abutments.

Table 2. 10. Loads due to superstructure, parapets and asphalt overlay.

Loads Due To: Superstructure, Parapets and Asphalt								
Concrete Unit Weight (γ) kN/m ³			23.563	Asphalt Unit Weight (kN/m ³)			22.992	
Gravitational Acceleration (g) m/s ²			9.806	Asphalt thickness (m)			0.1524	
	Areas (m ²)			Loads (kN/m)			Roadway Width (m)	17.84
Node #	Box Girder	Parapet	Asphalt	Box Girder	Parapet	Asphalt	Tributary Length (m)	Load/Node (kN)
101	11.813	0.333	2.72	278.34	15.68	62.51	7.75	2763
102	12.167	0.333	2.72	286.70	15.68	62.51	13.75	5017
103	13.008	0.333	2.72	306.52	15.68	62.51	10.00	3847
104	14.016	0.333	2.72	330.25	15.68	62.51	7.50	3063
105	14.725	0.333	2.72	346.97	15.68	62.51	6.00	2550
106	14.165	0.333	2.72	333.78	15.68	62.51	6.50	2677
107	13.204	0.333	2.72	311.13	15.68	62.51	10.00	3893
108	12.262	0.333	2.72	288.93	15.68	62.51	14.75	5415
109	11.929	0.333	2.72	281.08	15.68	62.51	20.25	7275

Table 2.14. Continuation.

110	12.573	0.333	2.72	296.25	15.68	62.51	17.50	6552
111	13.837	0.333	2.72	326.05	15.68	62.51	10.00	4042
112	15.091	0.333	2.72	355.58	15.68	62.51	7.50	3253
113	15.850	0.333	2.72	373.47	15.68	62.51	8.00	3613
114	14.880	0.333	2.72	350.63	15.68	62.51	8.50	3644
115	13.893	0.333	2.72	327.36	15.68	62.51	10.00	4055
116	13.458	0.333	2.72	317.10	15.68	62.51	16.50	6522
117	12.202	0.333	2.72	287.52	15.68	62.51	22.00	8045
118	12.573	0.333	2.72	296.25	15.68	62.51	17.50	6552
119	13.837	0.333	2.72	326.05	15.68	62.51	10.00	4042
120	15.091	0.333	2.72	355.58	15.68	62.51	7.50	3253
121	15.956	0.333	2.72	375.96	15.68	62.51	6.00	2724
122	15.291	0.333	2.72	360.30	15.68	62.51	6.50	2850
123	14.095	0.333	2.72	332.12	15.68	62.51	10.00	4103
124	12.708	0.333	2.72	299.44	15.68	62.51	18.50	6986
125	11.954	0.333	2.72	281.66	15.68	62.51	19.75	7107
126	12.034	0.333	2.72	283.56	15.68	62.51	11.25	4069
127	12.645	0.333	2.72	297.94	15.68	62.51	8.00	3009
128	13.389	0.333	2.72	315.48	15.68	62.51	7.50	2952
129	14.023	0.333	2.72	330.41	15.68	62.51	6.00	2451
130	13.550	0.333	2.72	319.27	15.68	62.51	6.50	2583
131	12.736	0.333	2.72	300.10	15.68	62.51	10.00	3782
132	12.046	0.333	2.72	283.84	15.68	62.51	12.25	4434
133	11.749	0.333	2.72	276.84	15.68	62.51	11.50	4082
134	11.970	0.333	2.72	282.06	15.68	62.51	11.25	4052
135	12.564	0.333	2.72	296.05	15.68	62.51	10.00	3742
136	13.389	0.333	2.72	315.48	15.68	62.51	7.50	2952
137	14.023	0.333	2.72	330.41	15.68	62.51	6.00	2451
138	13.550	0.333	2.72	319.27	15.68	62.51	6.50	2583
139	12.736	0.333	2.72	300.10	15.68	62.51	10.00	3782
140	12.046	0.333	2.72	283.84	15.68	62.51	12.25	4434
141	11.762	0.333	2.72	277.16	15.68	62.51	6.25	2220
Loads for nodes 201 to 241 are the same as those shown for nodes 101 to 141.								
Parapets were considered twice because there are two parapets on each bridge (see Figure 1.6).								

Table 2. 11. Pier loads.

Pier Loads				
Concrete Unit Weight (γ) (kN/m ³)				23.56
Pier	Node #	Area (m ²)	Tributary Length (m)	Load (kN)
Pier-1	401	47.34	1.46	13415
	402	47.34	2.91	3246
	403	47.34	2.91	3246
	404	47.34	1.46	1629
Pier-2	405	50.16	1.24	16384
	406	50.16	2.48	2931
	407	50.16	2.48	2931
	408	50.16	1.24	1466
Pier-3	409	50.16	1.40	16573
	410	50.16	2.80	3310
	411	50.16	2.80	3310
	412	50.16	1.40	1655
Pier-4	413	47.34	0.89	12779
	414	47.34	1.78	1986
	415	47.34	1.78	1986
	416	47.34	0.89	993
Pier-5	417	47.34	0.68	12545
	418	47.34	1.36	1517
	419	47.34	1.36	1517
	420	47.34	0.68	759

Table 2. 12. Abutment loads.

Abutment Loads				
Concrete Unit Weight (γ) (kN/m ³)				23.56
Abutment	Node #	Area (m ²)	Tributary Length (m)	Load (kN)
West Abutment	101/201	8.77	1.25	258
	501/601	8.77	1.25	1652
	502/602	8.77	2.5	517
	503/603	8.77	2.5	517
East Abutment	141/241	8.77	0.73	151
	504/604	8.77	0.73	1545
	505/605	8.77	1.47	304
	506/606	8.77	1.47	304

Table 2. 13. Pile cap loads.

Pile Cap Loads					
Concrete Unit Weight (γ) (kN/m ³)					23.56
Pier	Node #	Width (m)	Length (m)	Height (m)	Load (kN)
WA	501/601	13.60	3.00	1.45	1394
Pier-1	401	39.20	5.80	2.20	11786
Pier-2	405	40.25	7.15	2.20	14919
Pier-3	409	40.25	7.15	2.20	14919
Pier-4	413	39.20	5.80	2.20	11786
Pier-5	417	39.20	5.80	2.20	11786
WA	504/604	13.60	3.00	1.45	1394

2.4 Piled Foundation Model

Bridge No. 2001 is founded on deep foundation (piles). Pile foundations were represented with equivalent stiffness springs in the analytical model. Computer software GROUP7 was implemented to consider the soil-foundation interaction and to determine the spring's stiffness. This software performs p-y, q-w and t-z analyses internally to consider the soil-foundation-structure interaction analysis. The program can internally compute the deflection, bending moment, shear, and soil resistance as a function of depth for each pile. The main purpose of the program is to take into account the nonlinear behavior of soil and also to consider the group effect. When n -piles are installed in groups, the capacity of the group is less than the capacity of n -times the single pile capacity, because of the overlapping between stress zones which makes the soil to behave as if it has less resistance. Figure 2.2 presents an example of the overlapping between stress zones on adjacent piles.

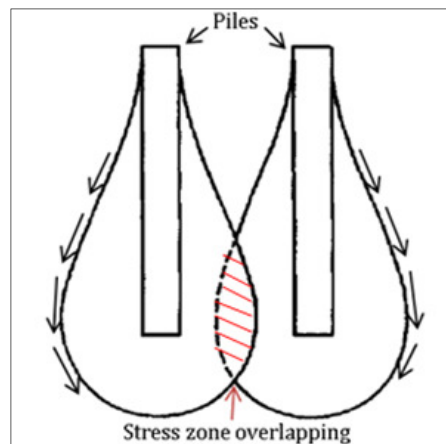


Figure 2. 2. Stress zone overlapping for group of piles.

The following soil properties were provided to the software for the soil modeling:

- layer depth (m),
- unit weight(γ),
- internal friction angle (ϕ) – for granular soils,
- unit strain (ϵ) – for cohesive soils, and
- soil stiffness(k).

These properties were obtained for soil layers underneath bridge piers. The standard penetration test (SPT) blow count (N), provided in the soil borings, was used to determine the appropriate soil properties using correlation tables for granular and cohesive soils. Tables 2.18 and 2.19 include the soil parameters for granular and cohesive soils, respectively. Figures 2.3 and 2.4 present the boring logs for each pier.

Table 2. 14. Soil parameters for granular soils (MoDOT, 2002).

	$(N_1)_{60}$ (blows/ft.)	ϕ (deg)	S_u (ksf)	D_r (relative density)	Grain Size	E (ksf)	Poisson's ratio, ν	Soil Type Distribution	γ (dry) (pcf)	γ (sat) (pcf)	Wet (below W.T.) Dry (above W.T.)	K (pci)
Very Loose	0 - 5	0 - 0.5	0 - 0.5	0.10	fine	100	0.25	uniform	88.00	115.00	wet	10
					medium	100	0.15	mixed	95.00	120.00	dry	15
Loose	5 - 10	0.5 - 10	0.5 - 1.0	0.2 - 0.4	fine	160 - 240	0.25	uniform	91.00	118.00	wet	20
					medium	200 - 600	0.2 - 0.25	mixed	99.00	123.00	dry	25
Medium	10 - 20	1.0 - 2.0	1.0 - 2.0	0.4 - 0.5	fine	240 - 300	0.25	uniform	97.00	122.00	wet	55
					medium	600 - 800	0.25 - 0.3	mixed	104.00	127.00	dry	92
Medium Dense	20 - 35	2.0 - 3.5	2.0 - 3.5	0.5 - 0.6	fine	300 - 400	0.25	uniform	103.00	126.00	wet	90
					medium	800 - 1000	0.3 - 0.35	mixed	110.00	131.00	dry	158
Dense	35 - 70	3.5 - 7.0	3.5 - 7.0	0.6 - 0.9	fine	400 - 600	0.25	uniform	109.00	130.00	wet	125
					medium	1000 - 1600	0.35 - 0.4	mixed	116.00	135.00	dry	225
Very Dense	75.00	7.50	8.00	0.95	fine	700	0.25	uniform	112.00	133.00	wet	15
					medium	1700	0.45	mixed	119.00	138.00	dry	15

Table 2. 15. Soil parameters for cohesive soils (MoDOT, 2002).

	N_{60} (blows/ft.)	$c = S_u$ (ksf)	E (ksf)	Poisson's ratio, ν	γ (dry) (pcf)	γ (sat) (pcf)	K (pci)	ϵ_{50} (in./in.)
Very Soft	0 - 5	0 - 0.5	50 - 150	0.50 (sat) 0.40 (unsat.)	73.00	105.00	50.00	0.02
Soft	5 - 10	0.5 - 1.0	150 - 300	0.50 (sat) 0.39 (unsat.)	76.00	110.00	100.00	0.01
Medium Stiff	10 - 20	1.0 - 2.0	300 - 650	0.50 (sat) 0.38 (unsat.)	86.00	116.00	500.00	0.007
Very Stiff	20 - 35	2.0 - 3.5	650 - 1000	0.50 (sat) 0.37 (unsat.)	96.00	123.00	1000.00	0.005
Hard	35 - 70	3.5 - 7.0	1000 - 1500	0.50 (sat) 0.36 (unsat.)	106.00	129.00	2000.00	0.004
Very Hard	75.00	7.50	1500 - 2000	0.50 (sat) 0.35 (unsat.)	108.00	134.00	3000.00	0.0035

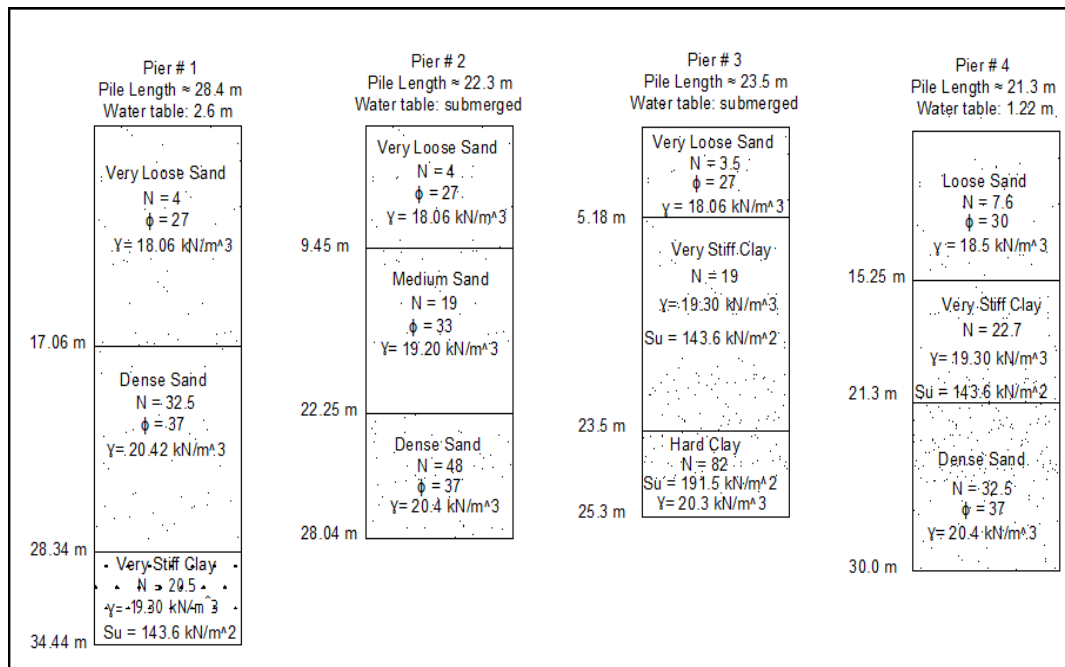


Figure 2.3. Boring logs: Piers 1, 2, 3, and 4.

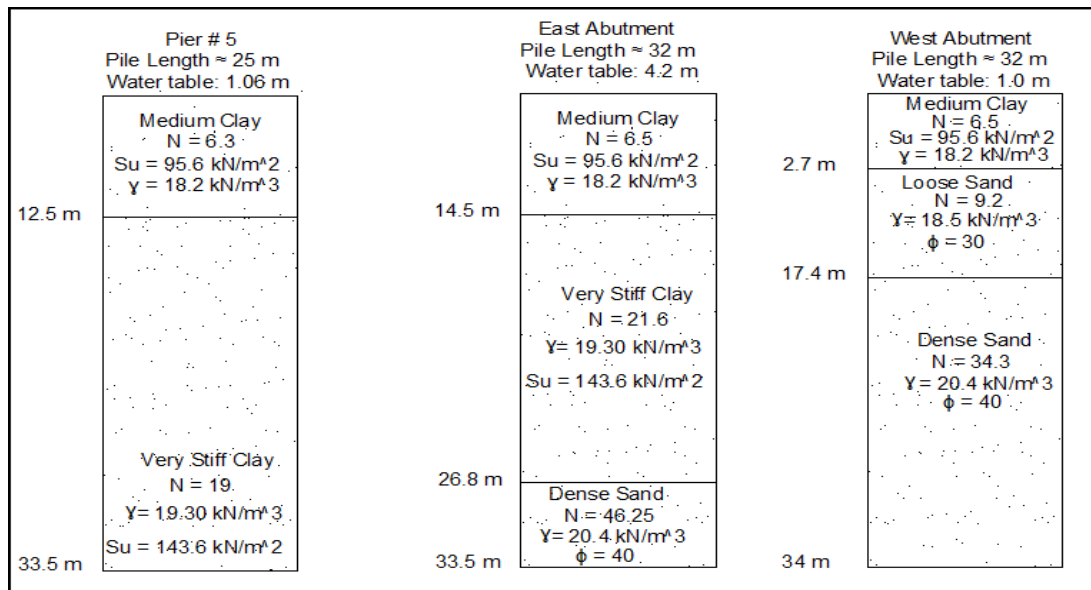


Figure 2.4. Boring logs: Pier 5 and Abutments.

In addition to the soil parameters, the computer software also requires the existing pile configuration: coordinates of piles (X, Y, and Z), the inclination angle for batter piles (β), and the orientation angle of piles (α). These coordinates and angles were obtained from the bridge design drawings. Figure 2.5 presents a detail of the parameters required to define the configuration of piles. Tables 2.20 to 2.30 summarize the pile configuration for bridge No. 2001.

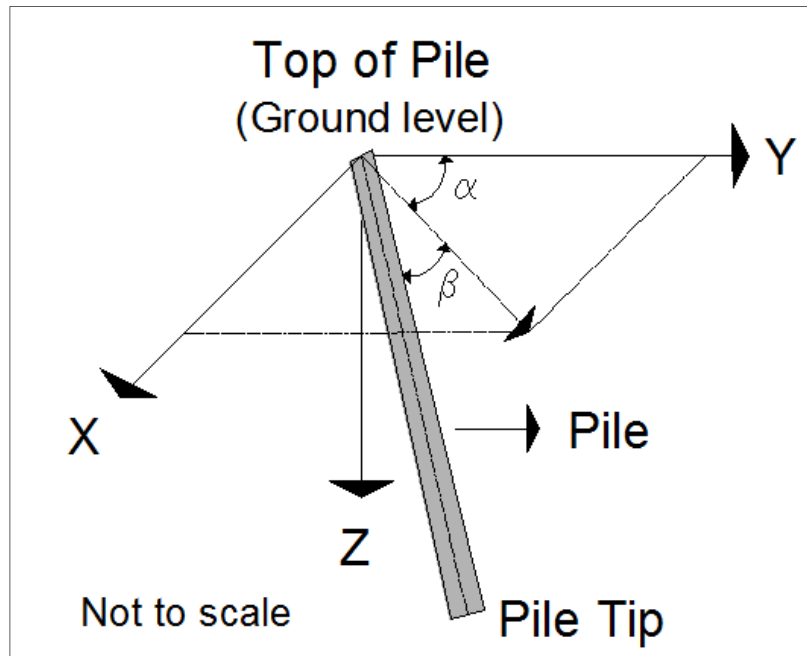


Figure 2. 5. Group7: Pile configuration requirements.

Table 2. 16. Piles configuration: Piers 1, 4 and 5, first row.

3.5 m Width Pier: Pile Configuration (118 Piles)				
First Row				
Pile #	Y(m)	Z(m)	β (degrees)	α (degrees)
1	-2.4	17.725	78.7	90
2	-2.4	16.375	78.7	90
3	-2.4	15.025	78.7	90
4	-2.4	13.675	78.7	90
5	-2.4	12.325	78.7	90
6	-2.4	10.975	78.7	180
7	-2.4	9.625	78.7	180
8	-2.4	8.275	78.7	180
9	-2.4	6.925	78.7	180
10	-2.4	5.575	78.7	180
11	-2.4	4.225	78.7	180
12	-2.4	2.875	78.7	180
13	-2.4	1.525	78.7	180
14	-2.4	-1.525	78.7	180
15	-2.4	-2.875	78.7	180
16	-2.4	-4.225	78.7	180
17	-2.4	-5.575	78.7	180
18	-2.4	-6.925	78.7	180
19	-2.4	-8.275	78.7	180
20	-2.4	-9.625	78.7	180
21	-2.4	-10.975	78.7	180
22	-2.4	-12.325	78.7	-90
23	-2.4	-13.675	78.7	-90
24	-2.4	-15.025	78.7	-90
25	-2.4	-16.375	78.7	-90
26	-2.4	-17.725	78.7	-90

Table 2. 17. Piles configuration: Piers 1, 4 and 5, second row.

3.5 m Width Pier: Pile Configuration (118 Piles)				
Second Row				
Pile #	Y(m)	Z(m)	β (degrees)	α (degrees)
27	-1.2	17.050	78.7	90
28	-1.2	15.700	78.7	90
29	-1.2	14.350	78.7	90
30	-1.2	13.000	78.7	90
31	-1.2	11.650	90	0
32	-1.2	10.300	90	0
33	-1.2	8.950	90	0
34	-1.2	7.600	90	0
35	-1.2	6.250	90	0
36	-1.2	4.900	90	0
37	-1.2	3.550	90	0
38	-1.2	0.000	90	0
39	-1.2	-3.550	90	0
40	-1.2	-4.900	90	0
41	-1.2	-6.250	90	0
42	-1.2	-7.600	90	0
43	-1.2	-8.950	90	0
44	-1.2	-10.300	90	0
45	-1.2	-11.650	90	0
46	-1.2	-13.000	78.7	-90
47	-1.2	-14.350	78.7	-90
48	-1.2	-15.700	78.7	-90
49	-1.2	-17.050	78.7	-90

Table 2. 18. Piles configuration: Piers 1, 4 and 5, third row.

3.5 m Width Pier: Pile Configuration (118 Piles)				
Third Row				
Pile #	Y(m)	Z(m)	β (degrees)	α (degrees)
50	0	17.725	78.7	90
51	0	16.375	78.7	90
52	0	15.025	78.7	90
53	0	13.675	78.7	90
54	0	10.975	90	0
55	0	9.625	90	0
56	0	6.925	90	0
57	0	5.575	90	0
58	0	4.225	90	0
59	0	2.875	90	0
60	0	-2.875	90	0
61	0	-4.225	90	0
62	0	-5.575	90	0
63	0	-6.925	90	0
64	0	-9.625	90	0
65	0	-10.975	90	0
66	0	-13.675	78.7	-90
67	0	-15.025	78.7	-90
68	0	-16.375	78.7	-90
69	0	-17.725	78.7	-90

Table 2. 19. Piles configuration: Piers 1, 4 and 5, fourth row.

3.5 m Width Pier: Pile Configuration (118 Piles)				
Fourth Row				
Pile #	Y(m)	Z(m)	β (degrees)	α (degrees)
70	1.2	17.050	78.7	90
71	1.2	15.700	78.7	90
72	1.2	14.350	78.7	90
73	1.2	13.000	78.7	90
74	1.2	11.650	90	0
75	1.2	10.300	90	0
76	1.2	8.950	90	0
77	1.2	7.600	90	0
78	1.2	6.250	90	0
79	1.2	4.900	90	0
80	1.2	3.550	90	0
81	1.2	0.000	90	0
82	1.2	-3.550	90	0
83	1.2	-4.900	90	0
84	1.2	-6.250	90	0
85	1.2	-7.600	90	0
86	1.2	-8.950	90	0
87	1.2	-10.300	90	0
88	1.2	-11.650	90	0
89	1.2	-13.000	78.7	-90
90	1.2	-14.350	78.7	-90
91	1.2	-15.700	78.7	-90
92	1.2	-17.050	78.7	-90

Table 2. 20. Piles configuration: Piers 1, 4 and 5, fifth row.

3.5 m Width Pier: Pile Configuration (118 Piles)				
Fifth Row				
Pile #	Y(m)	Z(m)	β (degrees)	α (degrees)
93	2.4	17.725	78.7	90
94	2.4	16.375	78.7	90
95	2.4	15.025	78.7	90
96	2.4	13.675	78.7	90
97	2.4	12.325	78.7	90
98	2.4	10.975	78.7	0
99	2.4	9.625	78.7	0
100	2.4	8.275	78.7	0
101	2.4	6.925	78.7	0
102	2.4	5.575	78.7	0
103	2.4	4.225	78.7	0
104	2.4	2.875	78.7	0
105	2.4	1.525	78.7	0
106	2.4	-1.525	78.7	0
107	2.4	-2.875	78.7	0
108	2.4	-4.225	78.7	0
109	2.4	-5.575	78.7	0
110	2.4	-6.925	78.7	0
111	2.4	-8.275	78.7	0
112	2.4	-9.625	78.7	0
113	2.4	-10.975	78.7	0
114	2.4	-12.325	78.7	-90
115	2.4	-13.675	78.7	-90
116	2.4	-15.025	78.7	-90
117	2.4	-16.375	78.7	-90
118	2.4	-17.725	78.7	-90

Table 2. 21. Piles configuration: Piers 2 and 3, first row.

4 m Width Pier: Pile Configuration (138 Piles)				
First Row				
Pile #	Y (m)	Z (m)	β (degrees)	α (degrees)
1	-3.075	17.725	78.7	90
2	-3.075	16.375	78.7	90
3	-3.075	15.025	78.7	90
4	-3.075	13.675	78.7	90
5	-3.075	12.325	78.7	180
6	-3.075	10.975	78.7	180
7	-3.075	9.625	78.7	180
8	-3.075	8.275	78.7	180
9	-3.075	6.925	78.7	180
10	-3.075	5.575	78.7	180
11	-3.075	4.225	78.7	180
12	-3.075	2.875	78.7	180
13	-3.075	1.525	78.7	180
14	-3.075	-1.525	78.7	180
15	-3.075	-2.875	78.7	180
16	-3.075	-4.225	78.7	180
17	-3.075	-5.575	78.7	180
18	-3.075	-6.925	78.7	180
19	-3.075	-8.275	78.7	180
20	-3.075	-9.625	78.7	180
21	-3.075	-10.975	78.7	180
22	-3.075	-12.325	78.7	180
23	-3.075	-13.675	78.7	-90
24	-3.075	-15.025	78.7	-90
25	-3.075	-16.375	78.7	-90
26	-3.075	-17.725	78.7	-90

Table 2. 22. Piles configuration: Piers 2 and 3, second row.

4 m Width Pier: Pile Configuration (138 Piles)				
Second Row				
Pile #	Y (m)	Z (m)	β (degrees)	α (degrees)
27	-1.875	17.050	78.7	90
28	-1.875	15.700	78.7	90
29	-1.875	14.350	78.7	90
30	-1.875	13.000	90	0
31	-1.875	11.650	90	0
32	-1.875	10.300	90	0
33	-1.875	8.950	90	0
34	-1.875	7.600	90	0
35	-1.875	6.250	90	0
36	-1.875	4.900	90	0
37	-1.875	3.550	90	0
38	-1.875	0.000	90	0
39	-1.875	-3.550	90	0
40	-1.875	-4.900	90	0
41	-1.875	-6.250	90	0
42	-1.875	-7.600	90	0
43	-1.875	-8.950	90	0
44	-1.875	-10.300	90	0
45	-1.875	-11.650	90	0
46	-1.875	-13.000	90	0
47	-1.875	-14.350	78.7	-90
48	-1.875	-15.700	78.7	-90
49	-1.875	-17.050	78.7	-90

Table 2. 23. Piles configuration: Piers 2 and 3, third row.

4 m Width Pier: Pile Configuration (138 Piles)				
Third Row				
Pile #	Y (m)	Z (m)	β (degrees)	α (degrees)
50	-0.675	17.725	78.7	90
51	-0.675	16.375	78.7	90
52	-0.675	15.025	78.7	90
53	-0.675	13.675	78.7	90
54	-0.675	10.975	90	0
55	-0.675	9.625	90	0
56	-0.675	6.925	90	0
57	-0.675	5.575	90	0
58	-0.675	4.225	90	0
59	-0.675	2.875	90	0
60	-0.675	-2.875	90	0
61	-0.675	-4.225	90	0
62	-0.675	-5.575	90	0
63	-0.675	-6.925	90	0
64	-0.675	-9.625	90	0
65	-0.675	-10.975	90	0
66	-0.675	-13.675	78.7	-90
67	-0.675	-15.025	78.7	-90
68	-0.675	-16.375	78.7	-90
69	-0.675	-17.725	78.7	-90

Table 2. 24. Piles configuration: Piers 2 and 3, fourth row.

4 m Width Pier: Pile Configuration (138 Piles)				
Fourth Row				
Pile #	Y (m)	Z (m)	β (degrees)	α (degrees)
70	0.675	17.725	78.7	90
71	0.675	16.375	78.7	90
72	0.675	15.025	78.7	90
73	0.675	13.675	78.7	90
74	0.675	10.975	90	0
75	0.675	9.625	90	0
76	0.675	6.925	90	0
77	0.675	5.575	90	0
78	0.675	4.225	90	0
79	0.675	2.875	90	0
80	0.675	-2.875	90	0
81	0.675	-4.225	90	0
82	0.675	-5.575	90	0
83	0.675	-6.925	90	0
84	0.675	-9.625	90	0
85	0.675	-10.975	90	0
86	0.675	-13.675	78.7	-90
87	0.675	-15.025	78.7	-90
88	0.675	-16.375	78.7	-90
89	0.675	-17.725	78.7	-90

Table 2. 25. Piles configuration: Piers 2 and 3, fifth row.

4 m Width Pier: Pile Configuration (138 Piles)				
Fifth Row				
Pile #	Y (m)	Z (m)	β (degrees)	α (degrees)
90	1.875	17.050	78.7	90
91	1.875	15.700	78.7	90
92	1.875	14.350	78.7	90
93	1.875	13.000	90	0
94	1.875	11.650	90	0
95	1.875	10.300	90	0
96	1.875	8.950	90	0
97	1.875	7.600	90	0
98	1.875	6.250	90	0
99	1.875	4.900	90	0
100	1.875	3.550	90	0
101	1.875	0.000	90	0
102	1.875	-3.550	90	0
103	1.875	-4.900	90	0
104	1.875	-6.250	90	0
105	1.875	-7.600	90	0
106	1.875	-8.950	90	0
107	1.875	-10.300	90	0
108	1.875	-11.650	90	0
109	1.875	-13.000	90	0
110	1.875	-14.350	78.7	-90
111	1.875	-15.700	78.7	-90
112	1.875	-17.050	78.7	-90

Table 2. 26. Piles configuration: Piers 2 and 3, sixth row.

4 m Width Pier: Pile Configuration (138 Piles)				
Sixth Row				
Pile #	Y (m)	Z (m)	β (degrees)	α (degrees)
113	3.075	17.725	78.7	90
114	3.075	16.375	78.7	90
115	3.075	15.025	78.7	90
116	3.075	13.675	78.7	90
117	3.075	12.325	78.7	0
118	3.075	10.975	78.7	0
119	3.075	9.625	78.7	0
120	3.075	8.275	78.7	0
121	3.075	6.925	78.7	0
122	3.075	5.575	78.7	0
123	3.075	4.225	78.7	0
124	3.075	2.875	78.7	0
125	3.075	1.525	78.7	0
126	3.075	-1.525	78.7	0
127	3.075	-2.875	78.7	0
128	3.075	-4.225	78.7	0
129	3.075	-5.575	78.7	0
130	3.075	-6.925	78.7	0
131	3.075	-8.275	78.7	0
132	3.075	-9.625	78.7	0
133	3.075	-10.975	78.7	0
134	3.075	-12.325	78.7	0
135	3.075	-13.675	78.7	-90
136	3.075	-15.025	78.7	-90
137	3.075	-16.375	78.7	-90
138	3.075	-17.725	78.7	-90

Pile cap dimensions were also provided to the software to take into account the passive pressure of the surrounding soil. Passive pressure is the force exerted by the soil in lateral contact with the pile cap, which helps to resist the shear forces acting at the pile cap level. Arbitrary loads and moments (100 kN and 1000 kN-m) were applied to the pile cap within the principal axes (see Figure 2.6), and pile cap displacements, due to these arbitrary loads, were obtained using software GROUP7. Loads applied to the pile cap and displacements obtained from the analysis were combined with *Method II – Matrix Coefficient Definition*, described in WSDOT 2012, to obtain the stiffness (K_{ij}) of the equivalent springs. Figure 2.7 presents the matrix used to obtain the equivalent stiffness of the springs. Table 2.31 presents a summary of the equivalent stiffness due to shear loads, axial loads and bending moments applied to the pile cap. These stiffness values were assigned to the analytical model developed in SAP2000 to represent the piled foundation.

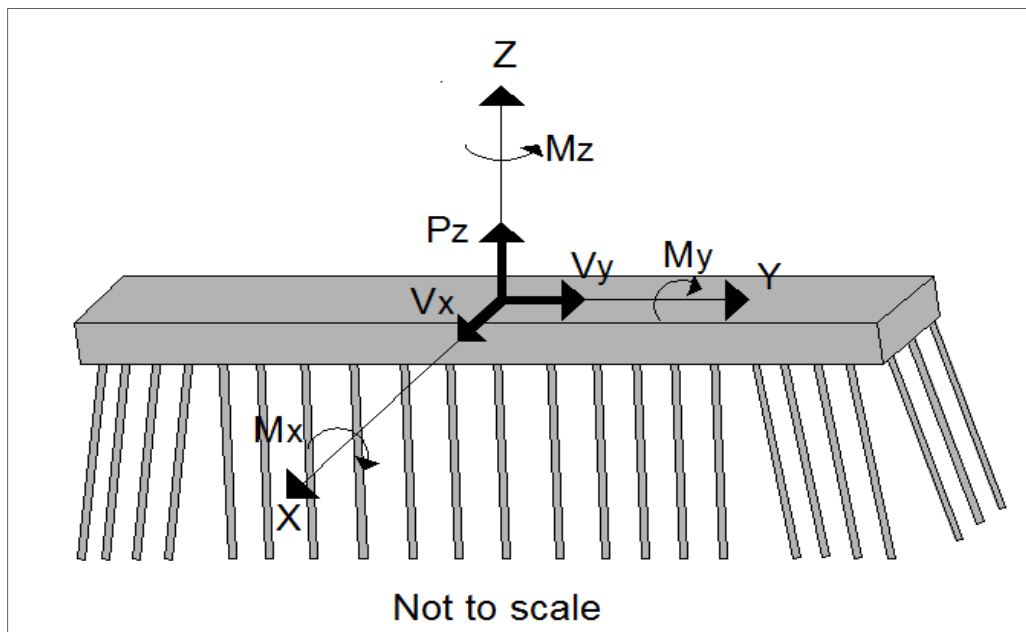


Figure 2. 6. Pile cap principal axes and arbitrary loads application.

$$\begin{bmatrix}
 & V_x & V_y & P_z & M_x & M_y & M_z \\
 V_x & K11 & 0 & 0 & 0 & 0 & 0 \\
 V_y & 0 & K22 & 0 & 0 & 0 & 0 \\
 P_z & 0 & 0 & K33 & 0 & 0 & 0 \\
 M_x & 0 & 0 & 0 & K44 & 0 & 0 \\
 M_y & 0 & 0 & 0 & 0 & K55 & 0 \\
 M_z & 0 & 0 & 0 & 0 & 0 & K66
 \end{bmatrix}
 \times
 \begin{bmatrix}
 \text{Disp.} \\
 \Delta x \\
 \Delta y \\
 \Delta z \\
 \Theta x \\
 \Theta y \\
 \Theta z
 \end{bmatrix}
 =
 \begin{bmatrix}
 \text{Force} \\
 V_x \\
 V_y \\
 P_z \\
 M_x \\
 M_y \\
 M_z
 \end{bmatrix}$$

Figure 2. 7. Stiffness matrix for piled foundation.

Table 2. 27. Equivalent stiffness for piled foundation.

Equivalent Stiffness for Piled Foundation						
Pier #	Kx(kN/m)	Ky(kN/m)	Kz(kN/m)	Kθx(kN-m/rads)	Kθy(kN-m/rads)	Kθz(kN-m/rads)
WA	811688	5767013	2714885	255819903	3802281	627352572
1	4405286	2598753	10539352	1483459427	38255547	301477238
2	2310002	4144219	15699319	436681223	41493776	635324015
3	4314064	5115090	12731681	44642857143	246548323	608642727
4	4880429	4761905	14003059	5854800937	92336103	547645126
5	1293995859	597728631	11947410	7968127490	234411627	31735956839
EA	4228330	8481764	3353681	676589986	8976661	691562932

2.5 Seismic Spectral Analysis

The seismic load used to perform the seismic analysis of bridge No. 2001 was generated using a multimodal response spectrum in the SAP2000 analytical model. Parameters used to define the acceleration response spectrum were obtained following the guidelines of AASHTO 2007. The following parameters were required to develop the response spectrum:

- Site Latitude = 18.4219°,
- Site Longitude = -66.1555°,
- $S_s = .64$ (short period (.20 sec) spectral acceleration),
- $S_1 = .22$ (long period (1.0 sec) spectral acceleration),
- Site Class = D,
- $F_a = 1.28$ (site coefficient in short period acceleration),

- $F_v = 1.96$ (site coefficient in long period acceleration),
- $SDS = .82 (F_a * S_s, \text{acceleration coefficient}), \text{ and}$
- $SD1 = .43 (F_v * S_1, \text{acceleration coefficient}).$

Coordinates of bridge site (latitude and longitude) were obtained using Google Earth 2006. Spectral accelerations at short and long period (S_s and S_1) were obtained from SAP2000 data base once provided the coordinates of the bridges site. Site class parameter was determined with the average standard penetration test (SPT) blow count (N). The overall N value was determined combining the values for each layer, shown in Figures 2.3 and 2.4, with following equation:

$$N = \frac{\sum_{i=0}^n d_i}{\sum_{i=1}^n \frac{d_i}{N_i}} \quad (2 - 1)$$

where:

d_i = thickness of the layer i , and

N_i = SPT blow count of the layer i .

With this N value and Table 1.4, an appropriate site class parameter was defined. Once determined the short and long period acceleration and the site class, the site coefficients were determined by linear interpolation using values from Tables 2.32

and 2.33. Once determined the acceleration coefficient ($SD1$) and using Table 2.34, it was possible to determine the seismic zone for bridge No. 2001.

Table 2. 28. Site coefficient (F_a) in short period acceleration (FHWA, 2006).

Site Class	Spectral Acceleration at Short-Period (0.2 sec), S_s ¹				
	$S_s \leq 0.25$	$S_s = 0.50$	$S_s = 0.75$	$S_s = 1.00$	$S_s \geq 1.25$
A	0.8	0.8	0.8	0.8	0.8
B	1.0	1.0	1.0	1.0	1.0
C	1.2	1.2	1.1	1.0	1.0
D	1.6	1.4	1.2	1.1	1.0
E	2.5	1.7	1.2	0.9	0.9
F ²					
Notes: 1. Use straight-line interpolation for intermediate values of S_s . 2. Site-specific geotechnical investigation and dynamic site response analysis should be performed for class F soils.					

Table 2. 29. Site coefficient (F_v) in long period acceleration (FHWA, 2006).

Site Class	Spectral Acceleration at Long-Period (1.0 sec), S_1 ¹				
	$S_1 \leq 0.1$	$S_1 = 0.2$	$S_1 = 0.3$	$S_1 = 0.4$	$S_1 \geq 0.5$
A	0.8	0.8	0.8	0.8	0.8
B	1.0	1.0	1.0	1.0	1.0
C	1.7	1.6	1.5	1.4	1.3
D	2.4	2.0	1.8	1.6	1.5
E	3.5	3.2	2.8	2.4	2.4
F ²					
Notes: 1. Use straight-line interpolation for intermediate values of S_1 . 2. Site-specific geotechnical investigation and dynamic site response analysis should be performed for class F soils.					

Table 2. 30. Seismic zone and seismic design category (AASHTO, 2007).

Seismic Zone & Seismic Design Category		
$SD1 = F_v * S1$	Seismic Zone	Seismic Design Category
$SD1 < 0.15$	1	A
$0.15 \leq SD1 \leq 0.30$	2	B
$0.30 \leq SD1 \leq 0.50$	3	C
$0.50 \leq SD1$	4	D

CHAPTER III: Bridge Analysis and C/D Ratios Determination

3.1 Introduction

Bridge No. 2001 was analyzed for load combinations discussed in section 1.5.4 using the analytical model defined in SAP2000. Bridge reactions (forces and moments) were obtained for each bridge component. Seismic demand on each component was compared with component capacity to determine the Capacity/Demand ratio. Procedures used to determine the different C/D ratios are discussed in detail in the following sections.

3.2 C/D Ratios for Reinforced Concrete Columns, Walls and Footings

Substructure components were analyzed following the flowchart presented in Table 1.6. However, due to the piled foundation of bridge No. 2001, it was also necessary to analyze the pile cap connecting the piles and piers. The procedure used to complete the analysis of the substructure is discussed below.

3.2.1 Piers

Capacity/Demand ratios for piers were determined using the following procedure based on the elastic demand forces and plastic hinging forces. This procedure can be described as follows:

- a. Determine the elastic moment demand (M_u) at top and bottom of piers for load cases defined in Section 1.5.4
- b. Determine the nominal moment capacity of the pier using an axial load resulting from plastic hinging analysis in columns. Plastic hinging methodology for single and multiple piers is described in sections 3.10.9.4.3b and 3.10.9.4.3c from AASHTO 2007.

Single Pier:

1. Determine the axial load corresponding to the dead load plus load combination presented in Section 1.5.4.
2. Determine the column nominal moment capacity (M_n) corresponding to the axial load determined in the previous step.

Multiple Piers:

1. Determine the axial load due to the dead load.
 2. Determine the column over-strength moment resistance ($1.3M_n$) corresponding to the axial load obtained in the previous step.
 3. Apply this over strength moment to the model to determine the shear forces on columns.
 4. Add these shear forces to obtain the maximum shear force on the structure.
 5. Apply this shear force to the center of mass of the superstructure to determine the axial forces in columns.
 6. With these axial loads, determine revised column over strength moment.
 7. With over strength moment, determine shear forces on columns and maximum shear force.
 8. If the difference between maximum shear force load and the one determined in the first step is greater than 10%, use this load and return to step five.
- c. Determine the C/D ratio for each pier (nominal moment capacity/elastic moment demand) using the following equation:

$$r_{ec} = \mu * \left[\frac{M_{nx}}{M_{ux}} + \frac{M_{ny}}{M_{uy}} \right] \quad (3 - 1)$$

where:

$\mu = 2$, ductility indicator. The ultimate moment capacity/demand ratios are multiplied by ductility indicators to enable elastic analysis results to be used for determining the C/D ratios of components subject to yielding (FHWA, 2006). The ductility indicator was determined with the following equation:

$$\mu = 2 + 4 * \left[\frac{k_1 + k_2}{2} \right] * k_3 \quad (3 - 2)$$

where:

k_1 , k_2 & k_3 are factors related to the spacing and size of reinforcement, and effectiveness of anchorage. However,

due to the age of the structure the minimum value ($\mu = 2$) was assumed to complete the analysis.

- d. Determine the plastic hinging case at the base of the column.
 - Case I – No hinging, r_{ec} and r_{ef} exceed 0.8. Calculate C/D ratios for anchorage and splices.
 - Case II – Hinging in footing only, $r_{ef} < 0.8$ and $r_{ec} > 0.8$. Calculate C/D ratios for anchorage, splices and confinement. Calculate C/D ratios for anchorage, splices and footing.
 - Case III – Hinging in column only, $r_{ec} < 0.8$ and $r_{ef} > 0.8$. Calculate C/D ratios for anchorage, splices and confinement.
 - Case IV – Hinging in column and or footing, r_{ec} and $r_{ef} < 0.8$. Calculate C/D ratios for anchorage splices, confinement and footing.
- e. Determine if plastic hinging ($r_{ec} < 0.8$) occurs at top of column.
 - If $r_{ec} > 0.8$, calculate C/D ratios for anchorage and splices. If $r_{ec} < 0.8$ calculate C/D ratios for anchorage, splices and confinement.
- f. Determine C/D ratios for column shear.

In order to determine the nominal moment capacity of piers it was necessary to define the interaction curve for piers cross-sections presented in Section 1.4. Section Designer Tool, included within computer program SAP2000, was used to determine the interaction diagram of piers. Piers cross section and vertical reinforcement (grade, size and spacing) were defined in the software to perform a finite element analysis and generate the interaction curves. Figures 3.1 to 3.6 shows the interaction curves and demand loads for bridge piers.

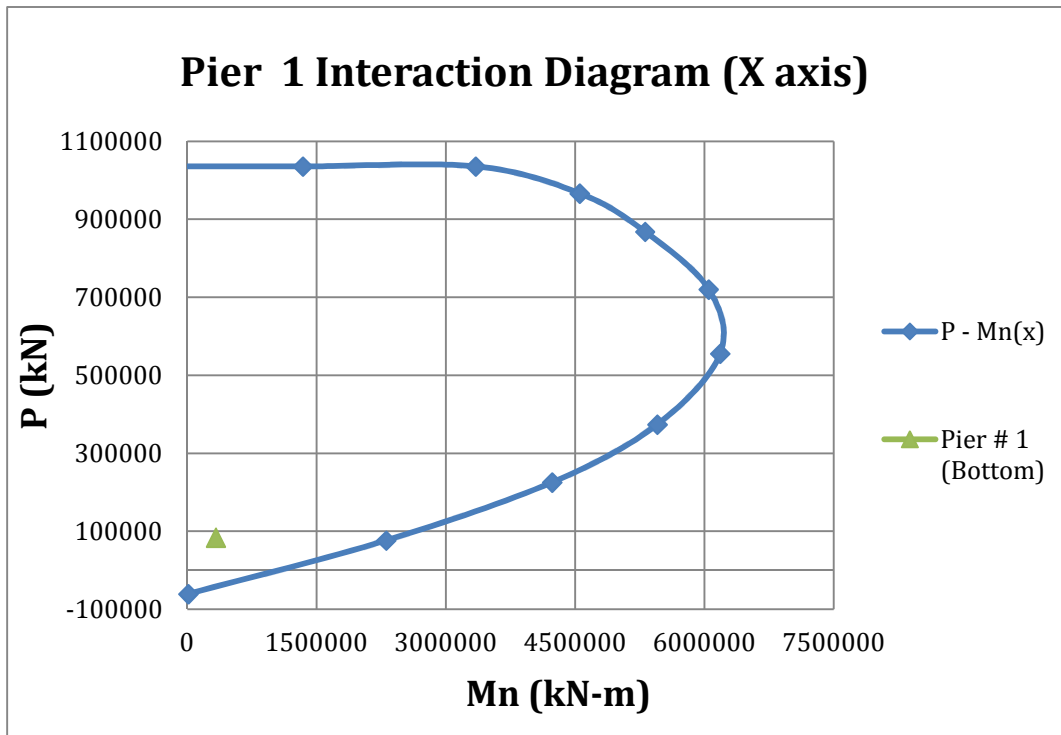


Figure 3. 1. Interaction diagram for Pier 1 about X axis.

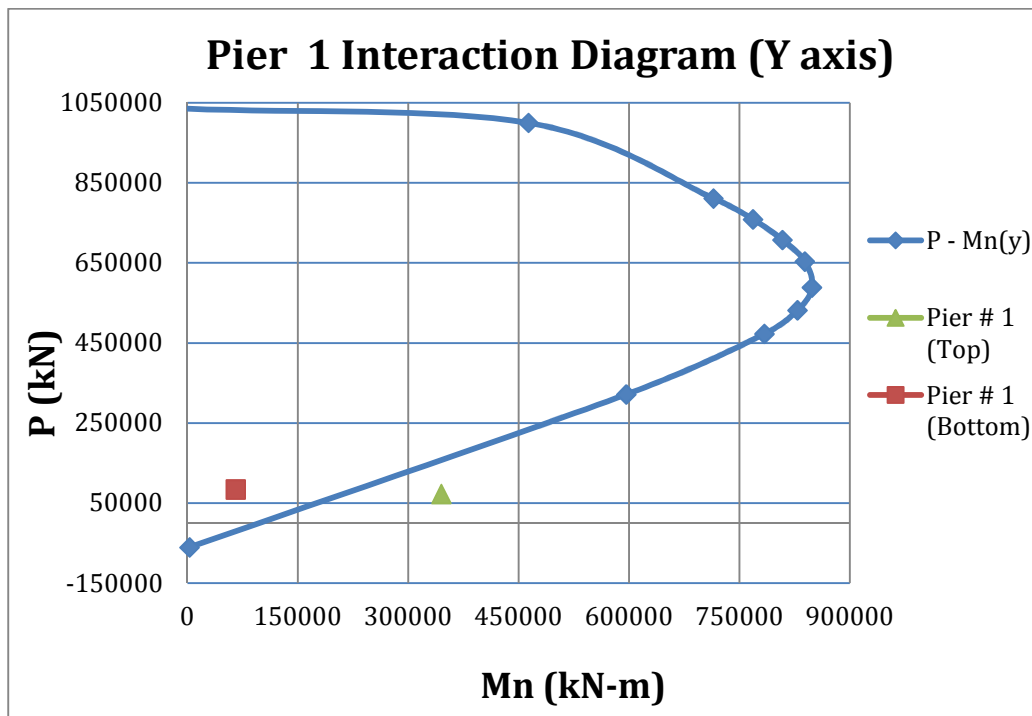


Figure 3. 2. Interaction diagram for Pier 1 about Y axis.

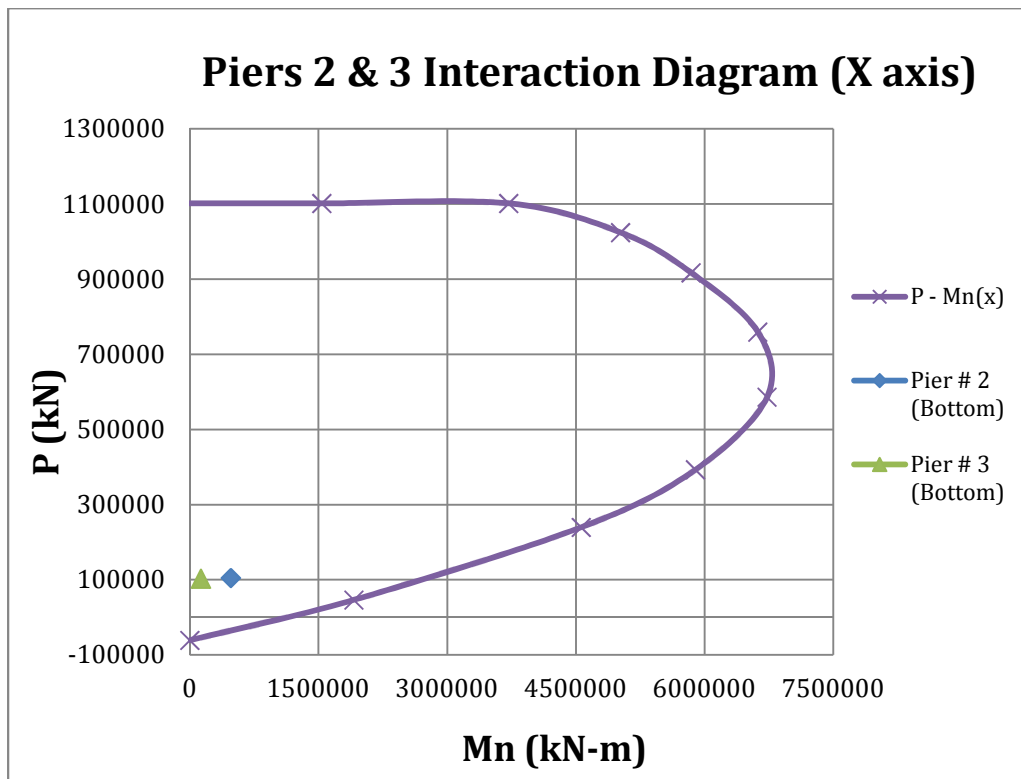


Figure 3. 3. Interaction diagram for Piers 2 and 3 about X axis.

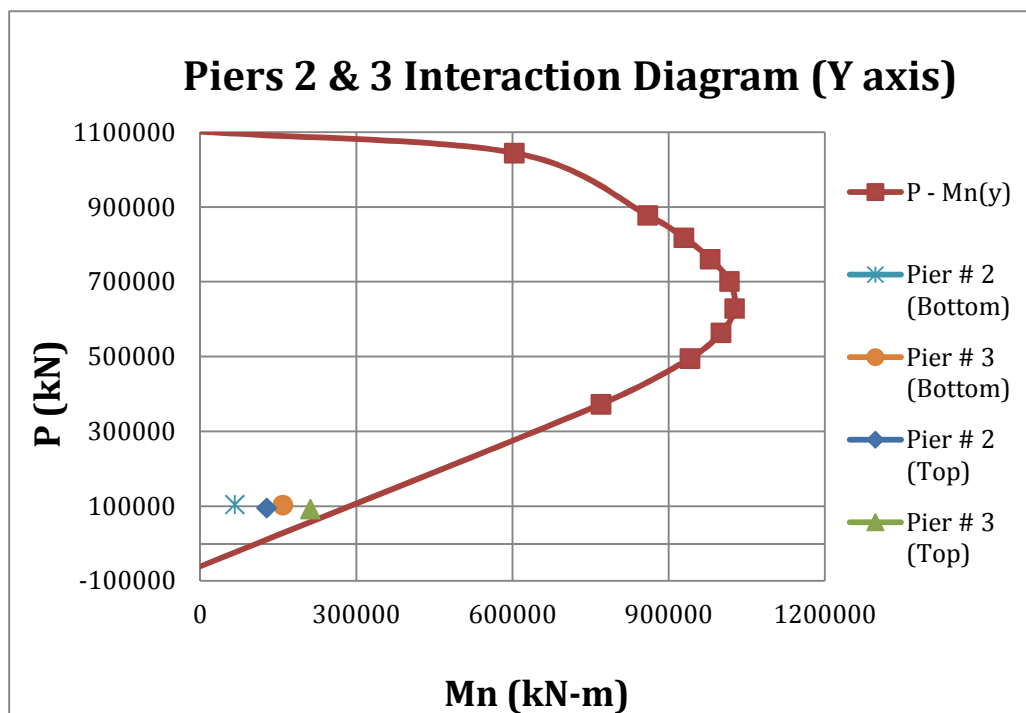


Figure 3. 4. Interaction diagram for Piers 2 and 3 about Y axis.

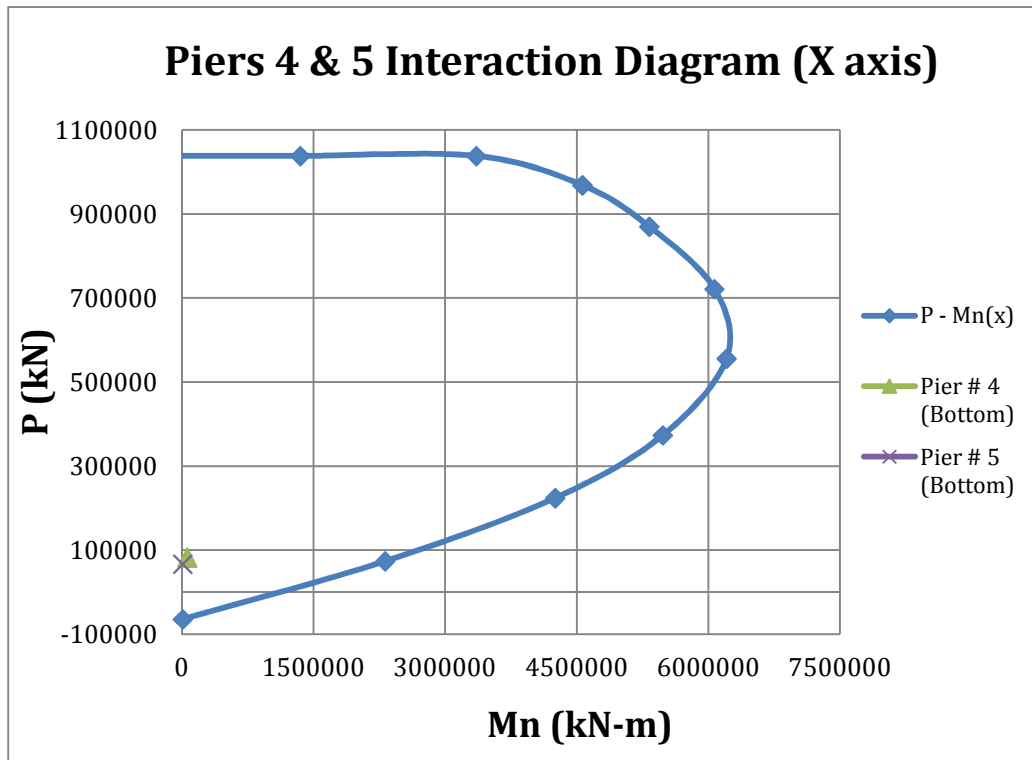


Figure 3. 5. Interaction diagram for Piers 4 and 5 about X axis.

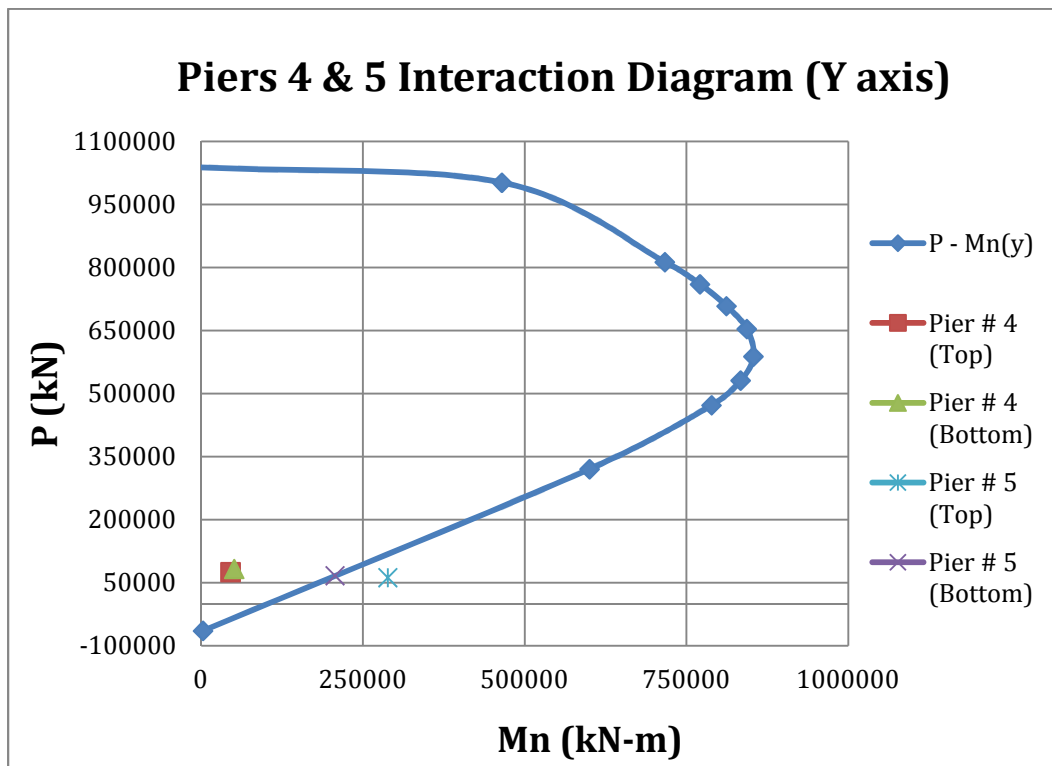


Figure 3. 6. Interaction diagram for Piers 2 and 3 about X axis.

Once determined the moment capacity and moment demand on piers, the C/D ratios were determined considering biaxial effects. This analysis was completed using the provisions of Section 5.7.4.5 from AASHTO 2007: Non Circular Members Subjected to Biaxial Flexure and Compression. The procedure included in this provision can be summarized with the following steps:

If $P_u < .10 \cdot f'_c \cdot A_g$ then:

$$\left[\frac{Mu_x}{Mn_x} + \frac{Mu_y}{Mn_y} \right] \leq 1 \quad (3 - 3)$$

where:

P_u = axial load on piers (top and bottom, kN),

f'_c = compressive strength of concrete (kPa),

A_g = gross area of pier Section (m²),

M_{ux} & M_{uy} = moment demand about respective axis (kN-m), and

M_{nx} & M_{ny} = nominal moment capacity about respective axis (kN-m).

Tables 3.1 and 3.2 include a summary of the results obtained for the biaxial analysis for top and bottom of piers respectively. As noted, all piers met the requirements set forth in AASHTO 2007 for biaxial flexure. However it was required to perform the analysis for anchorage and splicing of reinforcement. C/D ratios due to anchorage and splicing of longitudinal reinforcement are discussed further in this chapter.

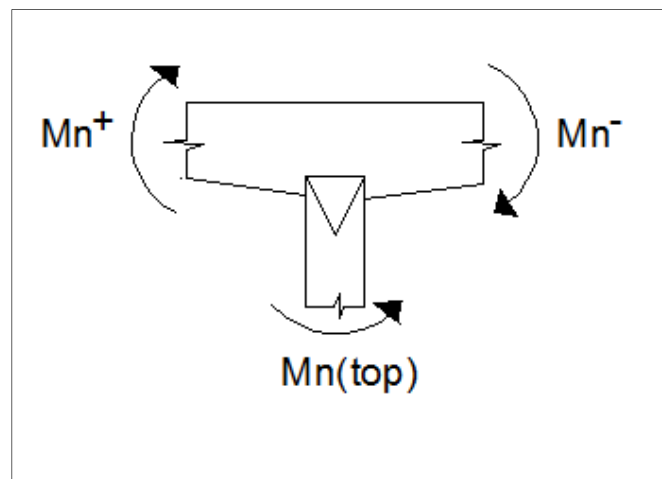
Table 3. 1. Biaxial flexure analysis: Top of Piers.

Biaxial Flexure Analysis (Top of Column)							
Pier #	P_u (kN)	$.10 \cdot f'_c \cdot A_g$ (kN)	M_{ux} (kN-m)	M_{uy} (kN-m)	M_{nx} (kN-m)	M_{ny} (kN-m)	r_{ec}
1	72802	146934	3542	345156	2246866	210468	1.21
2	95811	155687	14130	127460	2591137	277851	4.34
3	92980	155687	8570	211419	2552333	272831	2.56
4	75633	146934	271	45677	2341309	220312	10
5	62476	146934	137	288795	2128490	199885	1.38

Table 3. 2. Biaxial flexure analysis: Bottom of Piers.

Biaxial Flexure Analysis (Bottom of Column)							
Pier #	Pu (kN)	$.10*f_c*Ag$ (kN)	Mu_x (kN-m)	Mu_y (kN-m)	Mn_x (kN-m)	Mn_y (kN-m)	r_{ec}
1	80710	146934	332301	65761	2404007	227686	4.76
2	105693	155687	480664	66304	2718146	294282	5.0
3	103627	155687	132082	158487	2694556	291230	3.33
4	82768	146934	60638	51335	2438271	231988	8.33
5	69755	146934	9599	207178	2205326	208700	2.0

The analysis for top of piers was completed assuming that plastic hinging occurs first at top of pier than at superstructure. In order to validate this assumption it was necessary to compare the capacity at top of pier with the capacity of the superstructure, see Figure 3.7. If the capacity of the superstructure (Mn_s) results greater than piers capacity (Mn_p) then the assumption is validated. Superstructure capacity was determined using computer software SAP2000. Superstructure cross section properties and vertical reinforcement details, see Figure 3. 8, were provided to the software to determine its negative and positive moment capacity. Table 3.3 show the results obtained for the analysis of the superstructure. As noted, superstructure capacity was greater than piers capacity, which means that plastic hinging is expected to occur first at top of pier than at superstructure.

**Figure 3. 7. Plastic hinging analysis at pier–superstructure connection.**

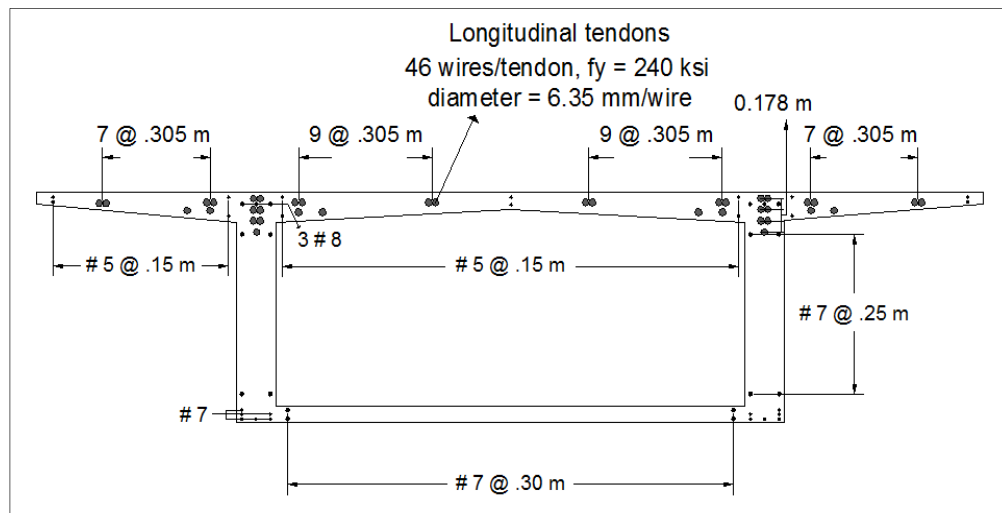


Figure 3. 8. Cross-section properties and reinforcement details for superstructure.

Table 3. 3. Plastic hinge location analysis.

Plastic Hinge Location Analysis					
Piers			Superstructure		
Pier #	Pu (top) (kN)	Mnp (top) (kN-m)	Mn+ (kN-m)	Mn- (kN-m)	Mns = \sum Mn (kN-m)
1	72802	210468	41640	294000	335640
2	95811	277851			
3	92980	272831			
4	75633	220312			
5	62476	199885			

3.2.2 Foundation

For foundation analysis, results were not presented as C/D Ratios as described in the SRMHB. Due to the amount of piles per foundation, the results of this analysis were not presented in tabular form. Bridge No. 2001 is founded on deep foundation and moments on piles are influenced by two of the forces existing at the pile cap level; shear and bending moment. It means that both forces contribute to the bending moment on piles; shear forces also contribute to moment on piles. However, in order to perform the foundation analysis it was necessary to generate the interaction diagram of the pile cross-section shown in Figure 1.12. Reactions on piles, due to the seismic analysis were obtained with computer software GROUP7. Seismic loads at piers base, obtained with SAP2000, were provided to the computer program GROUP7 to

obtain the reactions on each pile. The procedure used by this computer program to obtain the reactions on piles can be described with the following equations:

$$P_{pile} = \left[\frac{P_T}{\# Piles} \pm \frac{M_x * y_i}{\sum_1^n y_i^2} \pm \frac{M_y * x_i}{\sum_1^n x_i^2} \right] * \phi \quad (3 - 4)$$

$$V_{pile} = \left[\frac{V_T}{\# Piles} \right] * \phi \quad (3 - 5)$$

$$M_{pile} = \left[\frac{M_T}{\# Piles} \pm V_{pile} * d_p \right] * \phi \quad (3 - 6)$$

where:

P_{pile} = axial load on pile,

P_T = axial load at piers base,

M_x = bending moment around X-axis,

M_y = bending moment around Y-axis,

X_i = distance from center of pile cap to pile under analysis,

Y_i = distance from center of pile cap to pile under analysis,

V_{pile} = shear reaction on determined pile,

V_T = shear load at the base of the pier in the direction under analysis,

M_T = bending moment at the base of the pier in the direction under analysis,

d_p = distance from bottom of pile cap to the point of fixity of the pile. The point of fixity is that point below the ground level where the pile remains fixed due to the balance between the applied load and the passive pressure of the surrounding soil,

ϕ = group factor, it depends of the position of the pile within the group and the spacing between piles. It varies from 1 to 0.3. Higher values are used for the front row of piles and lower values are used for interior rows. Once the pile configuration is defined in GROUP7, the software determines this factor to automatically reduce the soil resistance.

Figures 3.9 to 3.15 show a summary of the results obtained for piles analysis. These figures include the interaction curve (nominal capacity) for pile cross-section obtained with computer software SAP2000 and also the reactions on

piles (demand loads) obtained with computer software GROUP7. Points out of the curve indicate that demand loads on piles exceed their structural capacity. As shown, the capacity of piles was exceeded in most cases. Foundation failures are unlikely to cause collapse, unless the ground deformations are extremely large due to widespread liquefaction or massive ground failure such as fault rupture (FHWA, 2006). However, retrofitting measures to improve the seismic performance of the piled foundation will be discussed in the following chapter.

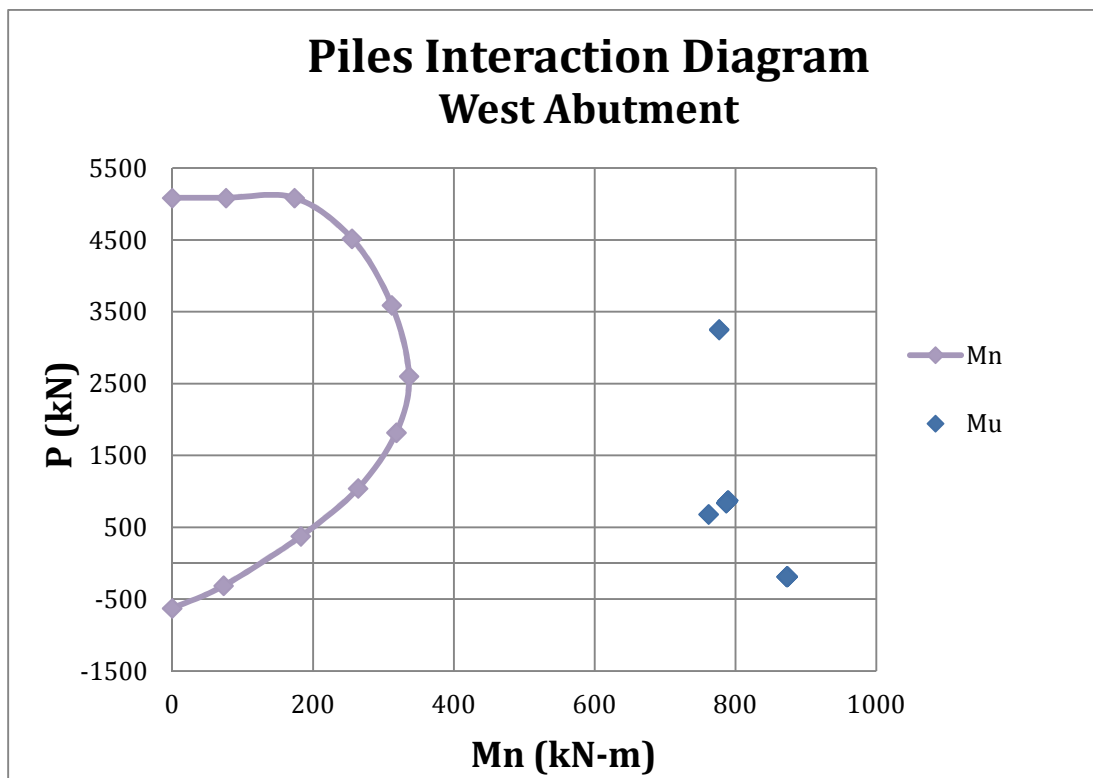


Figure 3. 9. Foundation analysis: West abutment.

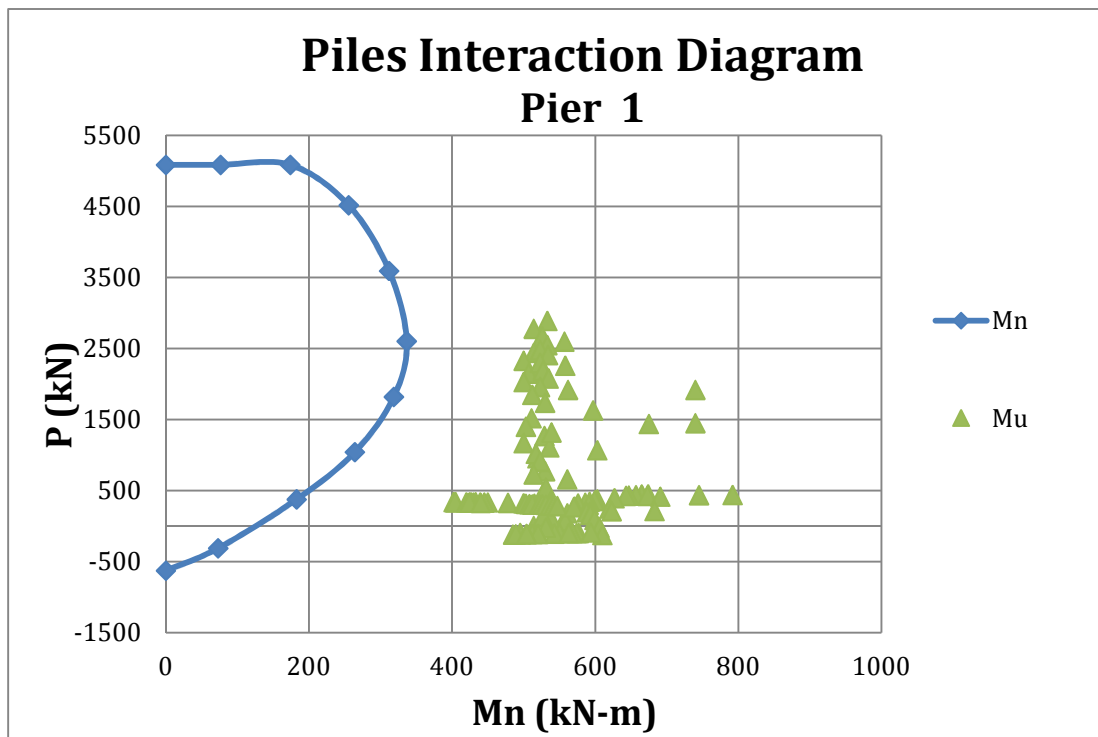


Figure 3. 10. Foundation analysis: Pier 1.

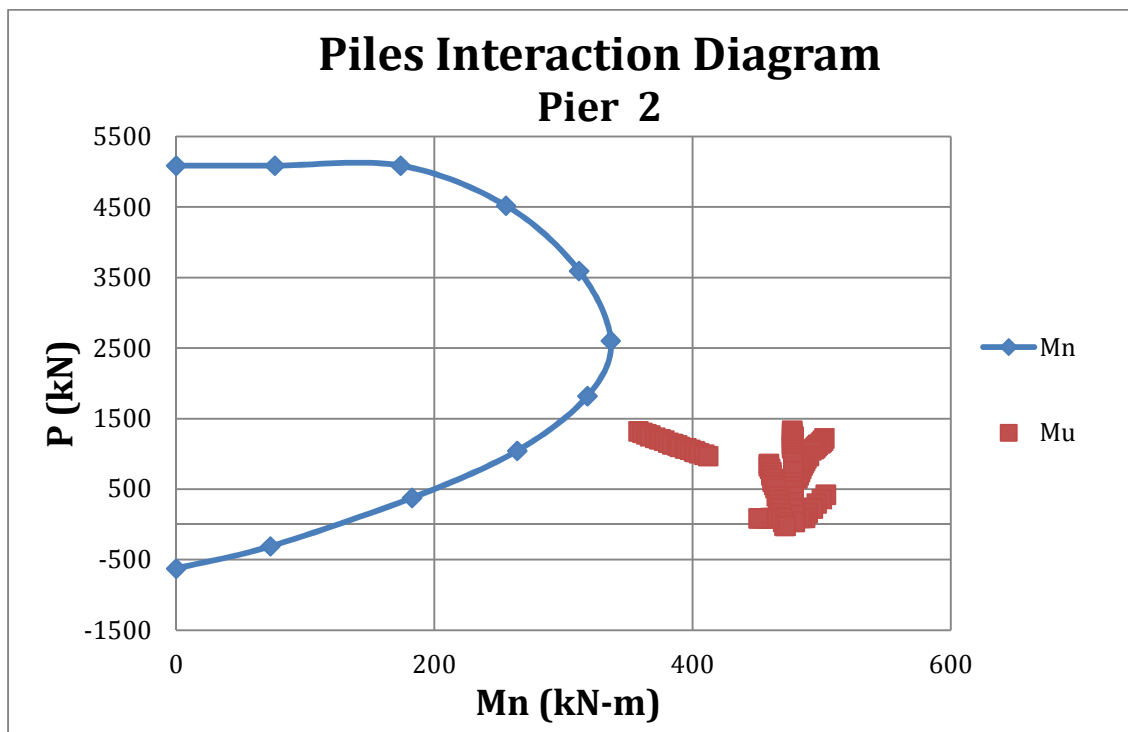


Figure 3. 11. Foundation analysis: Pier 2.

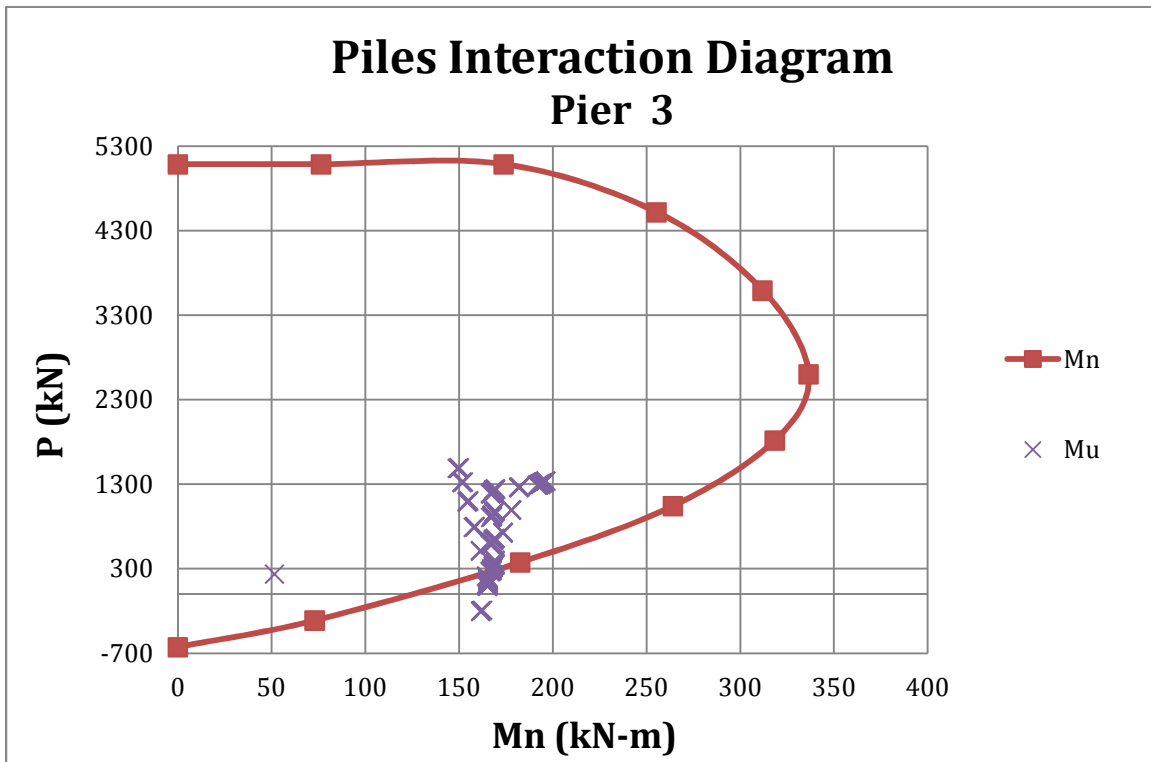


Figure 3. 12. Foundation analysis: Pier 3.

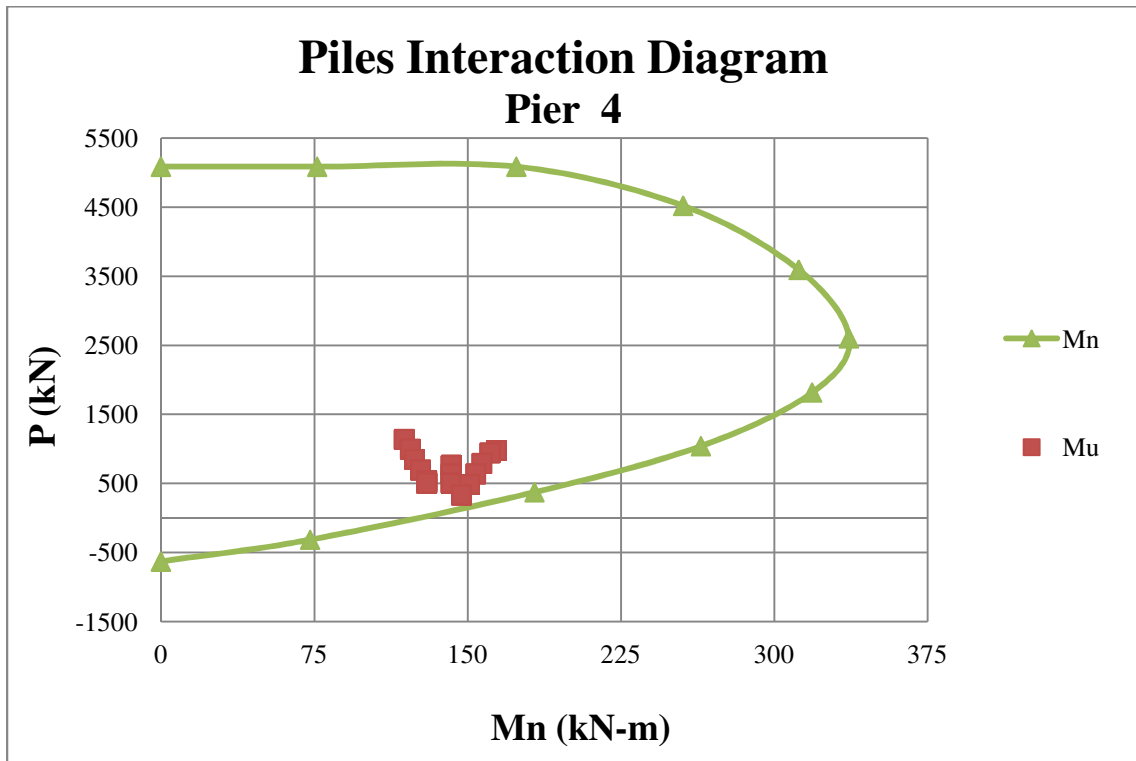


Figure 3. 13. Foundation analysis: Pier 4.

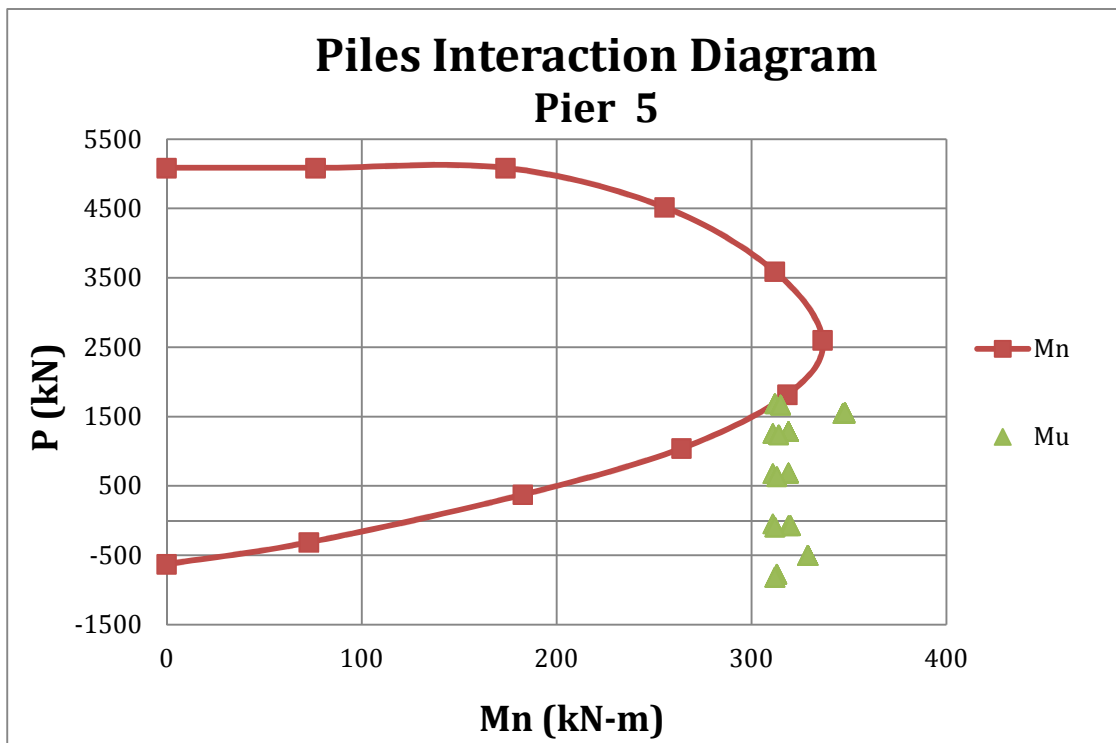


Figure 3. 14. Foundation analysis: Pier 5.

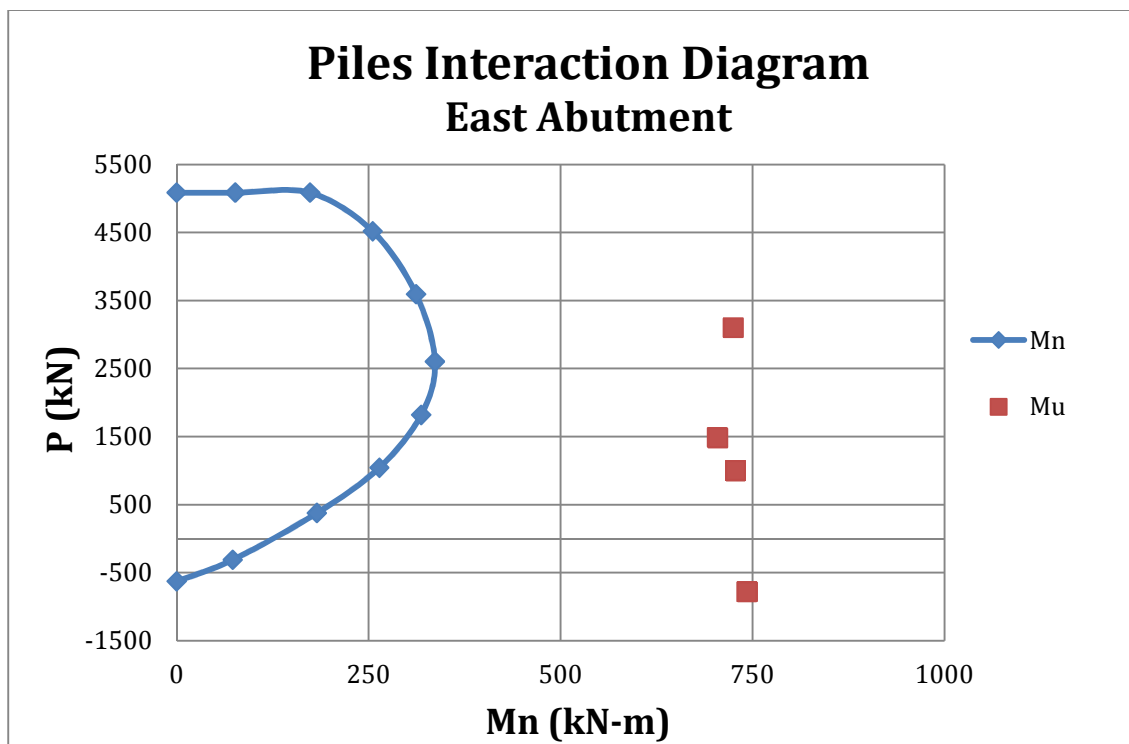


Figure 3. 15. Foundation analysis: East abutment.

3.2.3 Pile Cap

In addition to the analysis conducted for piles and piers, it was also necessary to analyze the component located between them, the pile cap. Pile caps are subjected to vertical reactions from piers and also to bending moments generated by piles located out of the critical section. The critical section is that section around the perimeter of the concentrated load where higher concentrations of stresses are expected to occur. Because of this, it was necessary to analyze the pile cap for punching shear and flexure. Figure 3.16 shows a plan view of the pile caps for bridge No. 2001 and also include the critical section for concentrated loads. The procedure used to complete the punching shear and flexure analyses are discussed in the following sections.

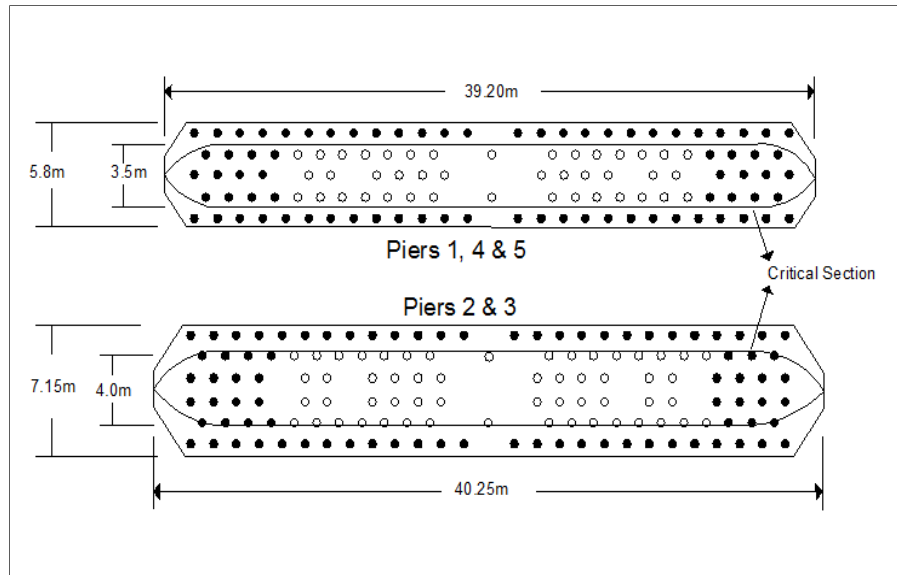


Figure 3. 16. Plan view of pier's pile cap and pile configuration.

3.2.3.1 Flexure

Longitudinal reinforcement is not provided in the short direction of the pile cap. However, due to the size of the pile cap, its capacity was determined based on the capacity of the concrete (cracking moment, M_{cr}). This M_{cr} was compared with the moment demand (M_u) at the critical section. The C/D ratio for flexure at the pile cap (r_{pm}) was determined with the following equation:

$$r_{pm} = M_{cr} / M_u \quad (3 - 7)$$

Moment demands were delivered by those piles located outside of the critical section. If the center of the pile is located within the critical section, it delivers no load to the critical section. As shown in Figure 3.16, most piles are located within piers footprint and only two rows of piles (exterior rows) generate moment with respect to the critical section. Figure 3.17 presents a sketch of those piles that delivers moment with respect to the face of the pier and also the moment arm for both type of piers.

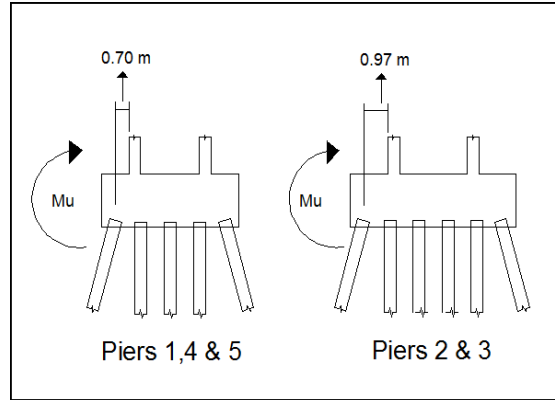


Figure 3. 17. Elevation view for pier's pile cap and piles.

The following equation was used to determine the cracking moment of the pile cap:

$$M_{cr} = \frac{(f_r * I_g)}{y_t * 1000^2} \quad (3 - 8)$$

where:

M_{cr} = cracking moment (kN-m),

f_r = modulus of rupture of concrete (MPa),

$$= .97 * \sqrt{f'_c},$$

f'_c = compressive strength of concrete (MPa, see Table 1.2),

I_g = moment of inertia of the gross concrete section (mm⁴),

$$I_g = \frac{b * y^3}{12} \quad (3 - 9)$$

where:

b = width of the pile cap (mm),

= 39200 mm (Piers 1, 4 & 5),

= 40250 mm (Piers 2 & 3),

y = height of the pile cap (mm),

= 2200 mm, and

y_t = distance from neutral axis to extreme tension fiber, taken conservatively as $(y/2)$ (mm).

Once completed the foundation analysis (Section 3.2.2), the greater loads were identified within the first row of piles (1 – 26). Those loads and the moment arm, see Figure 3.16, were used to complete the flexural analysis of the pile cap. Following equation was used to determine the moment demand at the critical section:

$$M_u = (\sum_1^{26} P_u) * Arm \quad (3 - 10)$$

where:

M_u = moment demand at critical section (kN-m),

P_u = vertical load on pile (kN), and

Arm = moment arm (as defined in Figure 3.16).

Results obtained for these analyses, see Table 3.4, show that concrete capacity (M_{cr}) is enough to withstand the moment demands (M_u) existing at the critical section. However, the lack of longitudinal reinforcement in the short direction of the pile cap reflects a poor seismic design. Recommendations to address this issue will be provided in Chapter IV.

Table 3. 4. Flexural analysis at pile cap.

Flexure at Pile Cap					
Pier #	Piles #	Arm (m)	M_u (kN-m)	M_{cr} (kN-m)	r_{pm}
1	1 @ 26	0.7	6326	40270	6.37
2	1 @ 26	0.97	23335	41349	1.77
3	1 @ 26	0.97	33669	41349	1.23
4	1 @ 26	0.7	18253	40270	2.21
5	1 @ 26	0.7	29162	160952	5.52

3.2.3.2 Punching Shear

Due to the magnitude of the vertical forces existing at piers base, it was required to verify the stresses existing at the pile cap level. The capacity of the pile cap was determined based on the stress capacity of concrete. The stresses due to pier reactions were determined within the footprint of the pier cross section using the following equation:

$$v_u (d) = \left[\frac{V_u}{b_o * d} \right] * 1000 \quad (3 - 11)$$

where:

$vu(d)$ = shear stress demand due to pier load (kPa),

V_u = shear force due to vertical reaction on piers (N),

$$b_o = 2 * [(b + d) + (h + d)] \quad (3 - 12)$$

where:

b_o = perimeter of the critical section, (mm),

b = long dimension of pier,

= 39200 mm (Piers 1, 4 & 5),

= 40250 mm (Piers 2 & 3),

d = 2.078m (effective depth of the pile cap), and

h = short dimension of column,

= 3500 mm (Piers 1, 4 & 5),

= 4000 mm (Piers 2 & 3).

The following equation was used to determine the capacity of the pile cap:

$$v(c) = (.166 * \sqrt{f'c}) * 1000 \quad (3 - 13)$$

where:

$v(c)$ = shear capacity of the pile cap (kPa), and

$f'c$ = compressive strength of concrete (MPa, see Table 1.2).

Once determined the capacity of the pile cap and the seismic demand, the C/D ratio for punching shear (r_{pv}) was determined with the following equation:

$$r_{pv} = v(c)/vu(d) \quad (3 - 14)$$

Table 3.5 present a summary of the results obtained for the punching shear analysis on the pile cap. As noted, the capacity of the pile cap, $[v(c)]$, was greater than the stresses delivered due to pier loads, $[vu(d)]$. These results were expected due to the size of the pile cap.

Table 3. 5. Punching shear analysis at pile cap.

Punching Shear Analysis at Pile Cap					
Pier #	$V_u(N)$	$b_o d (mm^2)$	$vu(d) (kPa)$	$v(c) (kPa)$	r_{pv}
1	72301000	194085200	373	872	2.34
2	90172000	200527000	450	872	1.94
3	88490000	200527000	441	872	1.98
4	71387000	194085200	368	872	2.37
5	55310000	194085200	285	872	3.06

3.3 C/D Ratios for Anchorage of Longitudinal Reinforcement

C/D ratios for anchorage of longitudinal reinforcement were determined at top and bottom of piers regardless of the results obtained once completed the yielding analysis for piers. If inadequate anchorage length is provided for the reinforcing steel, the ultimate capacity of the steel cannot be developed and failure will occur below the ultimate moment capacity of the column (FHWA, 2006). The minimum required anchorage length $[La(d)_{min}]$ was determined for both, straight and 90° hooks, and compared with the anchorage length provided $[La(c)]$, see Figure 3.18. C/D ratios for anchorage were determined with following equation:

$$r_{ca} = La(c)/La(d) \quad (3 - 15)$$

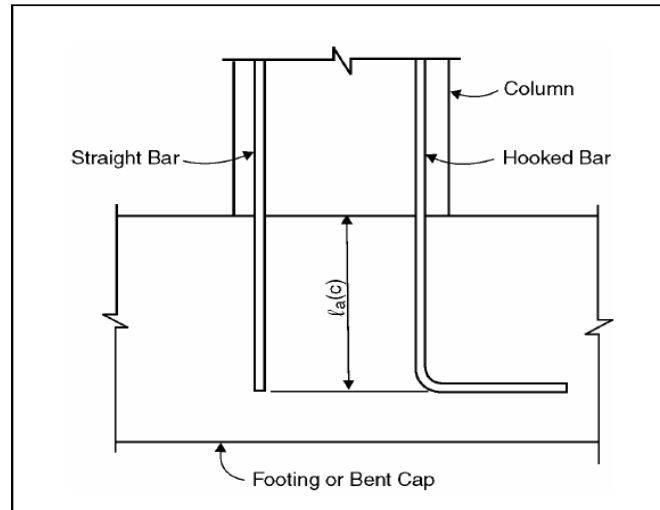


Figure 3. 18. Anchorage of longitudinal reinforcement (FHWA, 2006).

The anchorage length provided on piers was obtained from the design drawings for different type of anchorage:

$La(c) = 330 \text{ mm}$ (90° hooks - top of column),

$La(c) = 1040 \text{ mm}$ (straight bars - top of column), and

$La(c) = 1500 \text{ mm}$ (for 90° hooks - bottom of column).

The required anchorage length was obtained with the following equations for 90° hooks and straight hooks respectively:

$$La(d) = 1200 * km * d_b * \left(2.626 * \frac{f_y}{(60000 * \sqrt{f'_c})} \right) \geq 15d_b \quad (3 - 16)$$

$$La(d) = 2.626 * ks * \left[\frac{d_b}{\left[\left(1 + 2.5 * \frac{c}{d_b} + k_{tr} \right) * \sqrt{f'_c} \right]} \right] \geq 30d_b \quad (3 - 17)$$

where:

$d_b = 15.87$ mm (diameter of spliced bar, #5),

$f_y = 276000$ kPa (yield strength of reinforcing steel),

$f'_c = 31030$ kPa (compressive strength of concrete),

$k_m = 0.7$ for # 11 bars or smaller,

c = lesser of clear cover over the bar or half the clear spacing between adjacent bars,

$c/d_b \leq 2.5$,

$k_s = (f_y - 75845) / 33.1$ (constant for reinforcing steel with yield stress f_y),

$$k_{tr} = \frac{A_{tr}(c) * f_y}{(4137 * s * d_b)} \leq 2.5 \quad (3 - 18)$$

where:

$A_{tr}(c)$ = area of transverse reinforcement normal to potential splitting cracks, and

s = spacing of transverse reinforcement.

The minimum required anchorage length [$La(d)_{min}$] was determined using $c/d_b = 2.5$ and $k_{tr} = 2.5$:

For 90° hooks:

$$La(d)_{min} = 132 \text{ mm},$$

$$15d_b = 240 \text{ mm},$$

As $15d_b$ was greater than $La(d)_{min}$, $15d_b$ will be used as $La(d)_{min}$:

$$La(d)_{min} = 240 \text{ mm}.$$

For straight anchorage:

$$La(d)_{min} = 150 \text{ mm},$$

$$30d_b = 476 \text{ mm},$$

As $30d_b$ was greater than $La(d)_{min}$, $30d_b$ was used as $La(d)_{min}$:

$$La(d)_{min} = 476 \text{ mm}$$

Anchorage provided $L_a(c)$ was greater than $L_a(d)_{\min}$ for both, straight and 90° anchorage. Tables 3.6 and 3.7 show a summary of the anchorage for longitudinal reinforcement on top and bottom of columns. As noted, for all cases, the anchorage length provided exceeds the requirements. However, C/D ratios were determined following the provisions on the SRMHB. For Case B-5 the SRMHB recommends an $r_{ca} = 1$ when anchorage is provided with 90° hooks at top of footing and for Case B-6 recommends a $r_{ca} = 1$ if anchorage is provided at the bent cap.

Table 3. 6. Anchorage of longitudinal reinforcement: Top of Piers.

Anchorage of Longitudinal Reinforcement (Top of Columns)					
Detail #	Anchorage Type	$L_a(c)$ mm	$L_a(d)$ mm (minimum)	Case	r_{ca}
1	Straight	1050	476	B-6	1
2	90° hook	350	240	B-6	1

Table 3. 7. Anchorage of longitudinal reinforcement: Bottom of piers.

Anchorage of Longitudinal Reinforcement (Bottom of Columns)					
Pier #	Anchorage Type	$L_a(c)$ mm	$L_a(d)$ mm (minimum)	Case	r_{ca}
1	90° hook	1500	240	B-5	1
2	90° hook	1500	240	B-5	1
3	90° hook	1500	240	B-5	1
4	90° hook	1500	240	B-5	1
5	90° hook	1500	240	B-5	1

3.4 Splices of Longitudinal Reinforcement

C/D ratios for splices in longitudinal reinforcement (r_{cs}) were verified at top and bottom of piers disregarding if yielding of piers occur or not. The splice length provided at top and bottom of piers were determined from the design drawings. The C/D ratios were determined based on the area of transverse reinforcement provided $A_{tr}(c)$, and the minimum area of transverse reinforcement required for preventing splice failure $A_{tr}(d)$.

$A_{tr}(c) = 200 \text{ mm}^2$, cross-sectional area of confining hoop (# 5)

$$A_{tr}(d) = \frac{s \cdot f_y \cdot A_b}{(L_s \cdot f_{yt})} \quad (3 - 19)$$

where:

$A_b = 200 \text{ mm}^2$ (area of spliced bar (#5)),

$L_s = 760 \text{ mm}$ (existing splice length at bottom of column),

$L_s = 960$ mm (top of column),

$s = 300$ mm (spacing of transverse reinforcement),

$f_y = f_{yt}$ = yield strength of steel (MPa, see Table 1.2),

$A_{tr}(d) = 78.71$ mm² (bottom of column), and

$A_{tr}(c) = 62.58$ mm² (top of column)

$$L_{smin} = \frac{(4885 * db)}{\sqrt{f'_c}} = 440 \text{ mm.}$$

The following cases apply for splices of longitudinal reinforcement:

For:

$$L_s < 4885 * \frac{db}{\sqrt{f'_c}} \quad \text{or}$$

$$A_{tr}(c) < A_{tr}(d) \quad \text{or}$$

$s > 150$ mm, C/D ratios can be obtained with following equation:

$$r_{cs} = \frac{A_{tr}(c)}{A_{tr}(d)} * \left[\frac{\frac{150}{s} * L_s}{\left(4885 * \frac{db}{\sqrt{f'_c}} \right)} \right] * r_{ec} \leq \frac{A_{tr}(c)}{A_{tr}(d)} * r_{ec} \quad (3 - 20)$$

where:

$$150/s \leq 1,$$

$$4885 * \frac{db}{\sqrt{f'_c}} \geq 760,$$

As $4885 * \frac{db}{\sqrt{f'_c}} = 440$ mm ≤ 760 mm, use 760 mm instead of 440 mm.

Tables 3.8 and 3.9 present a summary of the results obtained for the analysis conducted for splicing of longitudinal reinforcement. The area of transverse reinforcement provided, at the top and bottom of piers, exceeded the area of transverse reinforcement required to prevent a splice failure $A_{tr}(d)$.

Table 3.8. Splices of longitudinal reinforcement: Bottom of Piers.

Splices of Longitudinal Reinforcement (Bottom of Column)					
Pier #	r_{ec}	L_s (mm)	$A_{tr}(c) / A_{tr}(d)$	$150/s$	r_{cs}
1	4.76	760	2.54	0.5	6.1
2	5.0	760	2.54	0.5	6.3
3	3.33	760	2.54	0.5	4.2
4	8.33	760	2.54	0.5	10.5
5	2	760	2.54	0.5	2.5

Table 3. 9. Splices of longitudinal reinforcement: Top of piers.

Splices of Longitudinal Reinforcement (Top of Column)					
Pier #	r_{ec}	Ls(mm)	Atr (c) / Atr (d)	150/s	r_{cs}
1	1.21	960	3.19	0.51	2.47
2	4.34	960	3.19	0.51	8.87
3	2.56	960	3.19	0.51	5.23
4	10	960	3.19	0.51	20.44
5	1.38	960	3.19	0.51	2.82

3.5 C/D Ratios for Column Shear

Column shear needs to be verified to determine if shear failure will take effect when shear demand exceeds shear capacity of columns. The procedure used to perform the shear analysis is shown in Table 1.9. C/D ratios for column shear were determined with the following equation:

$$r_{cv} = \frac{Vi(c)}{Ve(d)} \quad (3 - 21)$$

The elastic shear forces [Ve(d)] were obtained from the seismic analysis performed in SAP2000, while shear capacity [Vi(c)] was determined following the seismic requirements in Section 5.10.11 of the AASHTO 2007. The strong direction (transverse direction) was analyzed following the requirements for wall type piers, for weak direction (longitudinal direction), the shear capacity was determined using column requirements. The procedure used to determine the shear capacity of piers will be described in the next Sections.

3.5.1 Strong Direction Analysis

For wall type piers the initial shear resistance should be taken as:

$$Vi (c) = Vr = \frac{0.66\sqrt{f'c} * b * d}{1000} \quad (3 - 22)$$

where:

Vi (c) = Initial shear resistance of the column (kN),

$f'c$ = 31.03 MPa (compressive strength of concrete),

b = 1000 mm (width of the two flanges),

h = 31060 mm (height of the cross-Section), and

d = 0.72*h, per AASHTO LRFD (effective shear depth, mm)
= 22363 mm.

Table 3.10 show a summary of the C/D ratios determined for piers in the strong direction. As expected, shear capacity in the strong direction of piers is enough to resist the expected seismic demand.

Table 3. 10. Column shear C/D ratios: Bottom of Piers.

C/D ratios for Column Shear (Bottom of Column - Strong Direction)					
Pier #	r_{ec}	$V_e(d)$ (kN)	V_u (kN)	$V_i(c) = V_r$ (kN)	r_{cv}
1	4.76	39905	357952	82217	2.06
2	5.0	68805	474978	82217	1.19
3	3.33	15118	417127	82217	5.43
4	8.33	11637	593646	82217	7.06
5	2	2372	702811	82217	34.66

3.5.2 Weak Direction Analysis

As aforementioned, the shear capacity in the weak direction was determined following the column requirements in AASHTO 2007. The initial shear resistance [$V_i(c)$] of columns was determined with the following equations:

$$V_i(c) = V_c + V_s \quad (3 - 23)$$

$$V_c = \frac{.166 \cdot \sqrt{f'_c} \cdot b \cdot d}{1000} \quad (3 - 24)$$

where:

V_c = shear strength provided by concrete (kN),

b = 3998 mm (width of the web),

$d = .72 \cdot h = 2574$ mm (effective depth for piers 1, 4 & 5), and

$d = .72 \cdot h = 2870$ mm (effective depth for piers 2 & 3),

$$V_s = \frac{A_s \cdot f_y \cdot d}{1000 \cdot s} \quad (3 - 25)$$

where:

V_s = shear strength provided by reinforcing steel (kN),

$A_s = 4 \# 5 = 800$ mm² (area of transverse reinforcement),

$f_y = 276$ MPa (yield strength of steel reinforcement), and

$s = 250$ mm (spacing of transverse reinforcement).

Tables 3.11 and 3.12 show the results obtained for the shear analysis of piers in the weak and strong direction respectively. As noted, only two piers result with shear capacity exceeding shear demand. Retrofit measures, for the remaining cases, will be presented in the following chapter to increase the shear capacity as necessary.

Table 3. 11. Column shear C/D ratios: Top of piers, weak direction.

C/D ratios for Column Shear (Top of Piers – Weak Direction)					
Pier #	r_{ec}	V_e (d) (kN)	V_i (c) = $V_s + V_c$		r_{cv}
			V_s (kN)	V_c (kN)	
1	1.21	33605	2273	9515	0.35
2	4.34	9983	2574	10610	1.32
3	2.56	13377	2574	10610	0.98
4	10	8522	2273	9515	1.38
5	1.38	30840	2273	9515	0.38

Table 3. 12. Column shear C/D ratios: Bottom of piers, weak direction.

C/D ratios for Column Shear (Bottom of Piers – Weak Direction)					
Pier #	r_{ec}	V_e (d) (kN)	V_i (c) = $V_s + V_c$		r_{cv}
			V_s (kN)	V_c (kN)	
1	4.76	33864	2273	9515	0.35
2	5.0	10661	2534	10610	1.23
3	3.33	13612	2534	10610	0.97
4	8.33	8835	2273	9515	1.33
5	2.0	30872	2273	9515	0.38

3.6 Force C/D Ratios

Force C/D ratios (r_{bf}) were determined for hinge connections located at abutments and interior spans (see Figure 1.5). Hinge connections do not transmit moment in longitudinal direction but have the capability to transmit moment in the transverse direction. Forces existing at the hinge connection include: transverse shear, vertical shear (due to shear force and torsion), and axial forces (due to tension and transverse moment). Transverse shear is resisted by shear keys provided at abutments and hinge connection. Vertical shear and axial loads should be resisted by two steel beams provided at the web of the concrete box girder. Figure 3.19, obtained from the design drawings, show both components; shear key and hinge beam. C/D ratios for these forces were determined using equation 3 – 26. The procedure used to analyze these components is described in detail in the following sections.

$$r_{bf} = V_b(c)/V_b(d)$$

(3 - 26)

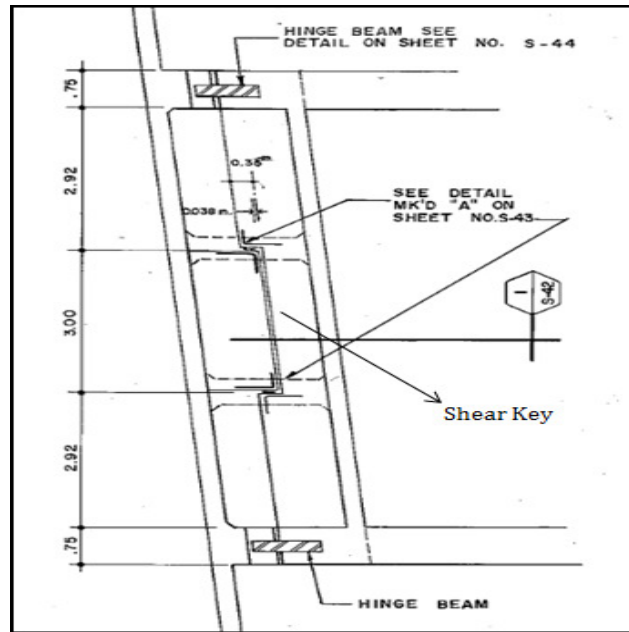


Figure 3.19. Elevation view for hinge beams and shear key.

3.6.1 Transverse Forces

As aforementioned, transverse forces delivered due to seismic loads, $[V_b(d)]$, should be resisted by shear keys located at the abutments and hinge connections at interior spans. The capacity of the shear key, $[V_b(c)]$, depend on the contribution of the reinforcing steel (V_s) and the contribution of the concrete (V_c), as defined by the following equation:

$$V_b(c) = V_c + V_s \quad (3 - 27)$$

$$V_c = \frac{.2 * \sqrt{f'c} * b * h}{1000} \quad (3 - 28)$$

where:

V_c = concrete contribution to the strength of the shear key (kN),

$f'c$ = compressive strength of concrete,

= 34.48 MPa (superstructure),

= 31.03 MPa (abutment),

h = height of shear key,

= 560mm (at hinge),

= 600 mm (at abutment), and

b = 3000 mm, width of the shear key

$$V_s = \frac{\mu * A_s * f_y}{1000} \quad (3 - 29)$$

where:

V_s = steel contribution to the strength of the shear key (kN),

A_s = area of vertical reinforcement within the shear key (12 # 4 & 19 # 5),

= 5277 mm² (at hinge, 12#4 & 19 # 5),

= 2573 mm² (at abutment, 12#4 & 13 # 5),

f_y = 275.89 Mpa (yield strength of reinforcement steel), and

μ = friction coefficient,

= 1.4 * α (α = 1.0 for normal weight concrete).

Table 3.13 shows a summary of the results obtained for the transverse forces analysis. As noted, the existing loads at interior spans, for three cases, exceed the capacity provided by the shear key. A failure at the hinge level could cause the failure or collapse of the superstructure. Recommendations to improve the connection at interior spans will be provided in the following chapter.

Table 3. 13. Transverse shear C/D ratios.

Force Capacity/Demand Ratio (Transverse Shear)				
Shear Key Location	V_b (d) (kN)	V_b (c) (kN)		r_{bf}
		V_s (kN)	V_c (kN)	
West Abutment	1556	1580	2005	1.80
Span 2	5369	2038	1972	0.74
Span 3	5135	2038	1972	0.78
Span 4	4093	2038	1972	0.97
Span 5	1085	2038	1972	3.69
East Abutment	343	1580	2005	10.45

3.6.2 Vertical Forces

Two steel beams are responsible for resisting the vertical shear forces existing at hinge connection. These forces are mostly resisted by the web of the steel beams. Figure 3.20 show the location of the hinge beam and Figure 3.21 shows a cross-section view of the steel beam. The shear capacity provided by the steel beams was determined with the following equation:

$$V_b(c) = 2 * (.6 * A_w * f_y) \quad (3 - 30)$$

where:

$V_b(c)$ = shear capacity for two beams (kN),

$A_w = .00533\text{m}^2$ (web area), and

$f_y = 344737 \text{ kPa}$ (yield strength of the steel beam).

Shear forces delivered to the steel beams can be defined as follows:

$$V_b(d) = V_u + \frac{T_u}{L} \quad (3 - 31)$$

where:

$V_b(d)$ = total vertical shear demand (kN),

V_u = vertical shear demand (kN),

T_u = torsion moment demand at hinge connection (kN-m), and

L = distance between steel beams (m).

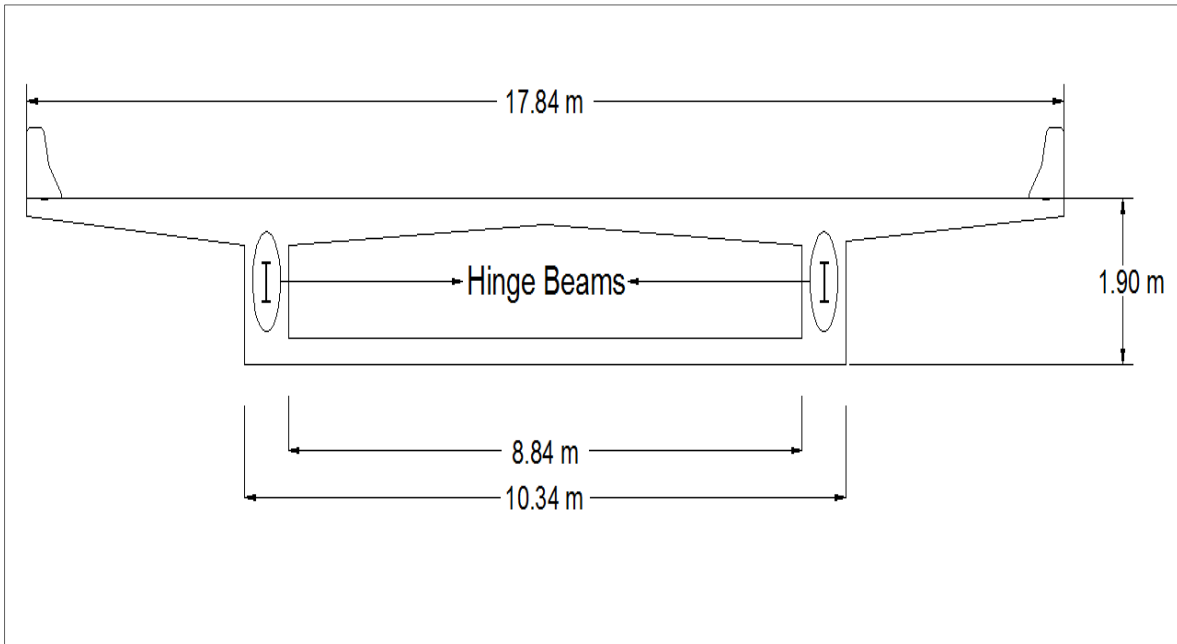


Figure 3. 20. Hinge beam location.

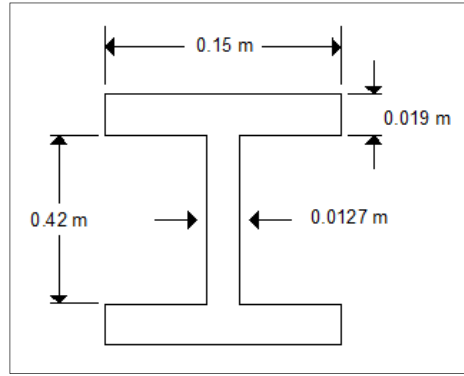


Figure 3. 21. Cross-section view of the hinge beam.

Table 3.14 shows a summary of the results obtained for the analysis of vertical shear forces. As noted, demand forces exceed the capacity provided by the steel beams at interior span hinges. Recommendations to improve the connection at interior spans will be provided in the next chapter.

Table 3. 14. Vertical shear C/D ratios.

Force Capacity/Demand Ratio (Vertical Shear)						
Hinge Location	V _u (kN)	T _u (kN-m)	L(m)	V _b (d) (kN)	V _b (c) (kN)	r _{bf}
West Abutment	1588	1999	9.6	1796	2206	1.23
Span 2	5728	4564	9.6	6203	2206	0.36
Span 3	5786	5606	9.6	6370	2206	0.35
Span 4	4658	110	9.6	4669	2206	0.47
Span 5	3670	74	9.6	3678	2206	0.60
East Abutment	2043	14	9.6	2044	2206	1.08

3.6.3 Axial Forces

Axial forces at hinge connection level were delivered by tensile forces and transverse moments. Two steel beams provided at this location, see Figure 3.20, are responsible for resisting these forces. The total axial load to be resisted by each steel beam can be obtained with the following equation:

$$P(d) = \frac{P_u}{2} + \frac{M_{tu}}{L} \quad (3 - 32)$$

where:

P (d) = total axial demand load (kN),

P_u = axial load at hinge connection (kN),

M_{tu} = transverse moment demand at hinge connection (kN-m), and

L = distance between steel beams (m).

The axial capacity of the steel beam was determined as follows:

$$P(c) = A_f * f_y \quad (3 - 33)$$

where:

$P(c)$ = axial capacity of the steel beam (kN),

$A_f = 0.0057 \text{ m}^2$ (flange area), and

$f_y = 344.87 \text{ MPa}$ (yield strength of the steel beam).

Table 3.15 includes a summary with the results obtained for the analysis of axial forces. As noted, the capacity provide by the steel beams is not enough to withstand the demand loads. Recommendations to address this lack of capacity at the hinge level will be provided in the following chapter.

Table 3. 15. Axial forces C/D ratios.

Force Capacity/Demand Ratio (Axial Forces)						
Hinge Location	Pu (kN)	Mu (kN-m)	L (m)	P _b (d) (kN)	P _b (c) (kN)	r _{bf}
Span 2	12763	208898	9.6	28142	2002	0.07
Span 3	14796	224647	9.6	30799	2002	0.06
Span 4	13700	123229	9.6	19686	2002	0.10
Span 5	12900	30523	9.6	9629	2002	0.20

3.7 Displacement C/D Ratios

Displacement C/D ratios were calculated to determine if the support length provided to the superstructure is enough to accommodate anticipated displacements. These ratios need to be determined for abutments, piers and expansion bearing joints. Due to the monolithic construction at the beam–pier level and hinge connections existing at interior spans of bridge No. 2001, displacement C/D ratios were determined only at the abutments. Following equation was used to determine displacement C/D ratios:

$$r_{bd} = N(c)/N(d) \quad (3 - 34)$$

The minimum support length required $[N(d)]$ was calculated and compared with the support length provided to the superstructure $[N(c)]$. The following equation was used to determine the minimum support length required:

$$N(d) = \left[100 + 1.7 * L + 7 * H + 50 * \sqrt{H} * \sqrt{1 + \left(2 * \frac{B}{L} \right)^2} \right] * \frac{1 + 1.25 * F_v * S_1}{\cos(\alpha)} \quad (3 - 35)$$

where:

N (d) = minimum seat width required (m),

L = distance between joints (m),

H = tallest pier between the joints (m),

B = width of the superstructure (m),

α = skew angle of the bridge (degrees),

Fv = site factor in long period range,

S1 = spectral acceleration at 1.0 sec. period, and

N(c) = seat width provided (m)

Table 3.16 present a summary of the C/D ratios obtained for the displacement analysis. Results obtained demonstrate that support length provided to the superstructure at the abutment level is appropriate to accommodate the displacement demands.

Table 3. 16. Displacement C/D ratios.

Displacement Capacity/Demand ratios							
Fv =	1.96	S1 =	0.22	α =	5.6	B(m) =	17.84
Location	L	H	B/L	N(c)	N(d)	r _{bd}	
West Abutment	42.5	9.06	0.420	0.920	0.655	1.40	
East Abutment	37.5	6.98	0.476	0.920	0.584	1.58	

3.8 C/D Ratios for Abutments

C/D ratio calculation to determine abutment failure was based on their displacement capacity vs. displacement demand. Usually these types of failures alone do not result in collapse or impairment of the ability of the structure to carry emergency traffic loadings (FHWA, 2006). Displacement demands [D(d)] were obtained from the seismic analysis while displacement capacity [D(c)] was taken as 75mm in the transverse direction and 150mm in the longitudinal direction as recommended by FHWA 2006. These values are based on engineering judgment as

result of experience with past earthquakes. Following equation was used to determine the C/D ratio for abutments:

$$r_{ad} = D(c) / D(d). \quad (3 - 36)$$

Table 3.17 presents a summary of the C/D ratio calculations for abutments. As noted, the displacement capacity at the abutment level is enough to accommodate the seismic demand.

Table 3. 17. Abutments C/D ratios.

Capacity Demand ratio for Abutments			
Location	D (d) (mm)	D(c) (mm)	r_{ad}
West Abutment	7.4	150	20.3
East Abutment	3.8	150	39.5

3.9 C/D Ratios for Soil Liquefaction

Liquefaction is a seismically induced loss of shear strength in loose, cohesionless soil that results from build-up of pore water pressure in the soil as it tries to consolidate during strong motion shaking (FHWA, 2006). When soil moves, due to the seismic event, pore water pressure increase, if water pressure reaches the cohesive resistance of soils, soil particles can't stay together resulting in a loss of foundation support due to liquefaction. Liquefaction is expected to occur within the first 9 meters below the ground surface and it depends on the soil properties, earthquake magnitude and earthquake duration. High magnitude with short duration may not induce liquefaction; otherwise, a moderate magnitude earthquake with long duration can easily induce soil liquefaction. C/D ratios for liquefaction were determined as the ratio between the effective peak ground acceleration at which liquefaction is expected to occur $[AL(c)]$ and the effective acceleration coefficient for the site under investigation $[AL(d)]$. The effective acceleration coefficient was determined as $.4 * S_s / g$, as recommended by FHWA 2006. The effective peak ground acceleration at which liquefaction is expected to occur was determined using the empirical method (Seed and Idriss, 1971) consisting on the following equation:

$$\frac{\tau}{\sigma'} = .65 * r_d * AL(c) * \left(\frac{\sigma}{\sigma'} \right) \quad (3 - 37)$$

where:

τ/σ' = average stress ratio at which liquefaction is expected to occur,

r_d = stress reduction factor (varies linearly from 1 at the ground surface to .9 at 9m depth),

$AL(c)$ = effective peak ground acceleration at which liquefaction is expected to occur (m/s^2),

σ = total overburden pressure at sand layer investigated (MPa), and

σ' = initial effective overburden pressure at sand layer investigated.

In order to determine the average stress ratio at which liquefaction is expected to occur, it was required to determine the modified penetration resistance (N_1) for the soil layer under investigation. The modified penetration resistance depends of the effective overburden pressure, average standard penetration resistance and the corrective factor for the average standard penetration resistance (C_N). The relation between the modified penetration resistance and the average standard penetration resistance can be described with the following equation:

$$N_1 = C_N * N \quad (3 - 38)$$

Figures 3.22 and 3.23 were used in combination with the average standard penetration resistance and the effective overburden pressure to determine the average stress ratio at which liquefaction was expected to occur in the layer under investigation. In addition to the average stress ratio, earthquake magnitude is also an important factor when determining susceptibility of soils to liquefy. Results obtained after the analysis show that for the same soil layer the susceptibility of soil to liquefy increases as earthquake magnitude increase. Tables 3.18 to 3.20 present a summary of the C/D ratios calculation for soil liquefaction at different earthquake magnitudes. As noted, for all cases C/D ratios were greater than 1. However, for the liquefaction analysis, having a C/D ratio greater than one is not enough to conclude that liquefaction is not expected to occur. It is suggested that a factor of safety of 1.5 is desirable to establish a reasonable margin of safety against liquefaction in the case of important bridge sites (AASHTO, 2007). Based on the three earthquake magnitudes considered during the analysis for bridge No. 2001, soils underneath Pier # 2 were the most susceptible to liquefy. However, as the earthquake magnitude increase to 8%,

there are three piers founded on soils with C/D ratios less than 1.5. Recommendations to address the susceptibility of soils to liquefy will be provided in the following chapter.

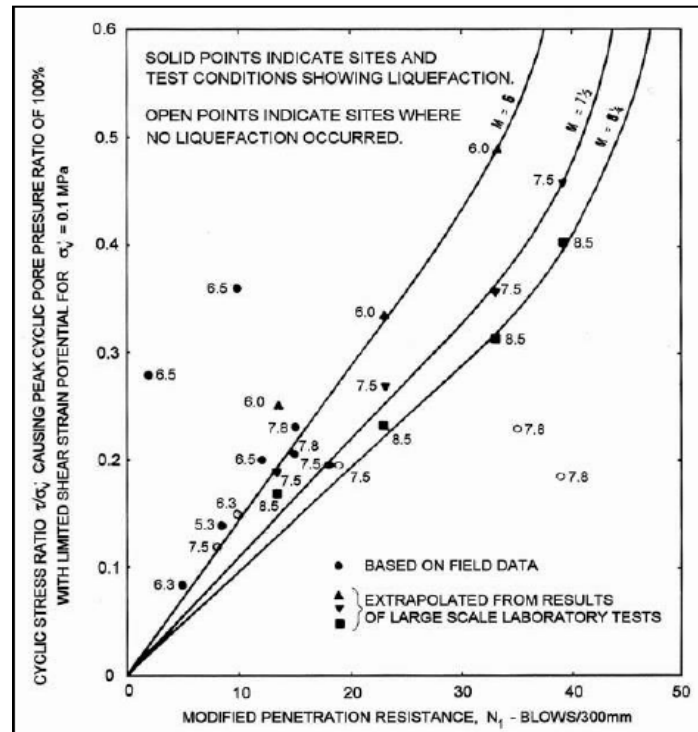


Figure 3. 22. Modified penetration resistance (AASHTO, 2007).

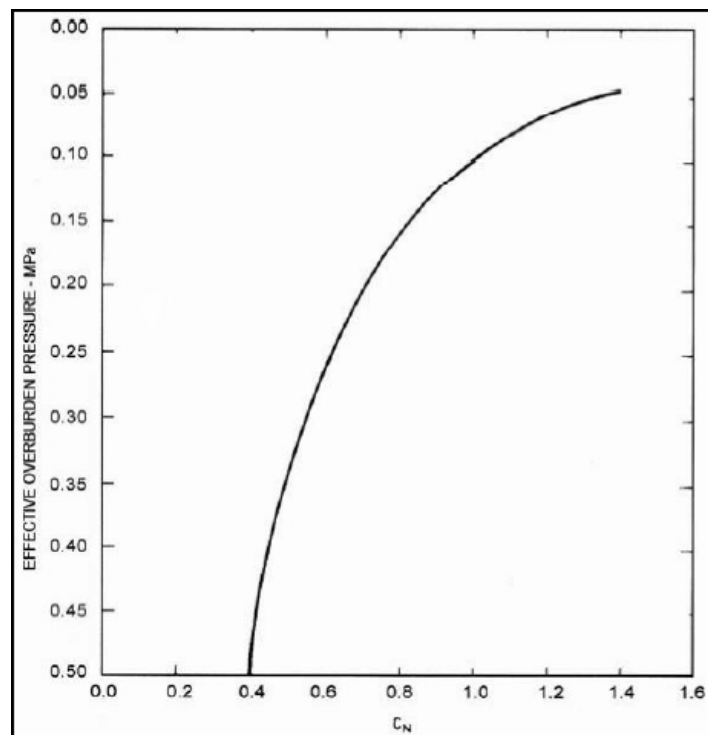


Figure 3. 23. Relationship between C_N and σ' (AASHTO, 2007).

Table 3. 18. Liquefaction C/D ratios: M = 6%.

Capacity/Demand Ratios for Liquefaction (Magnitude = 6%)									
Location	# of Layers	Thickness (m)	σ (Mpa)	σ' (Mpa)	r_d	τ/σ'	AL(c)	AL(d)	r_{sl}
WA	1	14.7	0.321	0.16	0.9	0.1	0.085	0.026	3.28
Pier 1	1	17.06	0.308	0.166	0.9	0.04	0.037	0.026	1.42
Pier 2	2	9.45	0.17	0.078	0.9	0.062	0.049	0.026	1.87
		12.8	0.416	0.198	0.9	0.19	0.155	0.026	5.95
Pier 3	1	5.18	0.093	0.042	0.95	0.075	0.055	0.026	2.11
Pier 4	1	15.25	0.282	0.144	0.9	0.09	0.079	0.026	3.02
Pier 5	N/A (Cohesive soils)								
EA	N/A (Cohesive soils)								

Table 3. 19. Liquefaction C/D ratios: M = 7%.

Capacity/Demand Ratios for Liquefaction (Magnitude = 7%)									
Location	# of Layers	Thickness (m)	σ (Mpa)	σ' (Mpa)	r_d	τ/σ'	AL(c)	AL(d)	r_{sl}
WA	1	14.7	0.321	0.16	0.9	0.075	0.064	0.026	2.44
Pier 1	1	17.06	0.308	0.166	0.9	0.03	0.028	0.026	1.06
Pier 2	2	9.45	0.17	0.078	0.9	0.048	0.038	0.026	1.44
		12.8	0.416	0.198	0.9	0.14	0.114	0.026	4.36
Pier 3	1	5.18	0.093	0.042	0.95	0.055	0.040	0.026	1.54
Pier 4	1	15.25	0.282	0.144	0.9	0.071	0.062	0.026	2.37
Pier 5	N/A (Cohesive soils)								
EA	N/A (Cohesive soils)								

Table 3. 20. Liquefaction C/D ratios: M = 8%.

Capacity/Demand Ratios for Liquefaction (M = 8%)									
Location	# of Layers	Thickness (m)	σ (Mpa)	σ' (Mpa)	r_d	τ/σ'	AL(c)	AL(d)	r_{sl}
WA	1	14.7	0.321	0.160	0.9	0.063	0.053	0.026	2.05
Pier 1	1	17.06	0.308	0.166	0.9	0.029	0.026	0.026	1.02
Pier 2	2	9.45	0.170	0.078	0.9	0.04	0.031	0.026	1.20
		12.8	0.416	0.198	0.9	0.12	0.097	0.026	3.73
Pier 3	1	5.18	0.093	0.042	0.95	0.049	0.035	0.026	1.37
Pier 4	1	15.25	0.282	0.144	0.9	0.061	0.053	0.026	2.04
Pier 5	N/A (Cohesive soils)								
EA	N/A (Cohesive soils)								

CHAPTER IV: Retrofitting Measures

4.1 Introduction

Once completed the seismic analysis for Bridge No. 2001, various components were determined to be in need of attention and possible retrofitting. The objective of retrofitting a bridge is to ensure that it will perform satisfactorily when subjected to the design earthquake (FHWA, 2006). Recommendations to improve the seismic performance of these components, as well as the seismic performance of the bridge will be provided in the following sections.

4.2 Cantilever Connection Strengthening

Forces C/D ratios were determined for hinge connections and shear keys existing at abutments and interior spans. These ratios were determined for transverse forces, vertical forces and axial forces. The seismic demand exceeded the capacity of the connection at interior spans, see Tables 3.13 to 3.15. Recommendations to improve the capacity at connection level will be discussed further in the following sections.

4.2.1 Hinge Connection

Forces existing at the hinge connection (vertical shear and axial loads) are mainly resisted by two steel beams provided at both webs of the concrete box girder. Results obtained after the seismic analysis demonstrated that seismic demand loads exceeded the capacity provided by the steel beams. The strengthening of the hinge connection can be achieved by increasing the size and strength of the steel section. A wider section with greater depth, web thickness and flange thickness should be able to resist the demand loads. A steel section with higher yield strength can also be considered for the strengthening of the hinge connection. Elastomeric bearing pads with continuous high strength anchor bolts drilled and grouted into existing concrete should be provided at one side of the steel beam to allow the rotation of the beam at the hinge connection. A fixed connection of the beam to the concrete should be provided at the other side of the beam. Anchor bolts should

be able to resist and transmit, by shear, the loads exerted on the steel section. Figures 4.1 and 4.2 show a cross section view and side view of the proposed steel section. However, the final size and the number of anchor bolts should be based on the design requirements.

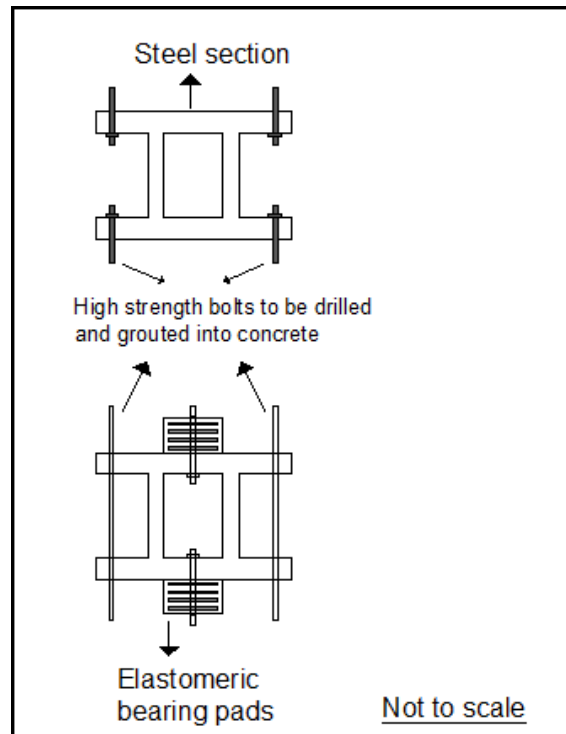


Figure 4. 1 Proposed steel section for hinge connection retrofitting.

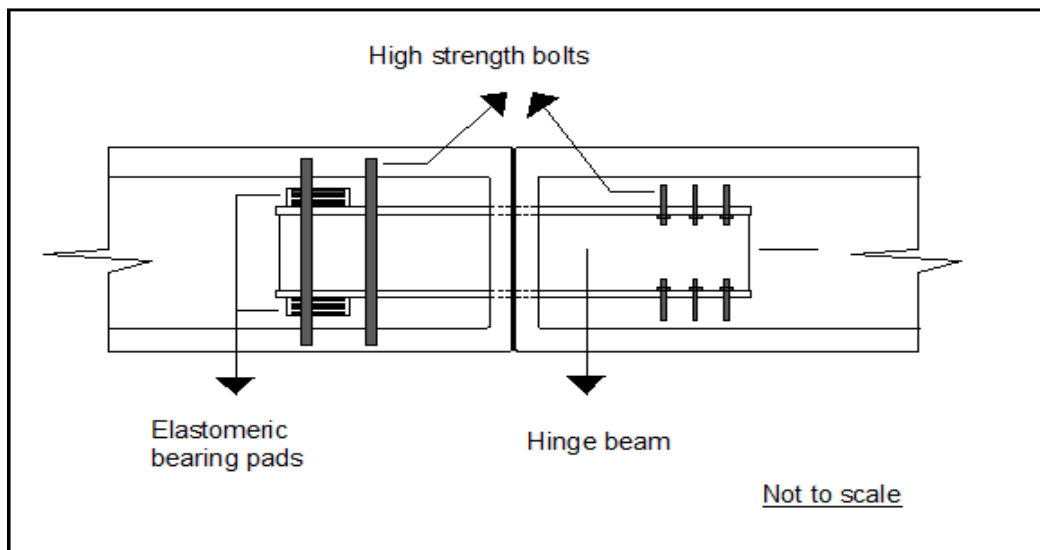


Figure 4. 2 Side view of the proposed hinge connection retrofitting.

4.2.2 Shear keys

Shear keys at interior spans were also determined to be in need of retrofitting, see Table 3.13. Strengthening of the shear keys can be obtained by providing additional shear keys at the connection level. Figures 4.3 and 4.4 show a cross section view and a plan view of the proposed alternative to improve the shear keys. This strengthening consists on providing the bottom slab of the concrete box girder with hollow structural steel sections (HSS) that creates a shear key. These HSS should be filled with concrete and welded to a steel plate. The steel plates should be bolted to the bottom slab by using high strength bolts. The number of HSS and bolts should be based on design requirements.

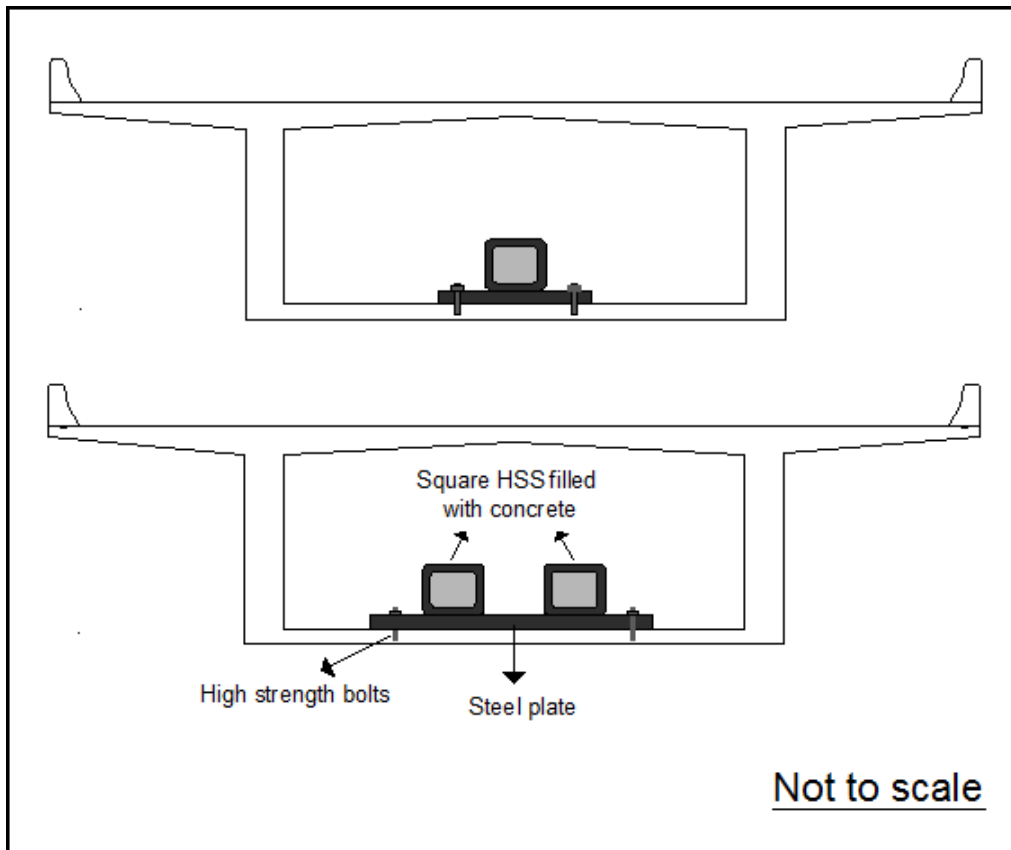


Figure 4. 3 Cross-section view of the proposed retrofitting measure for shear keys.

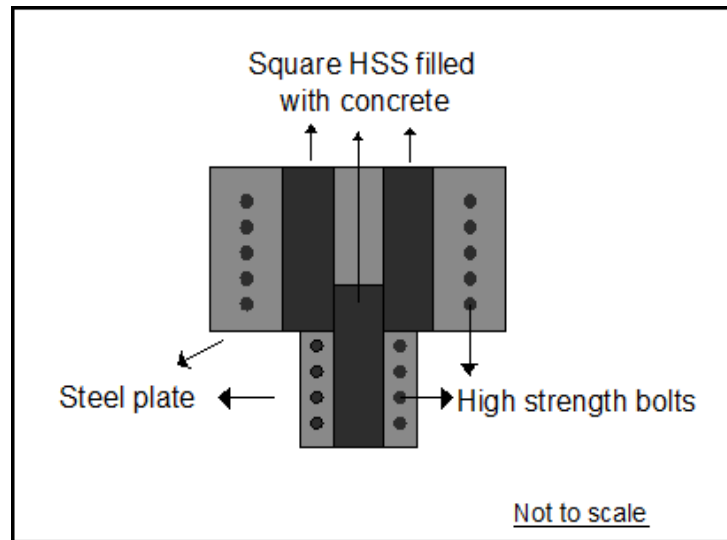


Figure 4. 4. Plan view of the proposed retrofitting measure for shear keys.

4.3 Diaphragm Strengthening

It was noted in the design drawings, see Figure 4.5, that diaphragms provided at the superstructure-pier level are not solid at all. If it is not practical to make diaphragms strong enough to resist loads elastically, brittle or non-ductile diaphragm failure modes could occur (FHWA, 2006). Strengthening of diaphragms can be reached by filling the hollow sections with concrete and providing adequate reinforcement to make it solid. In addition, an adequate connection should be provided between the new and existing concrete.

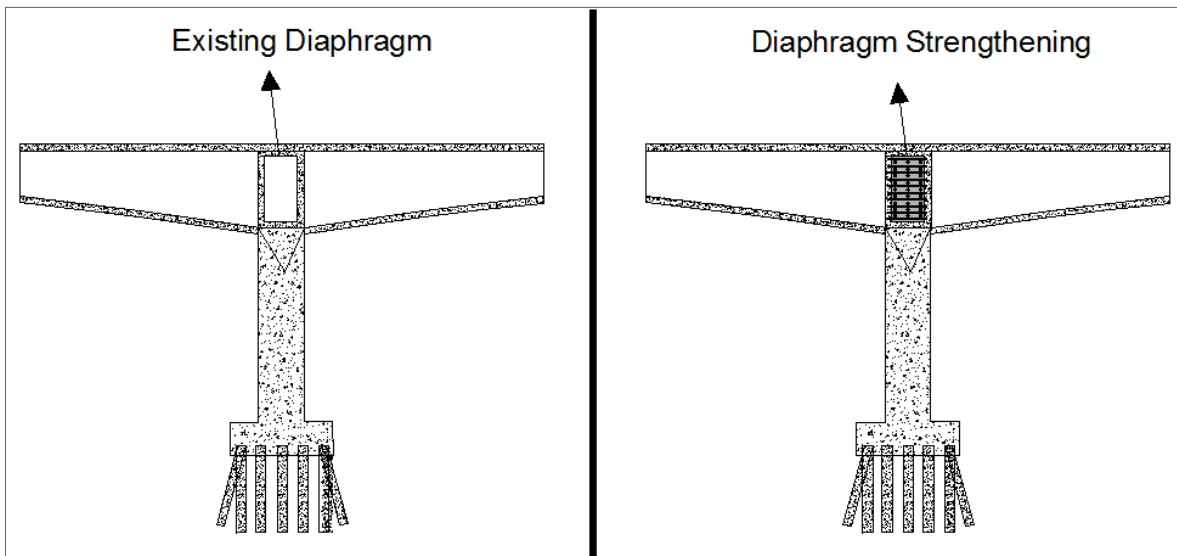


Figure 4. 5. Diaphragm strengthening.

4.4 Substructure Strengthening

After the completion of the seismic analysis for bridge No. 2001, various members of the substructure were found to be in need of attention and possible retrofitting. These members include; piers, pile caps and piled foundation. Retrofitting measures to strengthen these members will be discussed in the following sections.

4.4.1 Piers

Column shear C/D ratios demonstrated that the shear capacity of piers in the weak direction was exceeded by the seismic demand loads, see Tables 3.11 and 3.12. Strengthening of piers in the weak direction can be achieved by filling with concrete some of the hollows existing on piers, see Figure 4.6. An adequate connection should be provided between the existing and new concrete. With this retrofitting measure the capacity provided by the concrete (equation 3-24), will be increased.

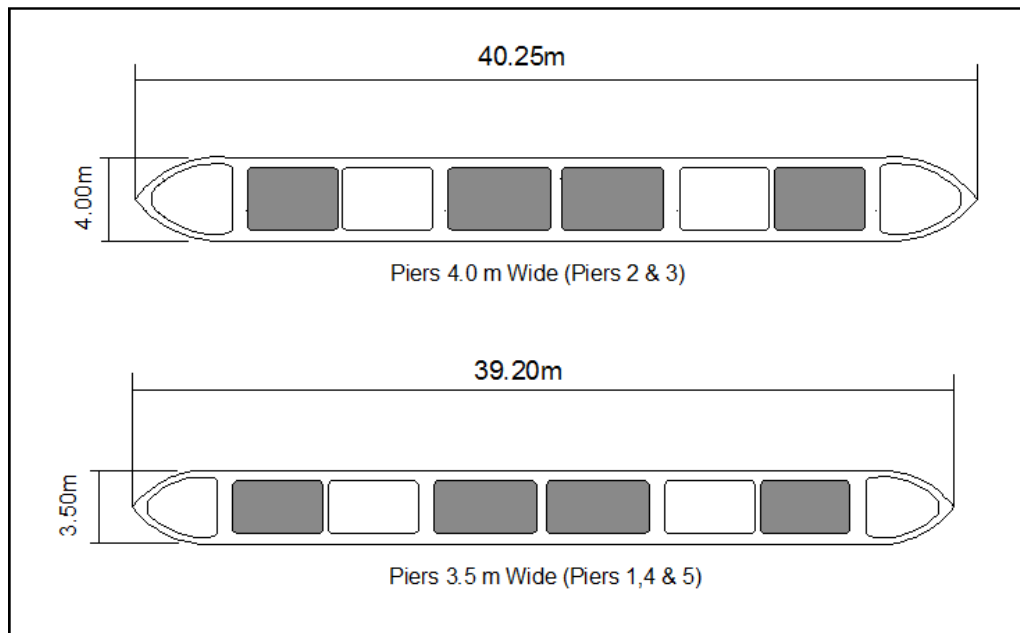


Figure 4. 6. Piers strengthening, plan view.

4.4.2 Pile Cap and Piled Foundation

The analysis performed on the pile cap, Sec. 3.2.2, demonstrated that the capacity of the pile cap is enough to withstand the seismic demand loads. However, it was noted the lack of longitudinal reinforcement in the short direction of the pile cap, which reflects a poor seismic design. In addition, once completed the analysis of the piled foundation, it was found that demand loads on piles exceeded the structural capacity for most piles. Strengthening of the piled foundation requires adding additional piles as well as increasing the size of the pile cap. With the increase on the size of the pile cap, it will be required to provide adequate transverse and longitudinal reinforcement in the new concrete and connect it to the existing concrete. The adequate connection between the old and new concrete can be achieved with the use of dowel bars. Figures 4.7 to 4.9 show a plan view, side view and elevation view of the proposed retrofit measure for the pile cap and piled foundation. The new piles should be provided with adequate reinforcement (transverse and longitudinal) and the embedment length into the pile cap should be at least 38 cm (15 in) to create a fixed connection.

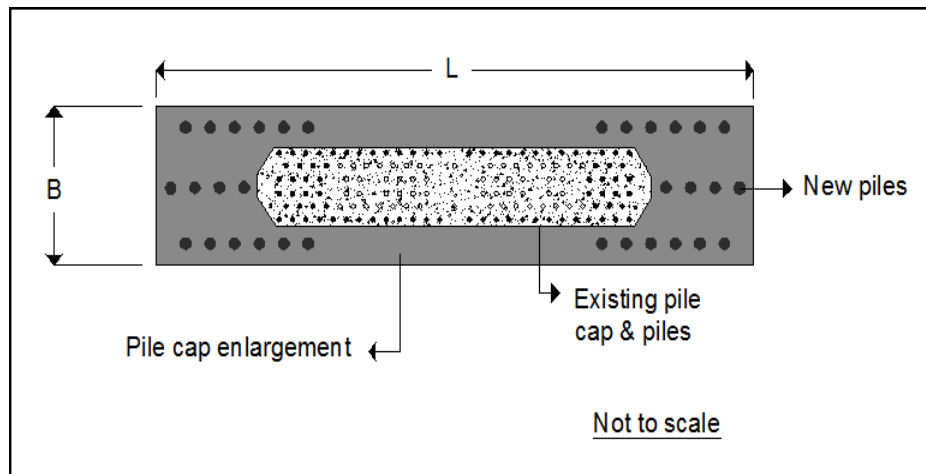


Figure 4. 7. Pile caps and pile foundations strengthening, plan view.

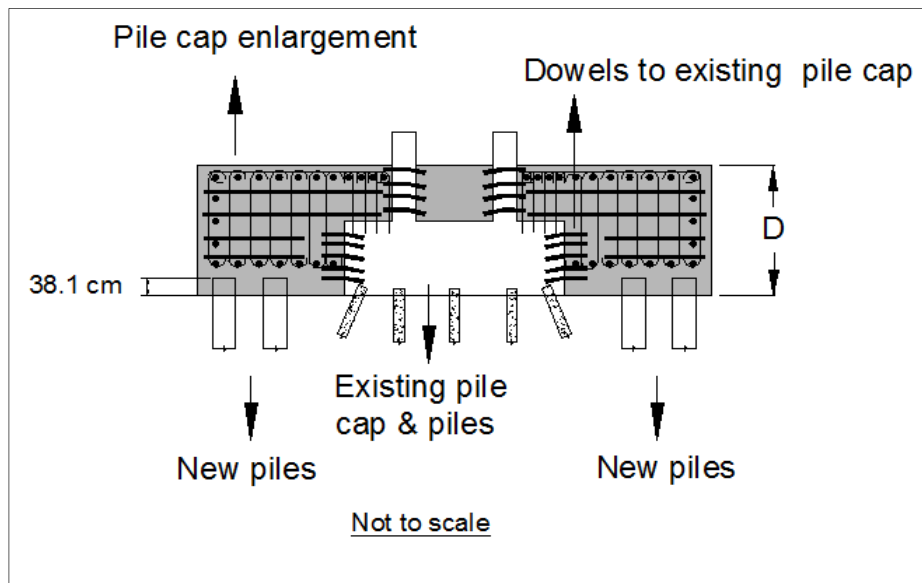


Figure 4. 8. Pile cap strengthening.

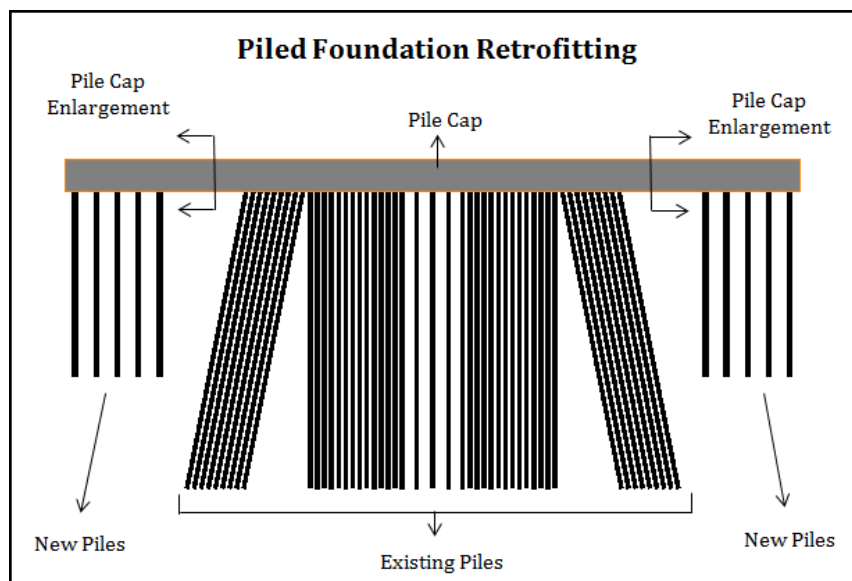


Figure 4. 9. Piled foundations strengthening.

A preliminary analysis was completed to have an estimate of the number of piles required to improve the seismic performance of the piled foundation. The size of the pile cap was also increased to accommodate the new piles. The diameter of the new piles was assumed as 61 cm (24 in) and 22 #10 rebars were assumed as the vertical reinforcement for these piles, see Figure 4.10. This preliminary analysis was completed assuming the same soil properties and the same loads used in the previous analysis. Table 4.1 presents a summary of the dimensions and number of piles required to retrofit the piled

foundation. The interaction diagram was defined for the new piles to complete their analysis. Figures 4.11 to 4.27 show the interaction diagram for the new piles as well as the reactions obtained after the analysis.

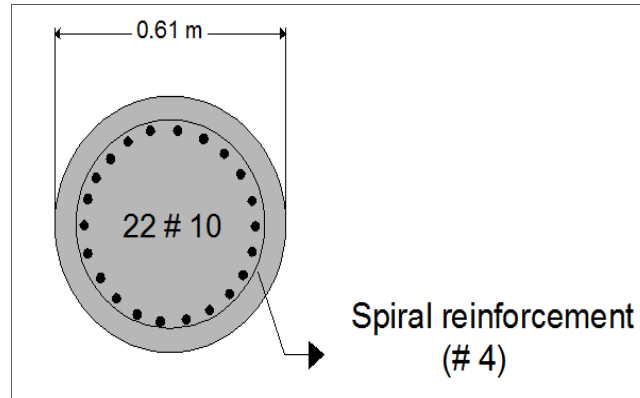


Figure 4. 10. Cross-section view and reinforcement for new piles.

Table 4. 1. Piled foundation retrofitting summary.

Piled Foundation Retrofitting Summary					
Location	Pile Cap Size			Number of Piles Required	Pile Length (m)
	B(m)	L(m)	D(m)		
East Abutment	8	48	3	12	28
Pier 1	14	70	3	60	18
Pier 2	16	62	3	72	15
Pier 3	14	68	3	48	16
Pier 4	12	39.2	3	N/A	N/A
Pier 5	12	62	3	48	24
West Abutment	8	48	3	12	20

Results obtained for this preliminary analysis can be observed from two different approaches; added piles acting together with existing piles to resist the demand loads or added piles providing enough capacity to withstand the demand loads without taking into account the structural capacity provided by the existing piles. The first two graphs for each foundation retrofitted present the results obtained considering both, existing and added piles working together. A third graph, was generated for those cases where the capacity provided by the new piles was enough to resist the demand loads, neglecting the contribution of the existing piles. In this case the existing piles were not considered as part of the analysis and the analysis was completed considering the new piles working alone.

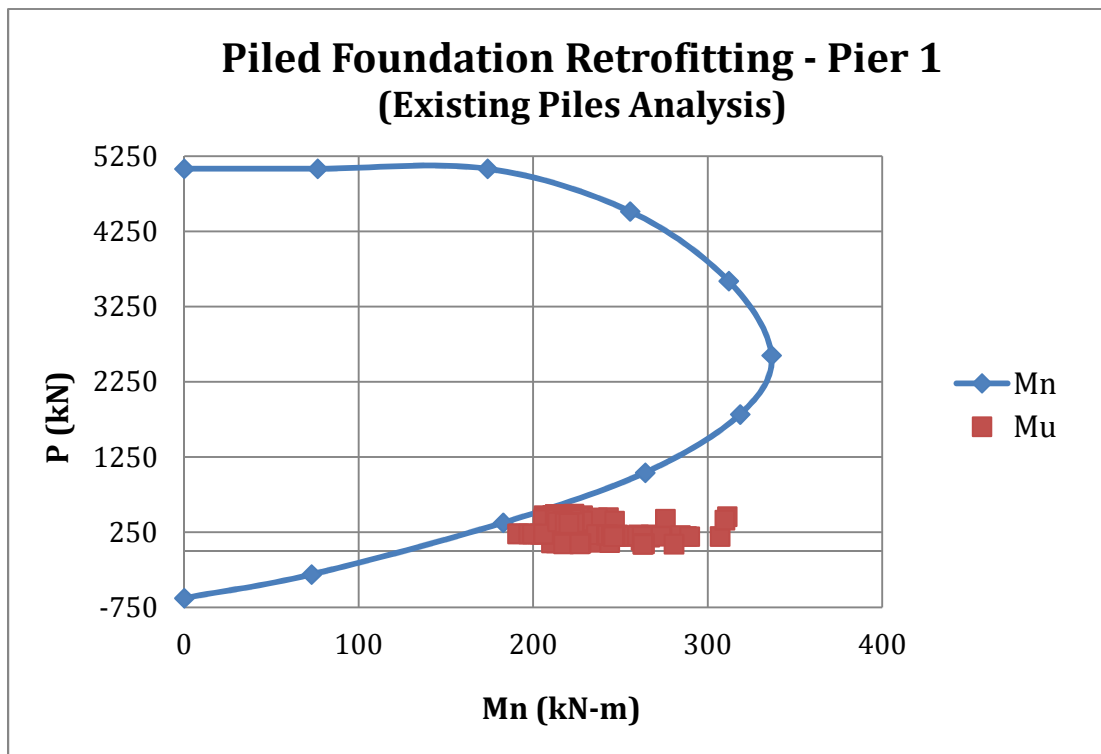


Figure 4. 11. Piled foundation retrofitting, existing piles analysis (Pier 1).

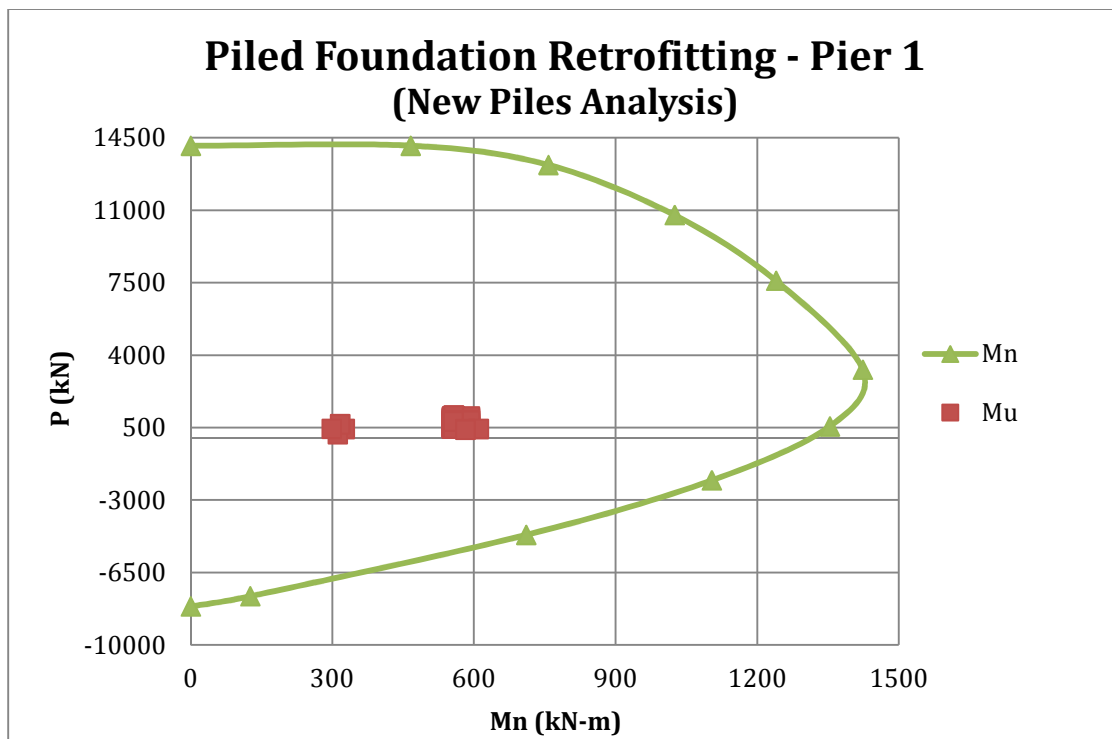


Figure 4. 12. Piled foundation retrofitting, new piles analysis (Pier 1).

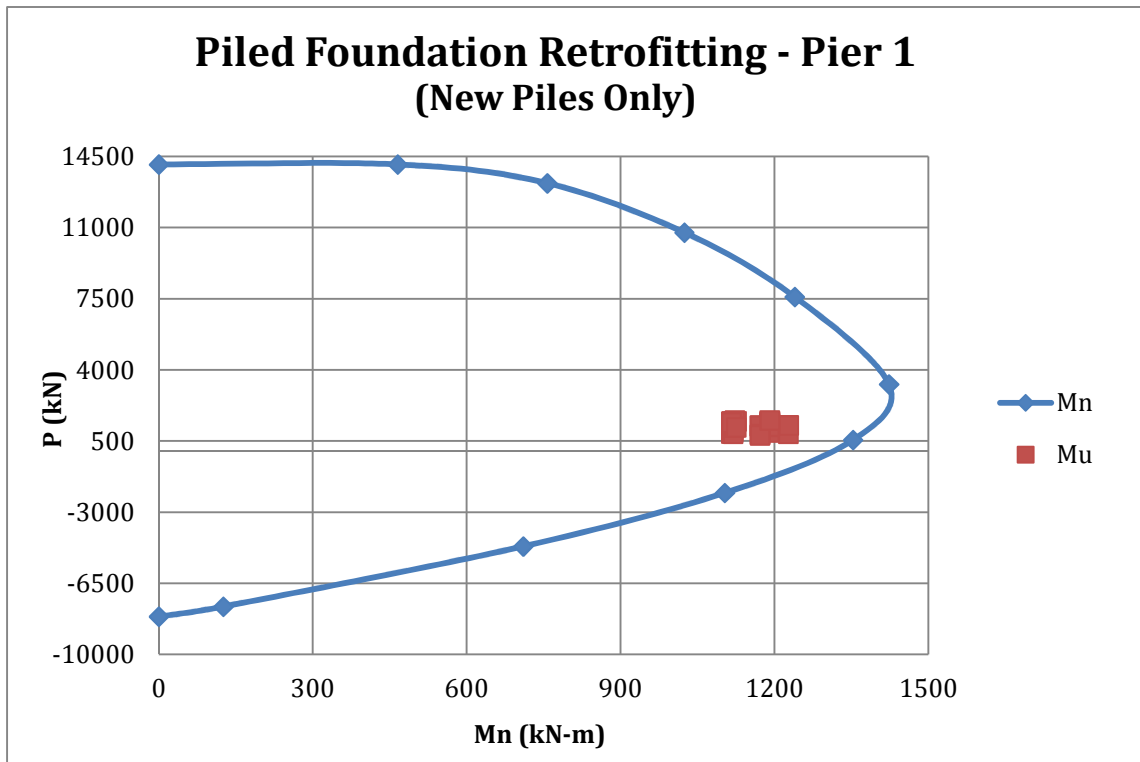


Figure 4. 13. Piled foundation retrofitting, analysis for new piles only (Pier 1).

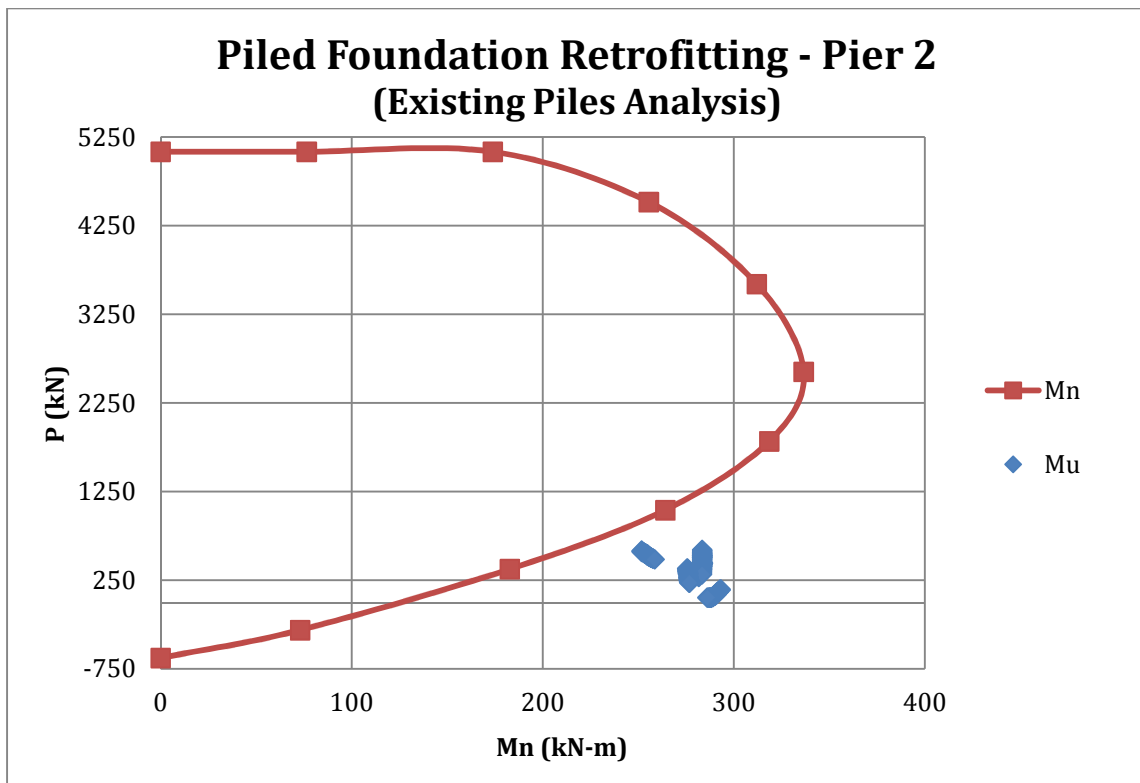


Figure 4. 14. Piled foundation retrofitting, existing piles analysis (Pier 2).

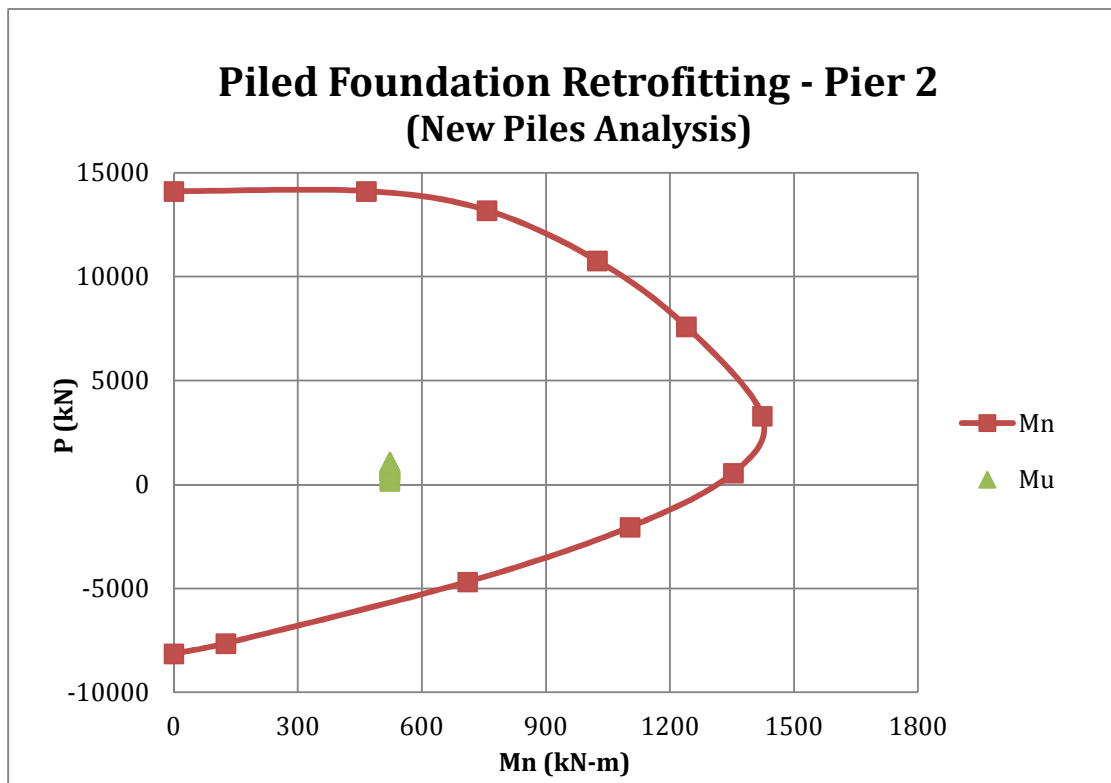


Figure 4. 15. Piled foundation retrofitting, new piles analysis (Pier 2).

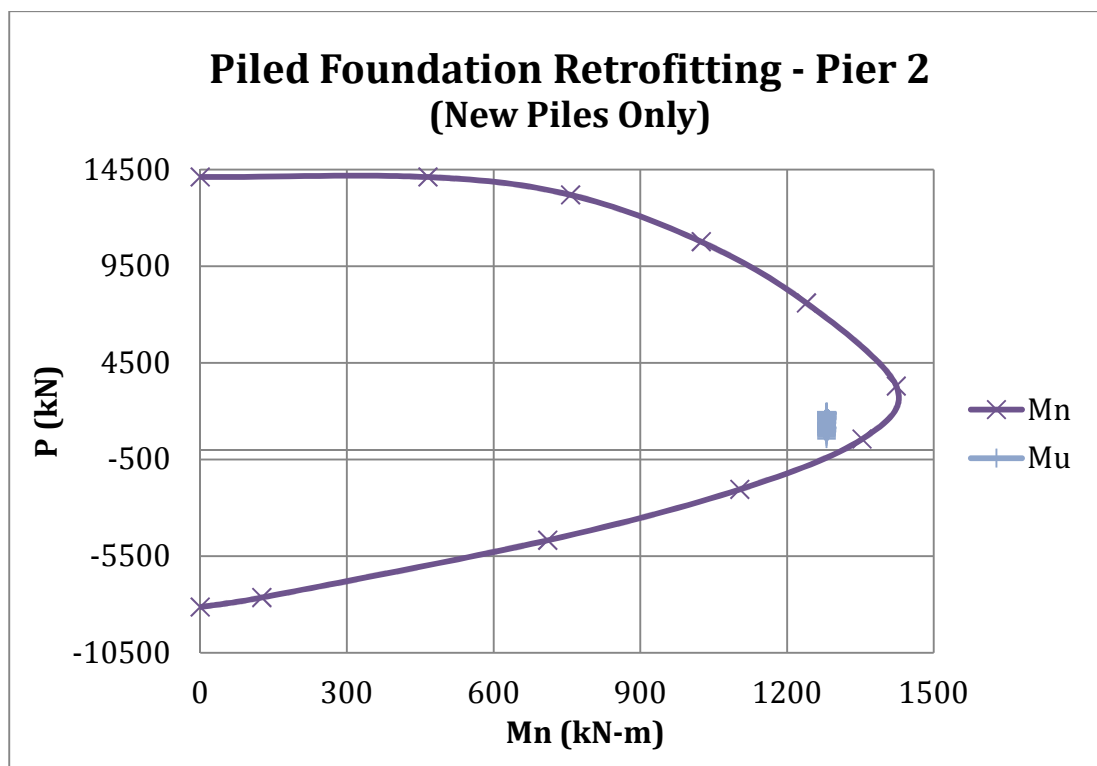


Figure 4. 16. Piled foundation retrofitting, analysis for new piles only (Pier 2).

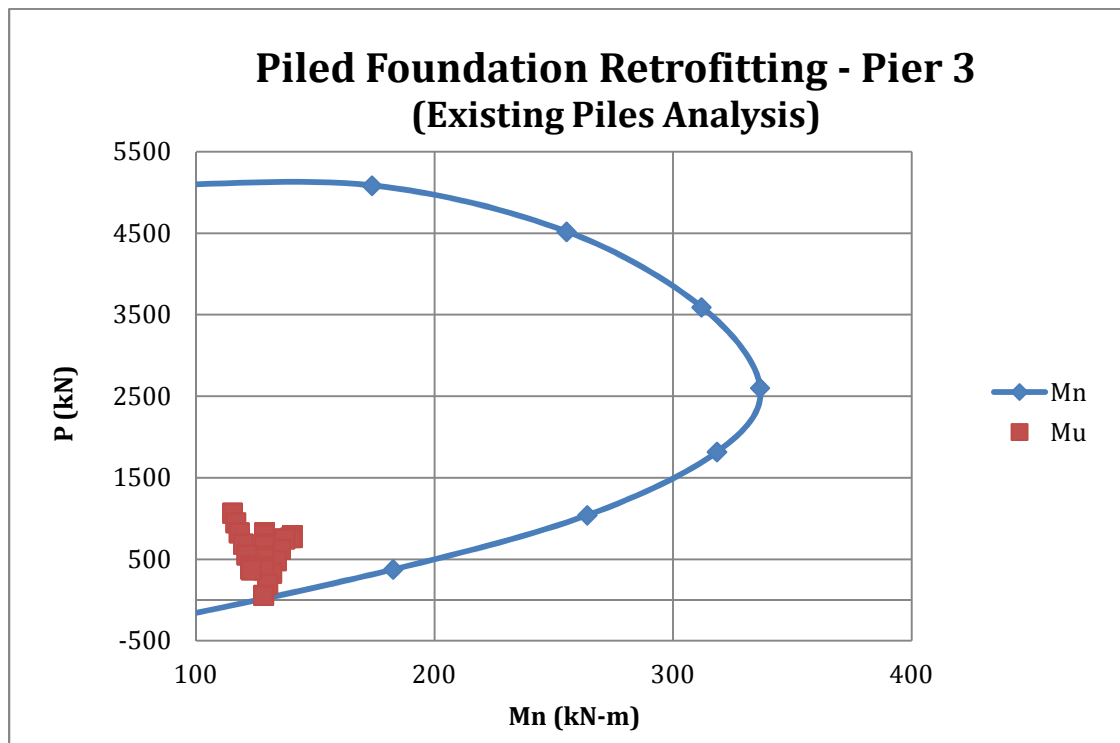


Figure 4. 17. Piled foundation retrofitting, existing piles analysis (Pier 3).

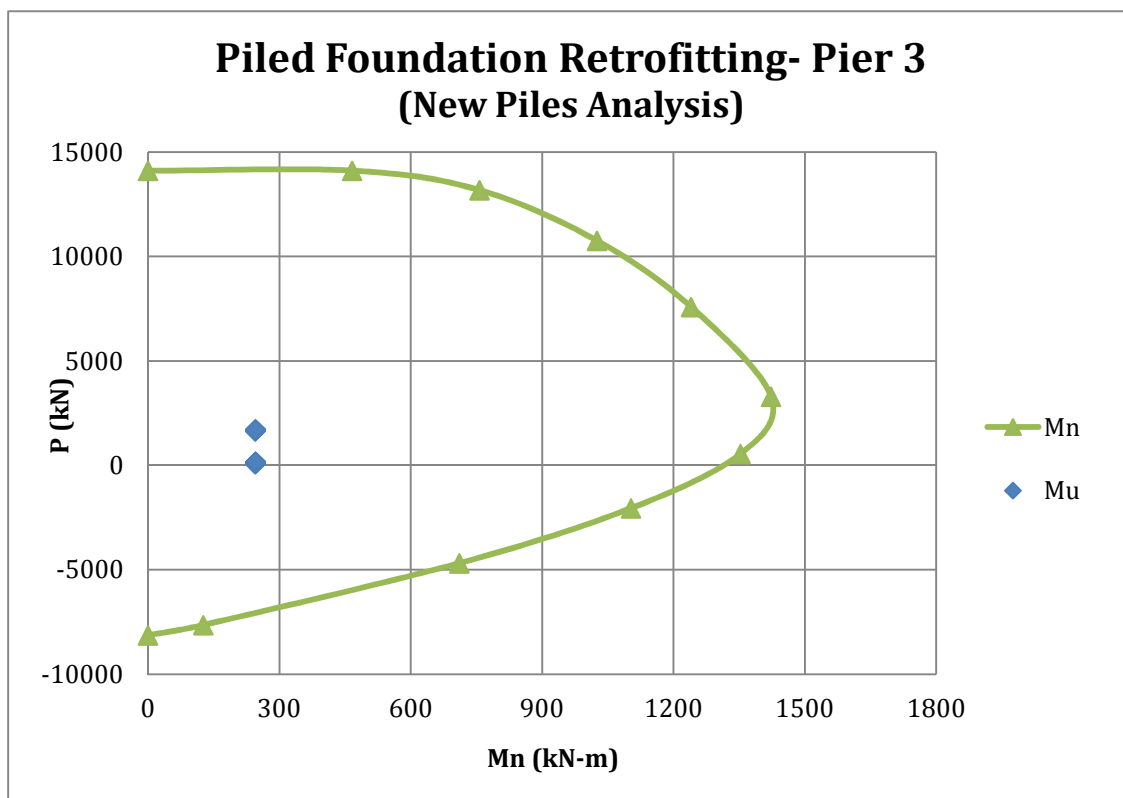


Figure 4. 18. Piled foundation retrofitting, new piles analysis (Pier 2).

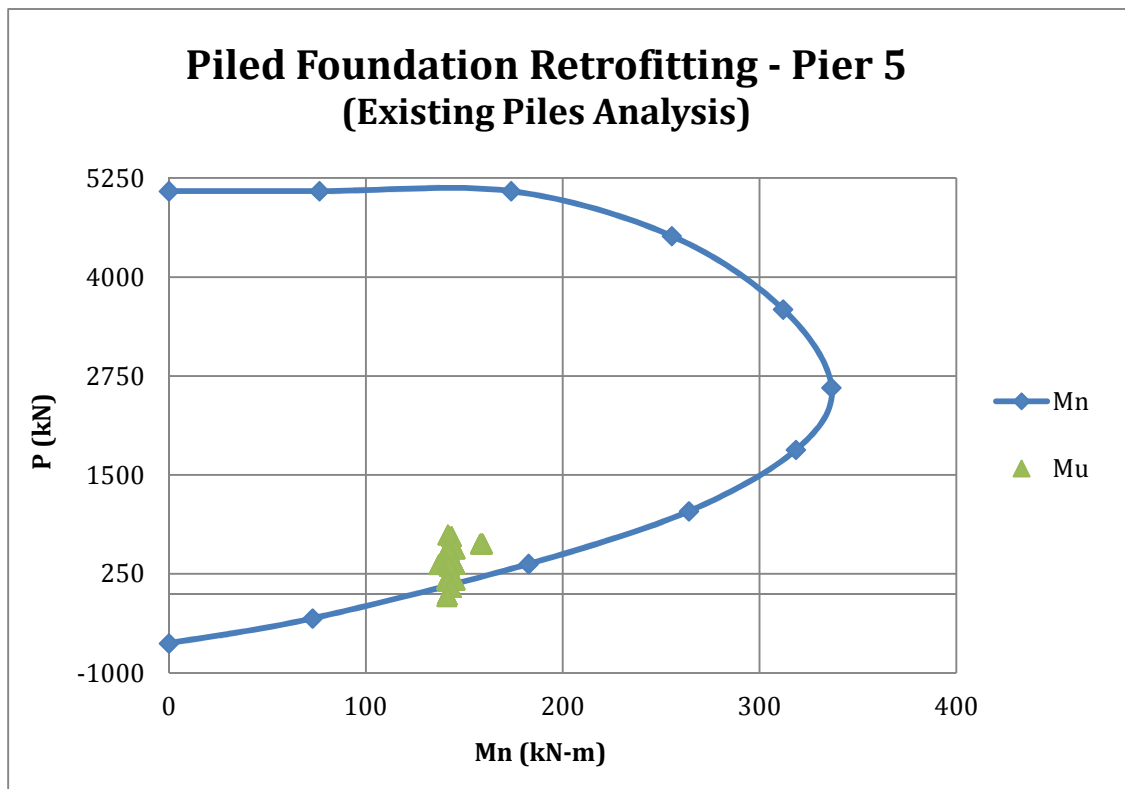


Figure 4. 19. Piled foundation retrofitting, existing piles analysis (Pier 5).

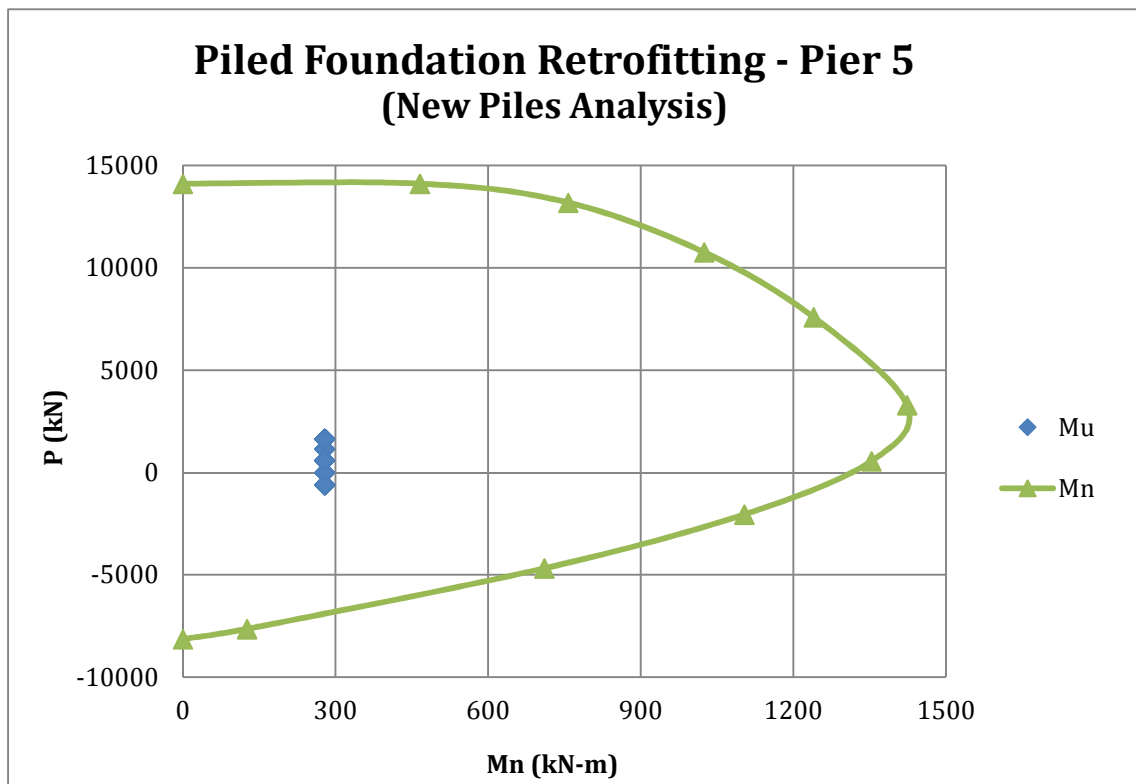


Figure 4. 20. Piled foundation retrofitting, new piles analysis (Pier 5).

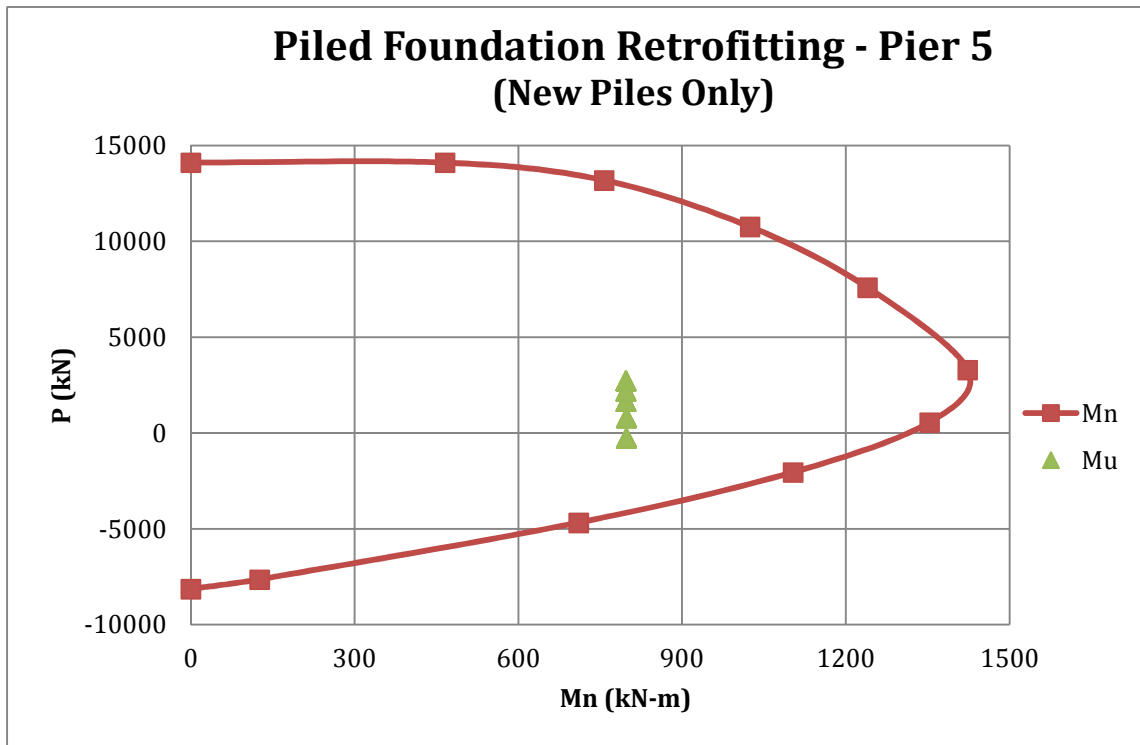


Figure 4. 21. Piled foundation retrofitting, analysis for new piles only (Pier 3).

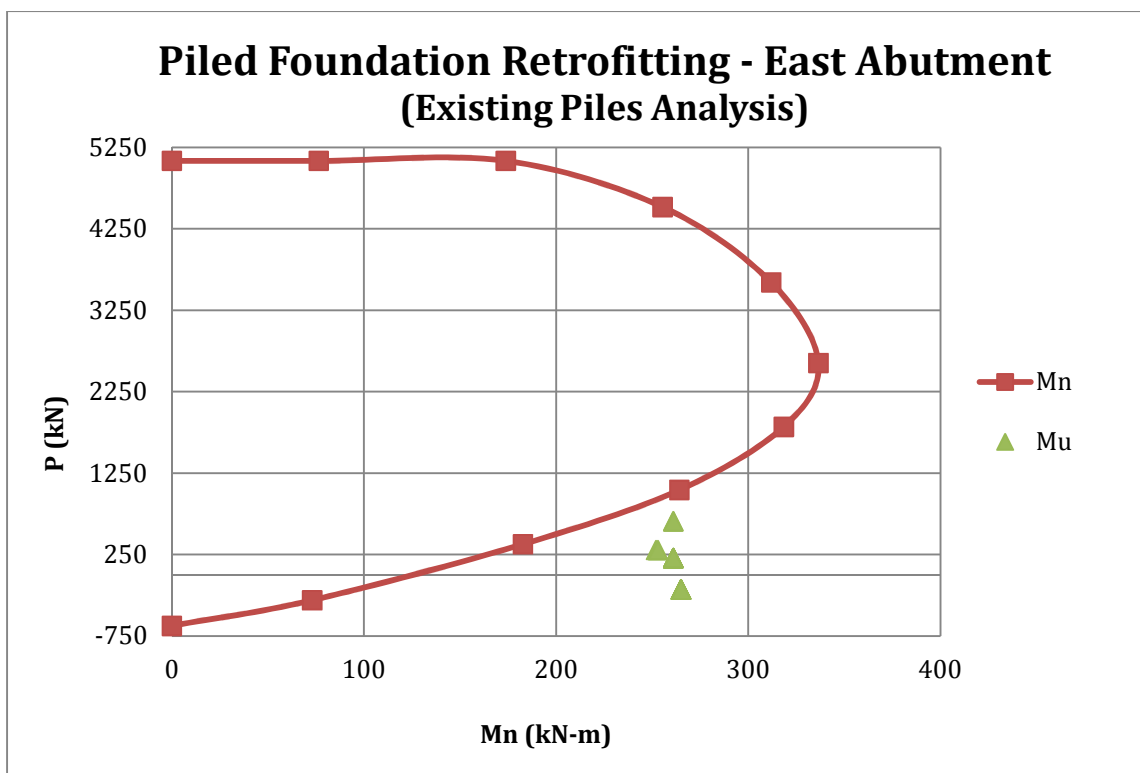


Figure 4. 22. Piled foundation retrofitting, existing piles analysis (East Abutment).

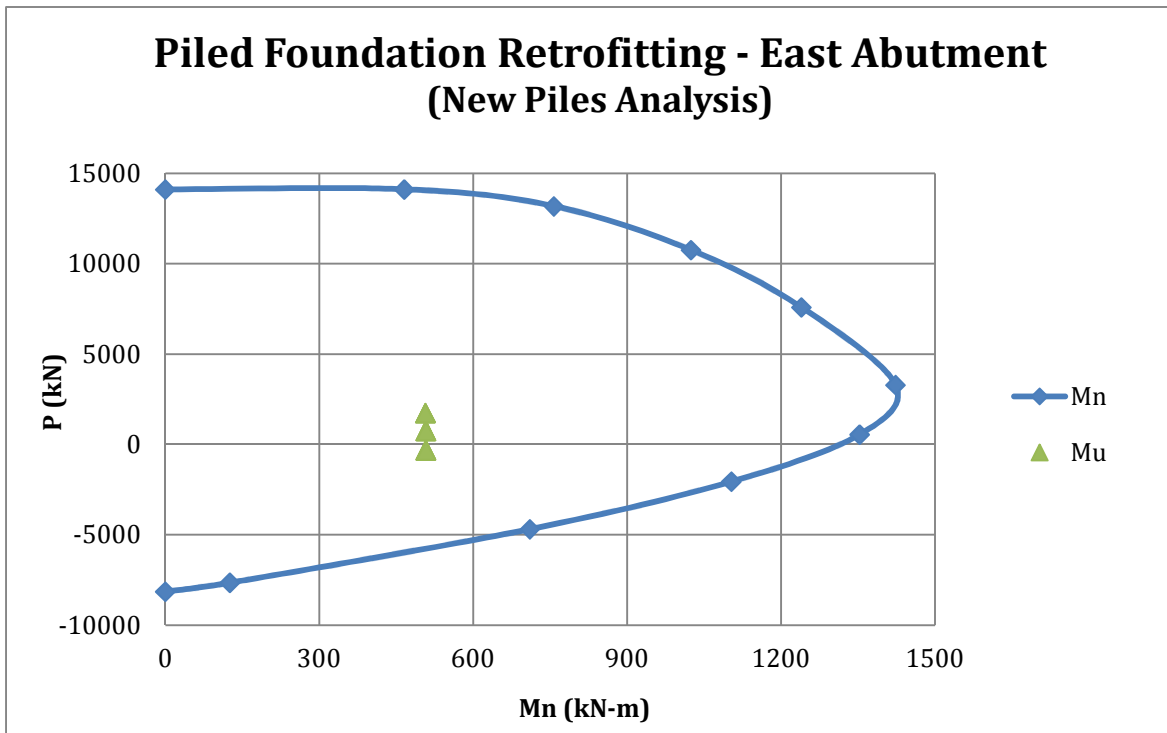


Figure 4. 23. Piled foundation retrofitting, new piles analysis (East Abutment).

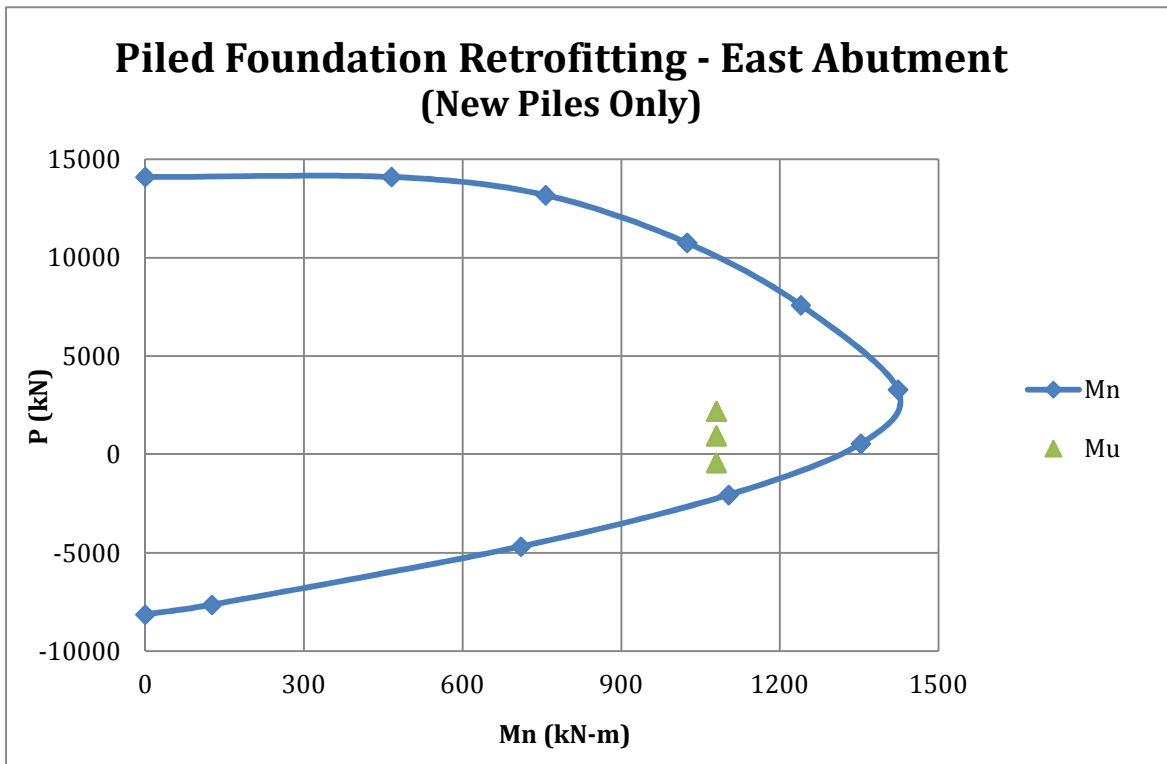


Figure 4. 24. Piled foundation retrofitting, analysis for new piles only (East Abutment).

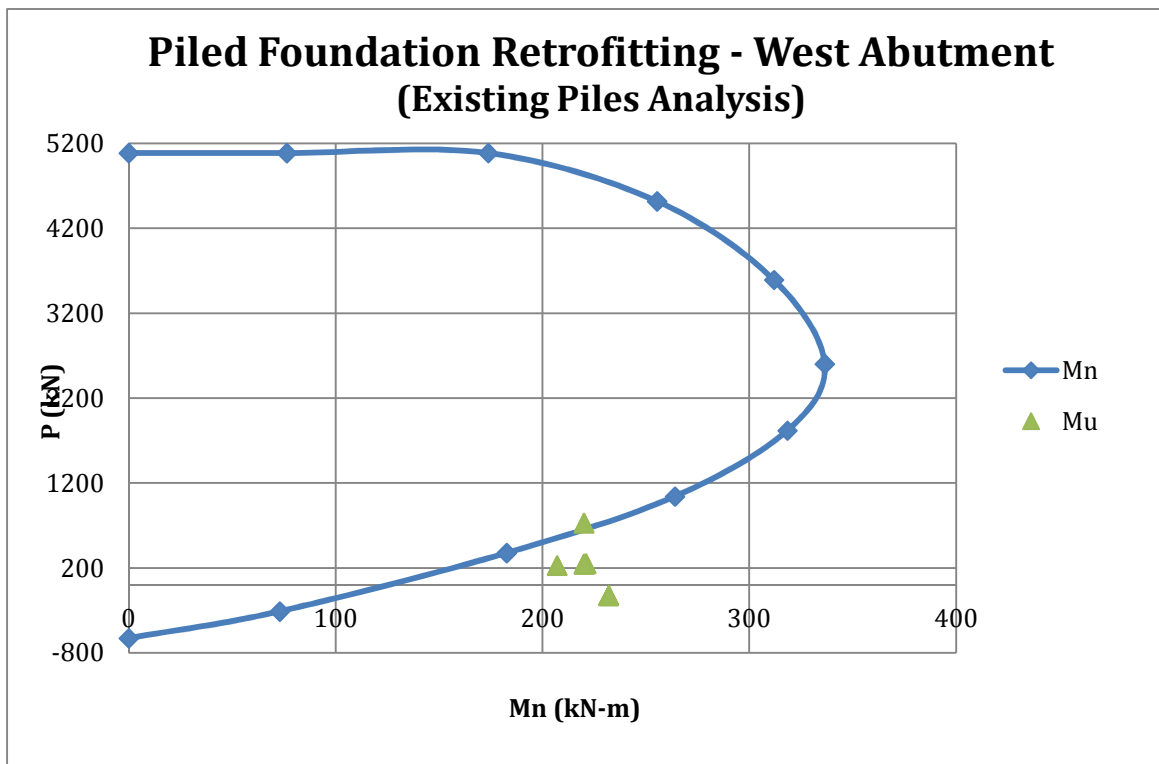


Figure 4. 25. Piled foundation retrofitting, existing piles analysis (West Abutment).

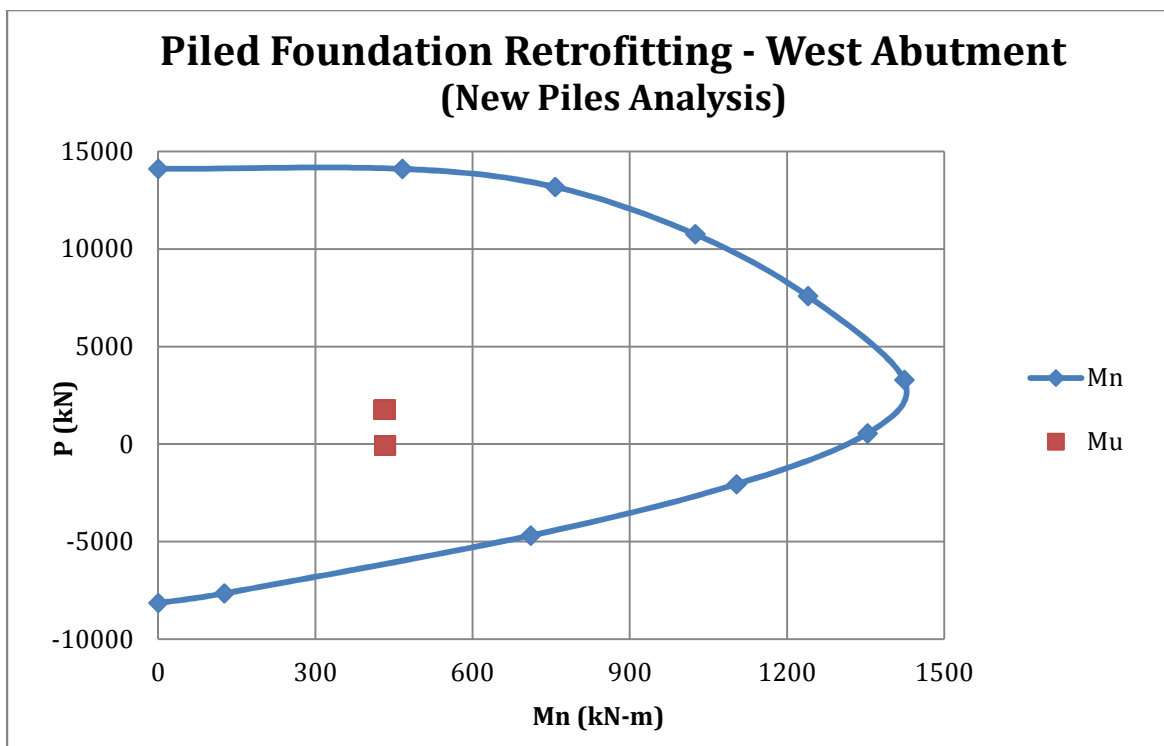


Figure 4. 26. Piled foundation retrofitting, new piles analysis (West Abutment).

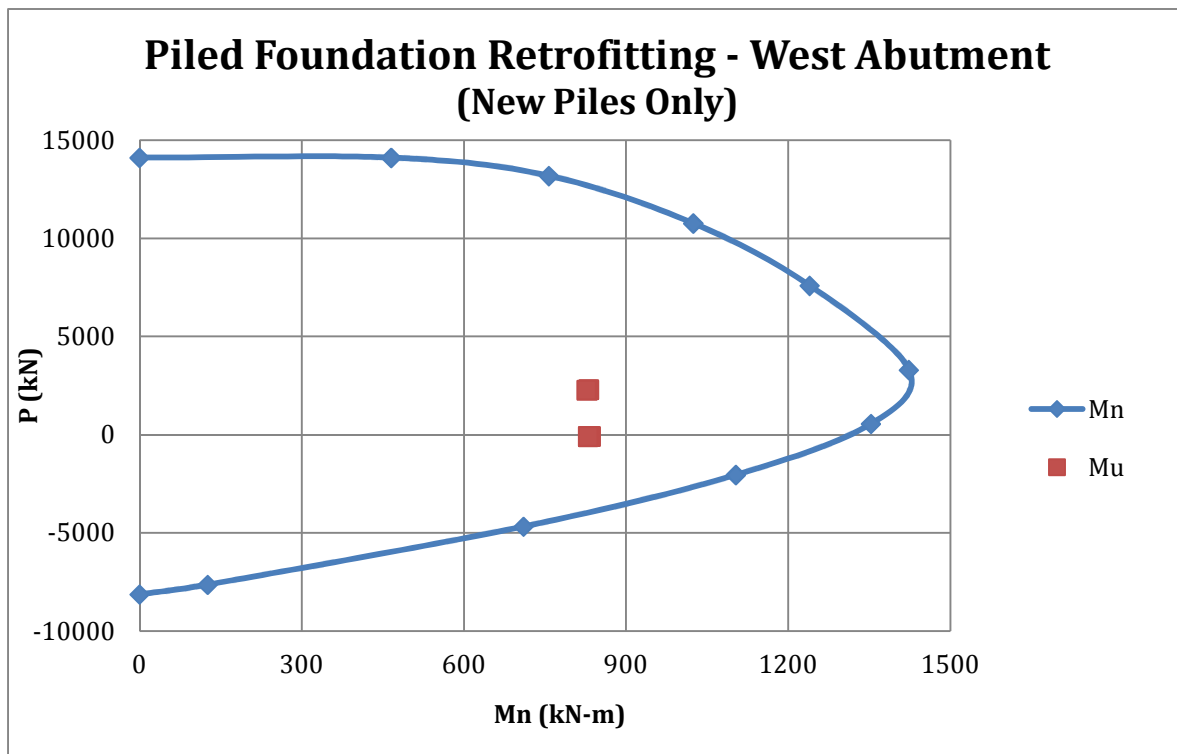


Figure 4. 27. Piled foundation retrofitting, analysis for new piles only (West Abutment).

4.5 Ground Improvement

Ground improvement techniques could be implemented to prevent soil liquefaction and maintain the lateral deformations of the bridge within tolerable limits. In order to accomplish the ground improvement, soils must be densified, drained, reinforced or replaced. Compaction grouting, permeation grouting, jet grouting and deep soil mixing are among the techniques which could be implemented for these purposes.

4.5.1 Compaction Grouting

Compaction grouting involves pumping a stiff mix of soil, cement and water into the ground under high pressure to compress or densify the soil. A very stiff soil-cement and water mixture is injected into the soil forming a grout bulb, which displaces and potentially densifies the surrounding ground, without penetrating the soil pores (FHWA, 2006). Figure 4.28 shows a conceptual drawing of the compaction grouting process.

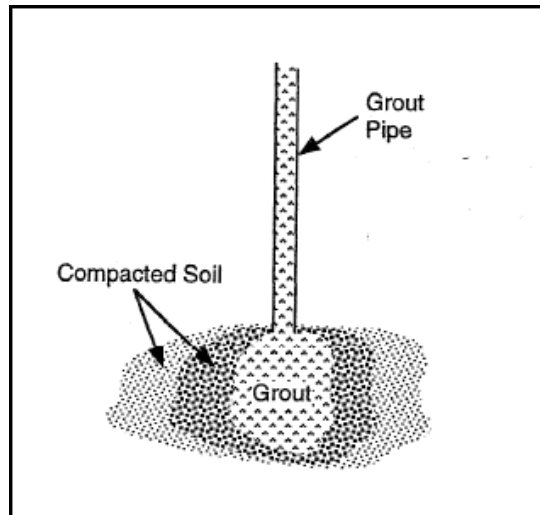


Figure 4. 28. Compaction grouting process (Andrus and Chung, 1995).

4.5.2 Permeation Grouting

This technique consists on injecting a low viscosity particulate into soil pore spaces to create changes in the physical structure of the soil. The major objective of permeation grouting is either to strengthen ground by cementing soil particles together or to reduce water flow by plugging soil pores (Andrus and Chung, 1995). Seismic induced settlements and liquefaction of soils can be reduced with the solidification of loose soils due to permeation grouting. Figure 4.29 shows a conceptual drawing of the permeation grouting process.

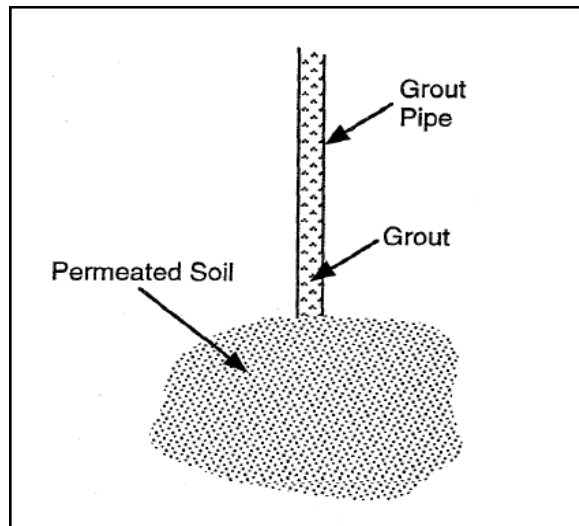


Figure 4. 29. Permeation grouting process (Andrus and Chung, 1995)

4.5.3 Jet Grouting

Jet grouting technique can be implemented to reinforce soil by increasing its shear strength. It consists mainly on eroding and replacing soils with grout using high pressure fluid jets. Jet grouting forms cylindrical or panel shapes of hardened soils to replace liquefiable, settlement sensitive or permeable soils with soil-crete having strengths up to 2500 psi (Baez, 1996). Figure 4.30 shows a diagram of the jet grouting process.

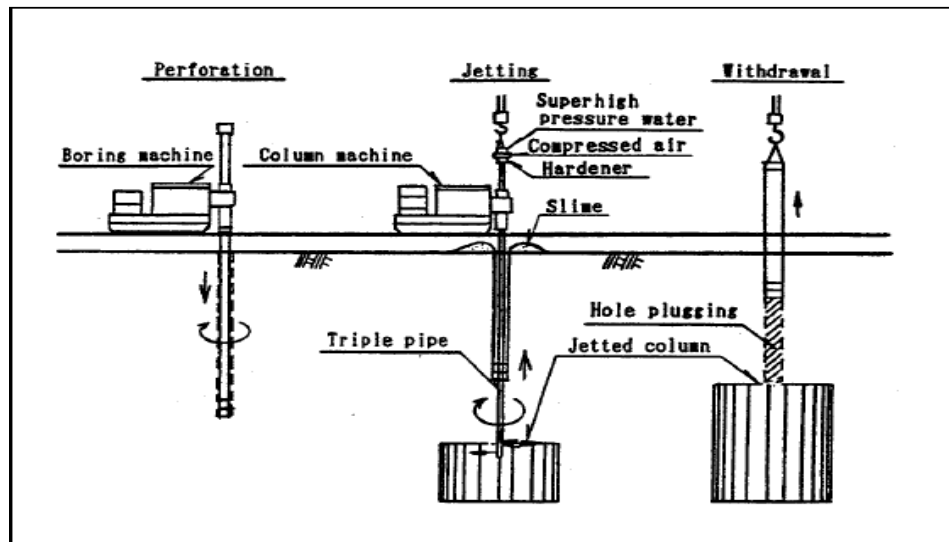


Figure 4. 30. Jet grouting process (Baez, 1996).

4.5.4 In Situ Soil Mixing

In situ soil mixing is the mechanical mixing of soil and stabilizer using rotation auger and mixing bar arrangements (Andrus and Chung, 1995). The result of this technique is the replacement of soils with grout. An increase in the bearing capacity of soils and prevention of liquefaction induced ground displacement can be achieved with this technique. Figure 4.31 shows a diagram of the In Situ Soil Mixing Technique.

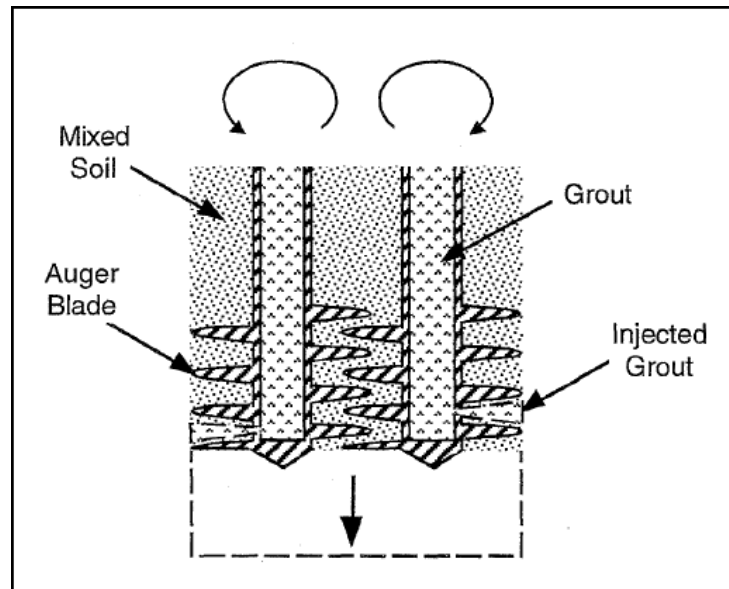


Figure 4. 31. In situ soil mixing technique (Andrus and Chung, 1995)

All these techniques mentioned above could be implemented to improve the seismic performance of soils by reinforcing or replacing liquefiable soils and controlling lateral deformation of soils. However, the selection of any one of these techniques should be based on engineering requirements, feasibility, cost consideration and environmental factors. It is recommended to consult geotechnical specialists to participate on the selection of an appropriate technique.

CHAPTER V: Conclusions and Recommendations

5.1 Conclusions

The main objectives of this study were to perform a detailed seismic analysis for a bridge located in one of the main routes of the National Highway System in Puerto Rico, to determine the seismic vulnerability of the bridge, and to present retrofitting measures, if necessary. This analysis was completed following the Capacity/Demand Ratio methodology presented in the FHWA publication entitled *Seismic Retrofitting Manual for Highway Bridges*. Two computer software programs were implemented to perform the computer modeling of the bridge and foundation. Once completed the seismic analysis of the bridge it was found that the capacity for various bridge components was exceeded by the seismic demand loads, resulting in C/D ratios smaller than 1. Bridge components in need of retrofitting include: hinge connections, shear keys, piers, pile caps, piled foundations and soils. The most relevant findings resulting from this study can be summarized as follows:

Hinge Connection:

The capacity provided at the hinge connections, was exceeded, in all interior spans, by the demand loads resulting from vertical shear and axial loads. The strengthening of the hinge connection can be achieved by increasing the size and strength of the steel section. A wider section with greater depth, web thickness and flange thickness should be able to increase the capacity of the hinge connection in order to resist the seismic demand. Elastomeric bearing pads with continuous high strength anchor bolts drilled and grouted into existing concrete should be provided at one side of the steel beam to allow the rotation of the beam.

Shear Keys:

Transverse forces resulting from the seismic analysis exceeded the capacity provided by the shear keys at the hinge level for the first three spans. The capacity provided by the steel and concrete was not enough to withstand the demand loads. The strengthening of the shear keys can be achieved by providing additional shear keys at the connection level. This strengthening

consists on providing the bottom slab of the concrete box girder with hollow structural steel sections (HSS) to create an additional shear key.

Piers:

The shear capacity of piers in the weak direction (Piers 1, 3 & 5) was exceeded by the seismic demand loads resulting from the analysis. Strengthening of piers in the weak direction can be achieved by filling some of the existing hollows with concrete. This measure increases the width considered to determine the capacity provided by the concrete (V_c). Adequate connection should be provided between the existing and new concrete.

Pile Caps:

The capacity provided by the pile caps was not exceeded by the seismic demand loads. However, it was noted the lack of longitudinal reinforcement in the transverse direction, which reflects a poor seismic design. It is recommended to increase the size (width, length and depth) of the pile cap in order to provide at least the minimum required reinforcement on both directions. Adequate connection should be provided between the existing and new concrete with the use of dowel bars. An increase in the size of the pile caps increase the shear capacity of the pile cap, by increasing the passive resistance of soils, and reduce the shear loads on piles.

Pile Foundations:

Based on the analysis completed for the piled foundations, it was demonstrated that the structural capacity of the piles was exceeded by the seismic demand loads. Strengthening of the piled foundation requires adding new piles or ground improvement techniques. With the increase in the size of the size of the pile cap it is possible to provide new piles to improve the seismic performance of the piled foundation. These new piles should be provided with a large diameter (24 in), adequate reinforcement (transverse and longitudinal), and the embedment length into the pile cap should be at least 38 cm (15 in) to create a fixed connection. The purpose of the piled foundation retrofitting is to

maintain the foundation within the elastic behavior to make sure that the plastic hinge occurs first at the pier than at the foundation.

Soils:

Once completed the analysis for potential soil liquefaction it was demonstrated that soils beneath Piers 1 and 2 are the most susceptible to liquefy. Ground improvement techniques could be implemented to prevent soil liquefaction and maintain lateral deformations of the bridge within tolerable limits. Compaction grouting, permeation grouting, jet grouting and deep soil mixing are among the techniques which could be implemented for these purposes.

Diaphragms:

Diaphragms are not among the primary components of the bridge but they provide additional capacity to the structure. Because of this, diaphragms were not analyzed as part of this study. However, it was noted in the design drawings that diaphragms located at the superstructure-piers intersection do not provide a solid connection. Strengthening of diaphragms can be achieved by filling the hollow sections with concrete and providing adequate reinforcement to make it solid. In addition, an adequate connection should be provided between the new and existing concrete.

5.2 Recommendations

The following recommendations should be taken into account previous to the retrofitting of the bridge:

- The selection of any of the retrofitting techniques should be based on engineering requirements, feasibility, cost considerations, and environmental factors.
- Consult a geotechnical specialist to participate on the selection of n appropriate technique to be implemented in the seismic improvement of the pile foundations and soils (liquefaction).
- A more detailed analysis to determine the susceptibility of soils to liquefy should be considered before taking any action to address liquefaction issues.
- Retrofitting measures are not limited to those presented as part of this study.

References

AASHTO LRFD, (2007). Bridge Design Specifications, SI Units, 4th Edition, American Association of State Highway and Transportation Officials, Washington D.C.

Andrus, R.D. and Chung, R.M. (1995). "Ground Improvement Techniques for Liquefaction Remediation near Existing Lifelines". Building and Fire Research Laboratory, National Institute of Standards and Technology.

Baez, J.I. (1996). "Seismic Ground Improvements for Bridge Sites: Proceedings of the Fourth CALTRANS Seismic Research Workshop", California Department of Transportation, Sacramento, CA.

Coll, M., (2003). "Seismic Evaluation & Retrofit Strategy for Bridge NO. 692 on Roadway PR-1 Over Guaynabo River & PR-834", Puerto Rico Highway & Transportation Authority.

FHWA, (2011), "LRFD Seismic Analysis and Design of Transportation Geotechnical Features and Structural Foundations". Publication No. FHWA-NHI-11-032, Federal Highway Administration, U.S. Department of Transportation.

FHWA, (2006), "Seismic Retrofitting Manual for Highway Bridges". Publication No. FHWA-HRT-06-032, Federal Highway Administration, U.S. Department of Transportation, January 2006.

Google Earth, (2011), Google Earth v6.1.0.5001 Software. Available from <http://www.google.com>

Group7, (2006). A Program for Analyzing Group of Piles Subjected to Axial and Lateral Loading, Group 7 for Windows. Ensoft Inc., Austin, TX.

Harik, E.I., Madasany, C., Chen, D., Zhou, L., Sutterer, K., Street, R., Allen, L.D., (1998). "Seismic Evaluation of the Ohio River Bridge on US 51 at Wickliffe, Kentucky". Research Report, Kentucky Transportation Center, College of engineering, University of Kentucky.

MoDOT, (2002), "Bridge Design Manual". Volume 6, Section 6.1 – Seismic Design, Missouri Department of Transportation.

SAP2000, (1995). Static and Dynamic Finite Element Analysis of Structures, SAP 2000, Educational Version. Computers and Structures, Inc., Berkeley, CA.

Seed, H.B., and Idriss, I.M., (1971), "Simplified Procedure for Evaluating Soil Liquefaction Potential", Journal of the Soil Mechanics and Foundation Division, American Society of Civil Engineers, Volume 97, Number SM9, September, pp. 1249-1273.

WSDOT, (2012), "Bridge Design Manual". Publication No. M-23-50, Washington State Department of Transportation.

APPENDIX A: Seismic Demand Loads on Piles

Table A. 1. Piles reactions: East Abutment.

East Abutment						
Pile #	Rz (kN)	Rx (kN)	Ry (kN)	Mz (kN-m)	Mx (kN-m)	My (kN-m)
1	-781	407	0.0591	0.0125	-0.0628	743
2	-781	407	0.0591	0.0125	-0.0628	743
3	-781	407	0.0591	0.0125	-0.0628	743
4	-781	407	0.0591	0.0125	-0.0628	743
5	-781	407	0.0591	0.0125	-0.0628	743
6	-781	407	0.0591	0.0125	-0.0628	743
7	-781	407	0.0591	0.0125	-0.0628	743
8	-781	407	0.0591	0.0125	-0.0628	743
9	1000	538	0.0515	0	-0.0554	728
10	1000	538	0.0515	0	-0.0554	728
11	1000	538	0.0515	0	-0.0554	728
12	1000	538	0.0515	0	-0.0554	728
13	1490	828	0.0538	0.0114	-0.0571	704
14	1480	824	0.0538	0.0113	-0.0571	705
15	1000	538	0.0515	0	-0.0554	728
16	1000	538	0.0515	0	-0.0554	728
17	1000	538	0.0515	0	-0.0554	728
18	1000	538	0.0515	0	-0.0554	728
19	3100	531	0.0438	0	-0.0479	725
20	3100	531	0.0438	0	-0.0479	725

Table A. 2. Piles reactions: West Abutment.

West Abutment						
Pile #	Rz (kN)	Rx (kN)	Ry (kN)	Mz (kN-m)	Mx (kN-m)	My (kN-m)
1	-186	491	2.88	0.313	-1.56	874
2	-186	490	2.88	0.313	-1.56	874
3	-186	490	2.89	0.313	-1.57	874
4	-186	490	2.89	0.313	-1.57	874
5	-186	490	2.91	0.313	-1.57	873
6	-186	489	2.91	0.313	-1.57	873
7	-186	489	2.92	0.313	-1.57	873
8	-186	489	2.92	0.313	-1.57	873
9	877	413	3.53	0	-2.27	790
10	873	412	3.53	0	-2.27	789
11	869	412	3.53	0	-2.27	789
12	864	412	3.53	0	-2.27	789
13	684	528	3.81	0.484	-2.42	762
14	681	526	3.81	0.48	-2.42	762
15	850	411	3.54	0	-2.28	788
16	846	410	3.54	0	-2.28	787
17	841	410	3.54	0	-2.29	787
18	837	410	3.55	0	-2.29	787
19	3260	412	3.88	0	-2.58	777
20	3250	411	3.88	0	-2.58	777

Table A. 3. Piles reactions: Pier 1.

Pier 1						
Pile #	Rz (kN)	Rx (kN)	Ry (kN)	Mz (kN-m)	Mx (kN-m)	My (kN-m)
1	322	394	326	95.9	234	480
2	335	296	262	81.4	193	407
3	337	274	252	77.9	189	390
4	335	276	259	78.3	197	392
5	334	279	267	78.8	206	394
6	449	313	328	74.9	375	560
7	447	306	326	74.6	373	551
8	443	305	331	75.2	376	548
9	438	300	330	75	375	540
10	432	291	326	74.4	372	529
11	428	289	328	74.6	373	524
12	429	316	360	79.5	398	543
13	438	381	434	90.1	451	593
14	439	426	499	98.8	494	619
15	416	332	403	85.4	427	543
16	394	278	347	77.2	386	494
17	379	260	331	74.6	373	474
18	368	259	334	75	375	469
19	357	259	338	75.6	378	465
20	344	255	337	75.4	377	457
21	332	250	336	75.1	376	449
22	321	278	307	79.8	416	399
23	276	278	310	79.7	408	399
24	183	276	319	79.3	397	397
25	73.6	278	338	79.6	391	398
26	-12.5	319	406	86.1	425	431
27	329	319	290	84.9	219	425
28	340	241	236	72.4	181	362
29	340	235	236	71.5	183	358
30	336	254	256	74.7	202	374
31	2890	253	307	0.0	367	386
32	2780	240	289	0.0	353	374
33	2670	249	301	0.0	361	382
34	2550	255	308	0.0	367	387
35	2440	241	289	0.0	351	375
36	2330	231	275	0.0	340	366
37	2220	246	296	0.0	356	380
38	1920	421	539	0.0	530	517
39	1630	304	375	0.0	415	429
40	1520	241	288	0.0	347	375
41	1400	235	280	0.0	341	370
42	1270	254	306	0.0	361	387
43	1110	260	314	0.0	366	392
44	957	247	296	0.0	352	381
45	774	256	307	0.0	360	389
46	110	261	309	76.7	377	384
47	4.04	248	306	74.3	354	372
48	-94.1	238	307	72.6	336	363
49	-111	254	326	75.3	346	377
50	317	376	348	93.4	264	467
51	335	261	260	75.7	204	379

Table A. 3. Continuation.

Pile #	Rz (kN)	Rx (kN)	Ry (kN)	Mz (kN-m)	Mx (kN-m)	My (kN-m)
52	339	233	242	71	193	355
53	336	245	257	73.1	207	366
54	2600	271	332	0.0	386	401
55	2480	247	299	0.0	360	380
56	2260	273	334	0.0	386	403
57	2150	236	284	0.0	346	371
58	2030	231	276	0.0	340	366
59	1920	277	339	0.0	389	406
60	1440	367	463	0.0	477	478
61	1320	261	316	0.0	369	393
62	1170	233	278	0.0	338	368
63	1020	246	294	0.0	351	379
64	660	279	340	0.0	385	408
65	477	255	306	0.0	359	387
66	-97	281	364	79.8	378	400
67	-115	244	312	73.6	332	368
68	-116	239	299	72.6	320	364
69	-103	288	355	81	362	405
70	322	323	324	85.7	256	429
71	334	249	265	73.8	215	369
72	334	243	264	72.8	217	364
73	329	255	280	74.8	232	374
74	2410	255	310	0.0	368	387
75	2300	247	299	0.0	359	380
76	2190	250	304	0.0	362	383
77	2080	256	311	0.0	368	388
78	1960	248	301	0.0	359	381
79	1850	240	289	0.0	350	374
80	1740	253	306	0.0	363	386
81	1450	421	540	0.0	529	517
82	1070	310	383	0.0	419	433
83	911	250	301	0.0	356	383
84	728	244	293	0.0	349	378
85	545	257	310	0.0	362	389
86	355	263	318	0.0	367	394
87	136	255	307	0.0	358	387
88	-20.3	259	312	0.0	361	390
89	-109	264	335	77	349	385
90	-111	256	319	75.6	334	378
91	-113	248	302	74.2	318	371
92	-109	263	314	76.6	326	384
93	303	412	418	98.6	326	493
94	318	327	346	86.3	280	432
95	316	311	337	83.9	277	420
96	311	311	342	83.9	285	420
97	306	312	348	84	293	420
98	312	278	396	83.2	416	316
99	307	284	393	82.9	415	323
100	302	290	393	82.9	415	331
101	296	297	395	83.2	416	340
102	292	302	393	82.9	415	348
103	284	308	393	82.9	415	356

Table A. 3. Continuation.

Pile #	Rz (kN)	Rx (kN)	Ry (kN)	Mz (kN-m)	Mx (kN-m)	My (kN-m)
104	269	324	414	85.9	430	374
105	250	361	470	93.6	468	407
106	215	412	531	102	509	456
107	212	368	448	90.8	454	427
108	205	345	405	84.7	424	414
109	195	342	392	82.9	415	416
110	161	342	392	82.9	415	424
111	88.7	335	391	82.9	415	432
112	-20.8	321	393	83.1	416	441
113	-123	306	390	82.8	414	448
114	-95.9	317	391	85.4	388	427
115	-95.5	319	386	85.7	382	429
116	-95.9	318	378	85.5	373	428
117	-95.9	318	371	85.6	365	428
118	-88.4	352	403	90.6	384	453

Table A. 4. Pile reactions: Pier 2.

Pier 2						
Pile #	Rz (kN)	Rx (kN)	Ry (kN)	Mz (kN-m)	Mx (kN-m)	My (kN-m)
1	1320	81.1	622	22.2	340	111
2	1300	81.4	621	22.3	343	111
3	1280	81.6	621	22.3	346	112
4	1260	81.9	620	22.4	349	112
5	1220	-56.8	475	90.6	454	215
6	1190	-55.7	475	90.6	454	212
7	1170	-54.7	475	90.6	454	209
8	1150	-53.6	476	90.6	454	206
9	1130	-52.6	476	90.6	454	203
10	1110	-51.6	476	90.6	454	200
11	1090	-50.5	476	90.6	454	197
12	1070	-49.5	476	90.6	454	194
13	1050	-48.4	476	90.6	454	190
14	972	-40.4	476	90.6	454	184
15	938	-36.6	476	90.6	454	180
16	903	-32.8	477	90.6	454	177
17	869	-29.1	477	90.6	454	174
18	834	-25.3	477	90.6	454	171
19	789	-19.5	477	90.6	454	168
20	744	-13.6	477	90.6	454	165
21	699	-7.66	477	90.6	454	162
22	653	-1.74	478	90.6	454	159
23	422	87.1	431	23.4	489	117
24	360	87.4	440	23.5	486	117
25	298	87.6	449	23.5	482	118
26	236	87.9	458	23.6	479	118
27	1250	81.3	620	22.2	350	111
28	1230	81.5	619	22.3	354	112
29	1210	81.8	618	22.3	357	112
30	1330	82.8	475	0.0	463	116
31	1300	83.1	476	0.0	463	116
32	1280	83.3	476	0.0	463	116

Table A. 4. Continuation.

Pile #	Rz (kN)	Rx (kN)	Ry (kN)	Mz (kN-m)	Mx (kN-m)	My (kN-m)
33	1250	83.6	476	0.0	463	117
34	1230	83.8	476	0.0	463	117
35	1210	84	476	0.0	463	117
36	1180	84.3	476	0.0	463	117
37	1160	84.5	476	0.0	463	118
38	1100	85.2	476	0.0	463	118
39	1020	85.9	477	0.0	463	119
40	980	86.1	477	0.0	463	119
41	937	86.4	477	0.0	463	119
42	895	86.6	477	0.0	463	120
43	852	86.9	477	0.0	463	120
44	800	87.1	477	0.0	463	120
45	740	87.4	478	0.0	463	120
46	681	87.7	478	0.0	463	121
47	225	87.3	460	23.5	479	117
48	161	87.6	470	23.5	475	118
49	95.8	87.9	480	23.6	472	118
50	1210	81.2	619	22.2	358	111
51	1190	81.4	618	22.3	361	111
52	1160	81.7	617	22.3	364	112
53	1140	81.9	616	22.4	368	112
54	1230	83.2	476	0.0	463	116
55	1200	83.4	476	0.0	463	116
56	1160	83.9	476	0.0	463	117
57	1130	84.2	476	0.0	463	117
58	1110	84.4	476	0.0	463	117
59	1080	84.7	477	0.0	463	118
60	930	85.8	477	0.0	463	119
61	888	86	477	0.0	463	119
62	845	86.3	477	0.0	463	119
63	790	86.5	478	0.0	463	120
64	671	87.1	478	0.0	463	120
65	611	87.3	478	0.0	463	120
66	95.6	87.2	480	23.4	471	117
67	94.7	87.5	476	23.5	468	118
68	93.9	87.7	473	23.5	465	118
69	93.1	88	470	23.6	462	118
70	1140	81.2	617	22.2	368	111
71	1120	81.4	616	22.3	371	112
72	1100	81.7	615	22.3	374	112
73	1080	81.9	614	22.4	378	112
74	1160	83.2	477	0.0	463	116
75	1130	83.5	477	0.0	463	116
76	1080	84	477	0.0	463	117
77	1060	84.2	477	0.0	463	117
78	1030	84.5	477	0.0	463	117
79	983	84.7	477	0.0	463	118
80	789	85.8	478	0.0	463	119
81	730	86.1	478	0.0	463	119
82	670	86.3	478	0.0	463	119
83	611	86.6	478	0.0	463	120
84	492	87.1	479	0.0	463	120
85	416	87.4	479	0.0	463	120

Table A. 4. Continuation.

Pile #	Rz (kN)	Rx (kN)	Ry (kN)	Mz (kN-m)	Mx (kN-m)	My (kN-m)
86	93.2	87.3	470	23.4	462	117
87	92.5	87.5	467	23.5	458	118
88	91.8	87.8	464	23.5	455	118
89	91	88	460	23.6	452	118
90	1080	81.3	615	22.3	379	111
91	1060	81.6	614	22.3	382	112
92	1040	81.8	613	22.4	385	112
93	1130	82.9	477	0.0	463	116
94	1100	83.1	477	0.0	463	116
95	1080	83.4	477	0.0	463	116
96	1060	83.6	477	0.0	463	117
97	1020	83.9	477	0.0	463	117
98	976	84.1	477	0.0	463	117
99	934	84.4	478	0.0	463	117
100	891	84.6	478	0.0	463	118
101	757	85.3	478	0.0	463	118
102	601	86	479	0.0	463	119
103	541	86.3	479	0.0	463	119
104	480	86.5	479	0.0	463	120
105	402	86.8	479	0.0	463	120
106	315	87.1	480	0.0	463	120
107	224	87.3	480	0.0	463	120
108	134	87.6	480	0.0	463	121
109	37.7	87.9	481	0.0	463	121
110	91	87.4	460	23.5	451	117
111	90.3	87.6	457	23.5	448	118
112	89.6	87.9	453	23.6	445	118
113	1030	81.2	613	22.2	386	111
114	1010	81.5	612	22.3	389	112
115	990	81.7	612	22.3	393	112
116	969	82	611	22.4	396	112
117	858	199	478	90.9	455	60.5
118	824	196	478	90.9	455	64.1
119	787	192	478	90.9	455	67.6
120	741	187	478	90.9	455	71.2
121	696	181	479	90.9	455	74.8
122	651	176	479	90.9	455	78.3
123	606	171	479	90.9	455	81.9
124	561	165	479	90.9	455	85.5
125	515	160	479	90.9	455	89.1
126	403	146	480	90.9	455	97.1
127	347	138	480	90.9	455	101
128	285	129	480	90.9	455	104
129	223	121	480	90.9	455	108
130	161	112	480	90.9	455	111
131	99.5	103	481	90.9	455	115
132	34.6	94.2	481	90.9	455	119
133	-17.7	87.4	481	90.9	455	122
134	-18.7	90.9	481	90.9	455	126
135	89.5	87.3	453	23.4	444	117
136	88.8	87.5	450	23.5	441	118
137	88.2	87.8	446	23.5	438	118
138	87.5	88	443	23.6	435	118

Table A. 5. Piles reactions: Pier 3.

Pier 3						
Pile #	Rz (kN)	Rx (kN)	Ry (kN)	Mz (kN-m)	Mx (kN-m)	My (kN-m)
1	1500	126	361	27.7	56.4	139
2	1490	126	360	27.7	56.5	139
3	1490	126	360	27.6	56.6	138
4	1490	126	359	27.6	56.7	138
5	1340	-104	98.9	18.1	90.8	174
6	1340	-104	98.9	18.1	90.8	174
7	1330	-104	98.9	18.1	90.8	173
8	1330	-104	98.9	18.1	90.8	173
9	1330	-103	98.9	18.1	90.8	173
10	1330	-103	98.9	18.1	90.8	173
11	1320	-103	98.9	18.1	90.8	172
12	1320	-103	98.9	18.1	90.8	172
13	1320	-102	98.9	18.1	90.8	172
14	1310	-102	98.9	18.1	90.8	171
15	1310	-102	98.9	18.1	90.8	171
16	1310	-101	98.9	18.1	90.8	171
17	1300	-101	98.9	18.1	90.8	171
18	1300	-101	98.9	18.1	90.8	170
19	1300	-101	98.9	18.1	90.8	170
20	1300	-100	98.9	18.1	90.8	170
21	1290	-99.8	98.9	18.1	90.8	169
22	1290	-99.2	98.9	18.1	90.8	169
23	1270	122	-121	27	123	135
24	1270	122	-120	27	122	135
25	1270	122	-120	27	122	135
26	1260	122	-119	26.9	122	135
27	1330	126	334	27.7	62.7	139
28	1330	126	333	27.7	62.8	138
29	1320	126	333	27.6	62.9	138
30	1250	126	98.8	0.0	92.4	142
31	1240	126	98.8	00.0	92.4	142
32	1240	126	98.9	0.0	92.4	142
33	1240	126	98.9	0.0	92.4	141
34	1230	126	98.9	0.0	92.4	141
35	1230	125	98.9	0.0	92.4	141
36	1230	125	98.9	0.0	92.4	141
37	1230	125	98.9	0.0	92.4	141
38	1220	125	98.9	0.0	92.4	141
39	1210	124	98.9	0.0	92.4	140
40	1210	124	98.9	0.0	92.4	140
41	1200	124	98.9	0.0	92.4	140
42	1200	124	98.9	0.0	92.4	140
43	1200	124	98.9	0.0	92.4	140
44	1200	123	98.9	0.0	92.4	139
45	1190	123	98.9	0.0	92.4	139
46	1190	123	98.9	0.0	92.4	139
47	1000	122	-74	27	116	135
48	999	122	-73.2	27	116	135
49	995	122	-72.4	27	116	135
50	1110	126	297	27.7	68.9	139
51	1100	126	296	27.7	69	139

Table A. 5. Continuation.

Pile #	Rz (kN)	Rx (kN)	Ry (kN)	Mz (kN-m)	Mx (kN-m)	My (kN-m)
52	1100	126	295	27.7	69.1	138
53	1090	126	294	27.6	69.2	138
54	988	126	98.9	0.0	92.3	142
55	983	126	98.9	0.0	92.3	142
56	973	126	98.9	0.0	92.3	141
57	969	125	98.9	0.0	92.3	141
58	964	125	98.9	0.0	92.3	141
59	959	125	98.9	0.0	92.3	141
60	939	124	98.9	0.0	92.3	140
61	934	124	98.9	0.0	92.3	140
62	929	124	98.9	0.0	92.3	140
63	925	124	98.9	0.0	92.3	140
64	915	124	98.9	0.0	92.3	140
65	910	124	98.9	0.0	92.3	139
66	737	123	-27.6	27	109	135
67	733	123	-26.8	27	109	135
68	729	122	-26.1	27	109	135
69	724	122	-25.3	27	109	135
70	805	126	244	27.7	75.9	139
71	801	126	243	27.7	76	139
72	796	126	242	27.7	76.1	139
73	792	126	242	27.7	76.2	138
74	665	126	98.9	0.0	92.1	142
75	660	126	98.9	0.0	92.1	142
76	650	126	98.9	0.0	92.1	141
77	646	126	98.9	0.0	92.1	141
78	641	126	98.9	0.0	92.1	141
79	636	125	98.9	0.0	92.1	141
80	616	125	98.9	0.0	92.1	140
81	611	125	98.9	0.0	92.1	140
82	606	124	98.9	0.0	92.1	140
83	600	124	98.9	0.0	92.1	140
84	590	124	99	0.0	92.1	140
85	585	124	99	0.0	92.1	139
86	405	123	31.1	27.1	102	135
87	400	123	32	27	102	135
88	395	123	32.9	27	102	135
89	390	122	33.8	27	102	135
90	519	127	194	27.7	82.2	139
91	514	126	193	27.7	82.3	139
92	509	126	192	27.7	82.4	139
93	366	127	98.9	0.0	92	142
94	361	127	99	0.0	92	142
95	356	126	99	0.0	92	142
96	351	126	99	0.0	92	142
97	346	126	99	0.0	92	142
98	340	126	99	0.0	92	141
99	335	126	99	0.0	92	141
100	330	126	99	0.0	92	141
101	317	125	99	0.0	92	141
102	303	125	99	0.0	92	140
103	298	125	99	0.0	92	140

Table A. 5. Continuation.

Pile #	Rz (kN)	Rx (kN)	Ry (kN)	Mz (kN-m)	Mx (kN-m)	My (kN-m)
104	293	124	99	0.0	92	140
105	288	124	99	0.0	92	140
106	283	124	99	0.0	92	140
107	278	124	99	0.0	92	140
108	273	124	99	0.0	92	139
109	267	124	99	0.0	92	139
110	104	123	84.3	27.1	95.6	135
111	98.9	123	85.1	27	95.5	135
112	94.1	123	86	27	95.4	135
113	239	13.1	54.3	9.45	20.5	47.3
114	217	127	140	27.7	88.5	139
115	212	126	140	27.7	88.6	139
116	207	126	139	27.7	88.7	139
117	197	165	98.8	18	90	139
118	191	164	98.8	18	90	139
119	186	163	98.8	18	90	139
120	181	162	98.8	18	90	139
121	176	161	98.8	18	90	139
122	171	160	98.8	18	90	139
123	165	159	98.8	18	90	139
124	160	158	98.8	18	90	139
125	155	157	98.8	18	90	139
126	143	154	98.8	18	90	139
127	138	153	98.8	18	90	139
128	133	152	98.9	18	90	139
129	128	151	98.9	18	90	139
130	123	150	98.9	18	90	138
131	117	149	98.9	18	90	138
132	112	148	98.9	18	90	138
133	107	147	98.9	18	90	138
134	102	145	98.9	18	90	138
135	-188	123	136	27.1	89.1	136
136	-193	123	137	27.1	89	135
137	-198	123	137	27	88.9	135
138	-203	123	138	27	88.8	135

Table A. 6. Piles reactions: Pier 4.

Pier 4						
Pile #	Rz (kN)	Rx (kN)	Ry (kN)	Mz (kN-m)	Mx (kN-m)	My (kN-m)
1	1140	84.4	288	20.6	60.1	103
2	1140	84.4	288	20.6	60.1	103
3	1140	84.4	288	20.6	60.1	103
4	1140	84.4	288	20.6	60.1	103
5	1140	84.4	288	20.6	60.1	103
6	980	-79.3	90.5	18.4	91.9	136
7	980	-79.2	90.5	18.4	91.9	136
8	979	-79.2	90.5	18.4	91.9	136
9	979	-79.2	90.5	18.4	91.9	136
10	979	-79.2	90.5	18.4	91.9	136
11	979	-79.1	90.5	18.4	91.9	136
12	979	-79.1	90.5	18.4	91.9	136

Table A. 6. Continuation.

Pile #	Rz (kN)	Rx (kN)	Ry (kN)	Mz (kN-m)	Mx (kN-m)	My (kN-m)
13	978	-79.1	90.5	18.4	91.9	136
14	978	-79	90.5	18.4	91.9	136
15	978	-79	90.5	18.4	91.9	136
16	978	-79	90.5	18.4	91.9	136
17	977	-78.9	90.5	18.4	91.9	136
18	977	-78.9	90.5	18.4	91.9	136
19	977	-78.9	90.5	18.4	91.9	136
20	977	-78.9	90.5	18.4	91.9	136
21	977	-78.8	90.5	18.4	91.9	136
22	945	84.3	-67.2	20.6	124	103
23	945	84.3	-67.1	20.6	124	103
24	945	84.3	-67.1	20.6	124	103
25	944	84.3	-67.1	20.5	124	103
26	944	84.3	-67	20.5	124	103
27	999	84.5	263	20.6	64.7	103
28	998	84.5	263	20.6	64.7	103
29	998	84.5	263	20.6	64.7	103
30	998	84.5	263	20.6	64.7	103
31	766	85	90.6	0.0	93.8	106
32	765	85	90.6	0.0	93.8	106
33	765	85	90.6	0.0	93.8	106
34	765	85	90.6	0.0	93.8	106
35	765	85	90.6	0.0	93.8	106
36	765	85	90.6	0.0	93.8	106
37	764	85	90.6	0.0	93.8	106
38	764	84.9	90.6	0.0	93.8	106
39	763	84.9	90.6	0.0	93.8	106
40	763	84.9	90.6	0.0	93.8	106
41	763	84.9	90.6	0.0	93.8	106
42	763	84.9	90.6	0.0	93.8	106
43	763	84.9	90.6	0.0	93.8	106
44	762	84.9	90.6	0.0	93.8	106
45	762	84.9	90.6	0.0	93.8	106
46	793	84.4	-41.3	20.6	119	103
47	793	84.4	-41.2	20.6	119	103
48	793	84.4	-41.2	20.6	119	103
49	793	84.4	-41.2	20.6	119	103
50	851	84.6	238	20.6	69.4	103
51	851	84.6	238	20.6	69.4	103
52	851	84.6	238	20.6	69.4	103
53	851	84.5	238	20.6	69.4	103
54	636	85.1	90.7	0.0	93.8	106
55	636	85.1	90.7	0.0	93.8	106
56	636	85	90.7	0.0	93.8	106
57	636	85	90.7	0.0	93.8	106
58	636	85	90.7	0.0	93.8	106
59	635	85	90.7	0.0	93.8	106
60	635	85	90.7	0.0	93.8	106
61	634	85	90.7	0.0	93.8	106
62	634	85	90.7	0.0	93.8	106
63	634	85	90.7	0.0	93.8	106
64	634	84.9	90.7	0.0	93.8	106
65	633	84.9	90.7	0.0	93.8	106

Table A. 6. Continuation

Pile #	Rz (kN)	Rx (kN)	Ry (kN)	Mz (kN-m)	Mx (kN-m)	My (kN-m)
66	640	84.5	-15.1	20.6	114	103
67	640	84.5	-15.1	20.6	114	103
68	640	84.5	-15	20.6	114	103
69	639	84.5	-15	20.6	114	103
70	698	84.6	212	20.6	74	103
71	698	84.6	212	20.6	74	103
72	698	84.6	212	20.6	74	103
73	698	84.6	212	20.6	74	103
74	508	85.1	90.8	0.0	93.8	106
75	507	85.1	90.8	0.0	93.8	106
76	507	85.1	90.8	0.0	93.8	106
77	507	85.1	90.8	0.0	93.8	106
78	507	85.1	90.8	0.0	93.8	106
79	507	85.1	90.8	0.0	93.8	106
80	506	85.1	90.8	0.0	93.8	106
81	506	85.1	90.8	0.0	93.8	106
82	505	85	90.8	0.0	93.8	106
83	505	85	90.8	0.0	93.8	106
84	505	85	90.8	0.0	93.8	106
85	505	85	90.8	0.0	93.8	106
86	505	85	90.8	0.0	93.8	106
87	504	85	90.8	0.0	93.8	106
88	504	85	90.8	0.0	93.8	106
89	487	84.6	11	20.6	110	103
90	487	84.6	11	20.6	110	103
91	487	84.6	11.1	20.6	110	103
92	486	84.5	11.1	20.6	110	103
93	545	84.7	187	20.6	78.6	103
94	545	84.7	186	20.6	78.6	103
95	545	84.7	186	20.6	78.6	103
96	544	84.7	186	20.6	78.6	103
97	544	84.7	186	20.6	78.7	103
98	511	175	90.7	18.4	91.9	91.3
99	511	175	90.7	18.4	91.9	91.3
100	511	174	90.7	18.4	91.9	91.3
101	511	174	90.7	18.4	91.9	91.3
102	510	174	90.7	18.4	91.9	91.3
103	510	174	90.7	18.4	91.9	91.3
104	510	174	90.7	18.4	91.9	91.3
105	510	174	90.7	18.4	91.9	91.3
106	509	174	90.7	18.4	91.9	91.3
107	509	174	90.7	18.4	91.9	91.3
108	509	174	90.7	18.4	91.9	91.3
109	508	174	90.7	18.4	91.9	91.3
110	508	174	90.7	18.4	91.9	91.3
111	508	174	90.7	18.4	91.9	91.3
112	508	174	90.7	18.4	91.9	91.3
113	508	174	90.7	18.4	91.9	91.3
114	334	84.7	37.1	20.6	105	103
115	334	84.6	37.1	20.6	105	103
116	334	84.6	37.2	20.6	105	103
117	334	84.6	37.2	20.6	105	103
118	333	84.6	37.2	20.6	105	103

Table A. 7. Piles reactions: Pier 5.

Pier 5						
Pile #	Rz (kN)	Rx (kN)	Ry (kN)	Mz (kN-m)	Mx (kN-m)	My (kN-m)
1	1690	297	300	62	31.9	310
2	1690	297	300	62	31.9	310
3	1690	297	300	62	31.9	310
4	1690	297	300	62	31.9	310
5	1690	297	300	62	31.9	310
6	1550	18.6	16.7	3	15	347
7	1550	18.6	16.7	3	15	347
8	1550	18.6	16.7	3	15	347
9	1550	18.6	16.7	3	15	347
10	1550	18.6	16.7	3	15	347
11	1550	18.6	16.7	3	15	347
12	1550	18.6	16.7	3	15	347
13	1550	18.6	16.7	3	15	348
14	1550	18.6	16.7	3	15	348
15	1550	18.6	16.7	3	15	348
16	1560	18.6	16.7	3	15	348
17	1560	18.6	16.7	3	15	348
18	1560	18.5	16.7	3	15	348
19	1560	18.5	16.7	3	15	348
20	1560	18.5	16.7	3	15	348
21	1560	18.5	16.7	3	15	348
22	1670	294	-262	61.7	63.1	309
23	1670	294	-262	61.7	63.1	309
24	1670	294	-262	61.7	63.1	309
25	1670	294	-262	61.7	63.1	309
26	1670	294	-262	61.7	63.1	309
27	1260	298	235	62.1	15.5	311
28	1260	298	235	62.1	15.5	311
29	1260	298	235	62.1	15.5	311
30	1260	298	235	62.1	15.5	311
31	1290	299	18.2	0.0	16.1	319
32	1290	299	18.2	0.0	16.1	319
33	1290	299	18.2	0.0	16.1	319
34	1290	299	18.2	0.0	16.1	319
35	1290	299	18.2	0.0	16.1	319
36	1290	299	18.2	0.0	16.1	319
37	1290	299	18.1	0.0	16.1	319
38	1290	299	18.1	0.0	16.1	319
39	1290	299	18.1	0.0	16.1	319
40	1290	299	18.1	0.0	16.1	319
41	1290	299	18.1	0.0	16.1	319
42	1290	299	18.1	0.0	16.1	319
43	1290	299	18.1	0.0	16.1	319
44	1290	299	18.1	0.0	16.1	319
45	1290	300	18.1	0.0	16.1	319
46	1240	296	-193	61.9	47	310
47	1240	296	-193	61.9	47	310
48	1240	296	-193	61.9	47	310
49	1240	296	-193	61.9	47	310
50	681	299	137	62.2	0.964	311
51	681	299	137	62.2	0.959	311

Table A. 7. Continuation.

Pile #	Rz (kN)	Rx (kN)	Ry (kN)	Mz (kN-m)	Mx (kN-m)	My (kN-m)
52	682	299	137	62.2	0.955	311
53	682	299	137	62.2	0.95	311
54	689	300	18.2	0.0	16.2	319
55	689	300	18.2	0.0	16.2	319
56	689	300	18.2	0.0	16.2	319
57	690	300	18.2	0.0	16.2	319
58	690	300	18.2	0.0	16.2	319
59	690	300	18.2	0.0	16.2	319
60	691	300	18.2	0.0	16.2	319
61	691	300	18.2	0.0	16.2	319
62	691	300	18.2	0.0	16.2	319
63	692	300	18.2	0.0	16.2	319
64	692	300	18.2	0.0	16.2	319
65	692	300	18.2	0.0	16.2	319
66	638	299	-92.1	62.1	30.8	311
67	638	299	-92.1	62.1	30.8	311
68	638	299	-92.1	62.1	30.8	311
69	639	299	-92.2	62.1	30.8	311
70	-43.4	300	11.4	62.2	17.4	311
71	-43.2	300	11.5	62.2	17.4	311
72	-43	300	11.5	62.2	17.4	311
73	-42.8	300	11.5	62.2	17.4	311
74	-70	301	18.3	0.0	16.2	319
75	-69.8	301	18.3	0.0	16.2	319
76	-69.6	301	18.3	0.0	16.2	319
77	-69.4	301	18.3	0.0	16.2	319
78	-69.1	301	18.3	0.0	16.2	319
79	-68.9	301	18.3	0.0	16.2	320
80	-68.7	301	18.3	0.0	16.2	320
81	-68.2	301	18.3	0.0	16.2	320
82	-67.6	301	18.3	0.0	16.2	320
83	-67.4	301	18.3	0.0	16.2	320
84	-67.2	301	18.3	0.0	16.2	320
85	-67	301	18.3	0.0	16.2	320
86	-66.8	301	18.3	0.0	16.2	320
87	-66.6	301	18.3	0.0	16.2	320
88	-66.4	301	18.3	0.0	16.2	320
89	-89.2	300	34.5	62.3	14.5	312
90	-89	300	34.5	62.3	14.5	312
91	-88.8	300	34.5	62.3	14.5	312
92	-88.6	300	34.4	62.3	14.5	312
93	-769	300	-115	62.1	33.8	311
94	-769	300	-115	62.1	33.8	311
95	-769	300	-115	62.1	33.8	311
96	-769	300	-115	62.1	33.8	311
97	-769	300	-114	62.2	33.8	311
98	-500	215	17.9	3.12	15.6	329
99	-500	216	17.9	3.12	15.6	329
100	-500	216	17.9	3.12	15.6	329
101	-499	216	17.9	3.12	15.6	329
102	-499	216	17.9	3.12	15.6	329
103	-499	216	17.9	3.12	15.6	329

Table A. 7. Continuation.

Pile #	Rz (kN)	Rx (kN)	Ry (kN)	Mz (kN-m)	Mx (kN-m)	My (kN-m)
104	-499	216	17.9	3.12	15.6	329
105	-499	216	17.9	3.12	15.6	329
106	-498	216	17.9	3.12	15.6	329
107	-498	216	17.9	3.12	15.6	329
108	-498	216	17.9	3.12	15.6	329
109	-497	216	17.9	3.12	15.6	329
110	-497	216	17.9	3.12	15.6	329
111	-497	216	17.9	3.12	15.6	329
112	-497	216	17.9	3.12	15.6	329
113	-496	216	17.9	3.12	15.6	329
114	-813	301	160	62.4	1.91	312
115	-813	302	160	62.4	1.91	312
116	-813	302	160	62.4	1.9	312
117	-813	302	160	62.4	1.9	312
118	-813	302	160	62.4	1.9	312